SAPIENZA
UNIVERSITÀ DI ROMA

PhD thesis in Environmental and Hydraulic Engineering

XXXIV cycle

Coupling bio- and electro-chemical processes for H_2 production from organic residues

PhD candidate
Eng. Tatiana Zonfa

Supervisor
Prof. Alessandra Polettini

Co-supervisors
Prof. Raffaella Pomi
Eng. Andreina Rossi

Abstract

Hydrogen is a carbon-free energy carrier and the research on alternative production methods, low energy-demanding and not based on fossil sources, plays a key role in the energy transition target. In that context, dark fermentation is considered a promising strategy for bio-hydrogen generation since it allows energy recovery from residual materials such as biodegradable waste. The present work addresses from different perspectives those which are currently believed to be the major challenges of the process. Firstly, a research study on the production yields and the assessment of long-term stability in continuous systems was performed; the results from the experimental campaign involving a number of combinations of operating conditions were reported. Secondly, the feasibility of combining the dark fermentation with electrochemical method was investigated with the aim to overcome the biochemical constraints associated with reduced hydrogen yields. To this purpose, an innovative integrated bio-electrochemical process was designed and tested under different configurations at lab-scale. Lastly, the concept of a multi-stage layout was investigated by means of two different bio-electrochemical systems serving as post processes for the dark fermentation effluent, with the overall aim of achieving a fully energy recovery from the starting substrate through bio-methane and electric current generation as well as providing an adequate level of stabilization of the residual organic matter.

Contents

Content of figures

Content of tables

1 Introduction

1.1 Background and problem statement

The Glasgow Climate Pact recently reached during COP26 (UNFCCC 2021) reiterated the urgency of maintaining the global temperature rise in this century well below 2 °C above pre-industrial levels and, possibly, to pursue efforts to limit the temperature increase to 1.5 °C, as stated at the 2015 Paris Agreement. However, it seems to be still far from a realistic achievement, moreover this is a very ambitious goal considering the expected economic and demographic growth over the coming years. The World Population Prospects (UN 2019) include projections at 30 years that expect the world population to reach 9.7 billion by 2050, that then get to 11 billion by the end of the century. This certainly leads to a pressure on the energy system that is responsible for almost three-quarters of the emissions (IEA 2021). A rapid and widespread change is needed in all areas of the energy sector in order to gain the sustainable development targets. An ever-increasing reduction of dependency on fossil fuels is strongly recommended as well as the use of innovative technologies able to provide efficient energy services.

The energy transition has indeed already begun and, since the early 2000s, research and use of alternative energy sources have been growing. To date, in most markets, wind or solar photovoltaic represents the most affordable and available source as new electricity generation and in 2020 also the sales of electric vehicles have set new records (IEA 2021).

Worldwide energy demand both from transport and heating sector also encourages biofuels production from biomass, such as bioethanol and biodiesel, that could represent another supporting measure to achieve independency from fossil fuels.

Nevertheless, biofuels are at the center of a wide debate concerning the competition with food crops. Nowadays bioethanol is produced for about 60% from corn, 25% from sugarcane, 7% from molasses, 4% from wheat and other cereals; biodiesel is made from vegetable oils such as soybean and palm oil for 77% and used cooking oils for 22% (OECD-FAO 2019). Biofuels produced from special dedicated energy crops and lignocellulosic feedstocks are just a small fraction. Although that category could represent a chance to avoid the conflict between food and fuel, some concerns remain regarding competition for land use or required land use changes. This resulted in a growing interest by research studies about the so-called third-generation biofuels (Nigam and Singh 2011), that are specifically derived from microorganisms or microalgae metabolic activities during organic waste treatment process.

In this context, hydrogen (H_2) plays a key role representing a competitive energy carrier thanks to its high net heating value per unit volume. H_2 can be used in both power generation systems and combustion processes, providing the great advantage of clean combustion. Nowadays, its use as a clean energy source is yet uncommon, while its main use is in ammonia production and hydrogenation of coal and petroleum during hydrocracking of traditional fuels (IEA 2019). However, the good environmental profile of H_2 is commonly counteracted by the fact that it is still primarily derived from non-renewable sources, with a high associated energy consumption and related relevant CO_2 emissions, posing an urgent need for sustainable production methods.

Several bioprocesses have been investigated over the last decades to produce H_2 through sustainable methods (Hallenbeck et al. 2012). Among them, dark fermentation (DF) is considered one of the most promising options. The main reason is that DF averts the major drawbacks of other biological processes (including direct or indirect photolysis and photo-fermentation), related to the intermittent production of H_2 and the need of a light source to support the process. Compared to other biological processes, dark fermentative H_2 production has the additional advantages of higher production rate, flexibility of operation under different temperatures and pressures, lower net energy input and, noteworthy, applicability to a range of renewable organic sources including organic waste and carbohydrate-based wastewaters (Ghimire et al. 2015; Da Silva Veras et al. 2017; Park et al. 2021).

The latter is a key point considering that, in 2019, about 931 million tons of food waste are generated (UNEP 2021). This suggests that around 17% of the world food production is disposed to landfill after it is lost along the entire food chain, as food production residues, expired goods or discarded surplus food. When food waste is landfilled, most of its energy content is lost. Under weak control and regulation condition, this practice leads to potential risks for public health caused by leachate dispersion, air pollution, nuisance and adverse sanitary conditions. Moreover, this is not even good practice from an economic point of view. Environmental policies also emphasize the importance of food waste reduction along with materials and energy recovery from organic materials.

DF of organic residues has been widely investigated over the past decades, but there are still some challenges along the way to full-scale implementation. These include mainly the poor stability of the biochemical process and the thermodynamic/biochemical limitations to the actual H_2 production yield attainable, which are the two aspects investigated in the first section of this thesis.

Lastly, the perspectives for DF application involve the integration in a wider multi-stage system, where the first step could be performed through DF of the organic waste along with H_2 collection. Afterwards, the organic matter in the original substrate is partially retained in the metabolic products, further treatment stages may include two main routes: value-added bio-molecules recovery (short-chain carboxylic acids and alcohols), or simultaneous energy recovery in various form and full removal of

the potentially polluting organic load (Moscoviz et al. 2018). The latter includes coupling DF with anaerobic digestion in a two-stage process for subsequent bio-CH_4 production, as widely reported in literature, or also DF combination with bio-electrochemical systems aimed at further H_2 or electricity production (De Gioannis et al. 2013).

The present thesis, which aims to broaden the knowledge of sustainable H_2 production processes pursuing the valorization of organic waste, is in line with the wide-ranging plan promoted through the European Green Deal (European Commission 2019). Indeed, among the key elements of this latter are a) increasing the EU's climate ambition for 2030 and 2050, b) supplying clean, affordable and secure energy, c) a zero pollution ambition for a toxic-free environment. It is evident that such challenging goals demand efforts on several fronts and there is no one single and easy solution. Nevertheless, in this framework, H_2 is intended to offer one of the clean energy options for tackling decarbonization goal, while at the same time is promoted a production method that involves the treatment of organic waste, which in turn addresses a second issue in the perspective of circular economy.

1.2 Aim of the thesis

The present thesis focuses on the valorization of organic waste from dairy industry assessing the feasibility of sustainable energy carriers production. The research study was organized according to several aims which are outlined hereafter:

i. Firstly, the possibility of producing bio-H_2 through DF of cheese whey and wastewater sludge was investigated, with special attention to drive the metabolic pathways of the fermentation process towards H_2 production. This included investigating the effect of a number of process conditions on the H_2 yield and operation stability.

ii. Then, a novel approach was used to explore the feasibility of overcoming the biochemical constraints associated with DF and maximise the energy recovery from this stage. To this aim, an integrated bio-electrochemical process meant to enhance the H_2 production yield of DF was designed.

iii. Lastly, the concept of a multi-stage process layout was assessed in order to provide an adequate level of stabilization of the organic matter as well as full recovery and exploitation of potentially valuable products from the initial substrate. Specifically, the degradation of the residual organic content in the fermentation effluent was evaluated by means of different options using microbial cells.

1.3 Structure of the thesis

In order to achieve the aforementioned aims, the work was arranged in three main experimental phases which are extensively discussed in the chapters of the thesis. A brief presentation of the content is provided below:

Chapter 1 outlines the context and the key elements for the topics addressed during the research and the structure of the thesis.

Chapter 2 focuses on DF of dairy-industry waste for bio-H_2 production. The experimental section shows the effect of different combinations of operating conditions on the H_2 yield in a continuous mode. This chapter also highlights the future perspectives and current shortcomings of DF, with specific focus on the stability of the biological process.

Chapter 3 presents an integrated bio-electrochemical process meant to enhance the H_2 production yield of DF. The experimental set-up is designed as a galvanic cell combined with the fermentation reactor that allows to achieve higher H_2 yield through the electrochemical conversion of the protons released by the organic acids generated during fermentation. Moreover, the electrochemical process simultaneously produces electricity and also has the positive outcome of contrasting acidification thanks to proton conversion.

Chapter 4 addresses the opportunity to further exploit the DF effluent through bio-electrochemical post-processes. The experimental investigation was carried out by means of a single-chambered microbial fuel cell, whereby organic matter is degraded and electricity is generated by the electrogenic biomass, and through a dual-chamber microbial electrolysis cell equipped with both a bioanode and a biocathode, to attain VFAs degradation and CO_2 upgrade to bio-methane.

Chapter 5 summarizes the main results achieved and highlights future perspectives in the field.

2 Biochemical hydrogen production through dark fermentation

2.1 Metabolic pathways

H_2 production from DF is the result of various biochemical reactions brought by the metabolic activity of chemoheterotrophic microorganisms. The primary aim of the process is cell synthesis and energy production to support biomass growth under anaerobic and light-independent conditions, pursued through organic substrate degradation that also gives rise to various metabolic end-products. Thus, the analysis of end products in fermentative processes is a key issue since their distribution pattern reflects the metabolic routes followed by the hydrogenogenic biomass and is correlated with the H_2 yield.

DF starts with the disintegration of macromolecules, contained in the organic matter, into simpler substances such as carbohydrates, lipids and proteins. This process is naturally performed by enzymes secreted by microorganisms, but it can be enhanced by several substrate pre-treatments, that could be of a mechanical, physical, biological or chemical nature. The main products from the first stage undergo the hydrolysis phase, performed by hydrolytic microorganisms, that leads to the formation of monosaccharides from carbohydrates, amino acids from proteins, glycerol and long-chain fatty acids (LCFAs) from lipids. They are then transformed into various organic acids and alcohols by fermentative bacteria, leading to the so-called acidogenic phase, characterized by a decrease in pH. The acidification of the system occurs almost simultaneously with hydrolysis. However, too low pHs can also inhibit the microorganisms themselves, due to the fact that dissociated acids can cross the cell membrane, in turn causing a change in the intracellular pH (Elbeshbishy et al. 2017). For these reasons a fair trade-off of the process is essential; to this regard, the proteins breakdown appears to be useful as it releases ammonia, producing a buffering effect that helps prevent excessive acidification.

The carbohydrates breakdown is the most important transformation that leads to H_2 production. The aminoacids from proteins disintegration are principally fermented in pairs by the so-called Strickland reactions, where one aminoacid serves as the electron acceptor for the oxidation of the second aminoacid, with no H_2 production. Concerning LCFAs, they can be transformed into acetate and H_2 by syntrophic bacteria, but this reaction needs specific environmental conditions such as extremely low H_2 partial pressures (Hallenbeck 2009). Consequently, the choice of a carbohydrate-rich substrate is essential.

The transformation of monomers resulting from the first step is described below using hexose ($C_6H_{12}O_6$) as a model substrate.

The first key reaction is the transformation of hexose into two pyruvate molecules ($CH_3COCOOH$) during glycolysis, that allows energy production in the form of adenosine triphosphate (ATP). During

glycolysis, the electrons and protons transfer is regulated by nicotinamide adenine dinucleotide, a coenzyme that acts as a H_2 acceptor, present in both the reduced (NADH) and the oxidized (NAD^+) form, as follows:

$$C_6H_{12}O_6 + 2NAD^+ \rightarrow 2CH_3COCOO^- + 4H^+ + 2NADH \quad (1)$$

This process produces two ATP molecules.

The pyruvate transformation continues through various possible fermentative pathways, during which protons are the electron surplus acceptors. The NADH from the previous stage can be newly oxidized in NAD^+ form, leading to H_2 production as a result of protons reduction. However, this kind of operation is largely connected to the H_2 partial pressure, with high partial pressures hindering further electrons transfer to protons, and routing to other acceptors such as the acetyl-coenzyme A (acetyl-CoA), that is produced in the following phases.

The aforementioned pyruvate transformation pathways can be driven by two different enzymes, that are the pyruvate/formate lyase (Pfl), typical of the enteric-type fermentation, and the pyruvate/ferredoxin oxidoreductase (Pfor), in clostridial-type fermentations. Both pathways can transform pyruvate into acetyl-CoA.

In the Pfl pathway, the acetyl-CoA generation is accompanied by formate ($HCOO^-$), as follows:

$$CH_3COCOO^- + CoA\text{-}H \rightarrow \text{acetyl-CoA} + HCOO^- \quad (2)$$

In this case, appropriate conditions, such as an acidic medium, can promote the transformation of formate into H_2 and CO_2 through the formate:hydrogen lyase (Fhl) pathway:

$$HCOO^- + H^+ \rightarrow CO_2 + H_2 \quad (3)$$

This conversion has no advantage for the microorganism growth, except for the raise in pH caused by protons transformation. As a result, it occurs spontaneously only when conditions become too acidic for microorganisms.

During this process, the electrons transport is performed by hydrogenases, key enzymes for many microorganisms to dispose of the electron excess by reducing protons (Hallenbeck 2009). The most common are [Ni-Fe] and [Fe-Fe] hydrogenases, which differ for the active site. The [Fe-Fe] hydrogenases are especially active in proton reduction, while [Ni-Fe] hydrogenases catalyse H_2 oxidation, but there could be exceptions depending on the microorganisms.

Nevertheless, acidic conditions can also improve the catalytic action of lactate dehydrogenase (LDH), that leads to the conversion of pyruvate into lactate, inhibiting H_2 generation through subtraction of pyruvate and NADH. According to the homolactic fermentation, 2 mol of pyruvates produced from glycolysis can be reduced to lactate (Asunis et al. 2019):

$$C_6H_{12}O_6 \rightarrow 2CH_3CHOHCOOH \quad (4)$$

Alternatively, in the heterolactic fermentation, one mol of pyruvate can be transformed into lactate and the other one into acetic acid or even ethanol:

$C_6H_{12}O_6 \rightarrow CH_3CHOHCOOH + CO_2 + CH_3COOH$ (5)

$C_6H_{12}O_6 \rightarrow CH_3CHOHCOOH + CO_2 + CH_3CH_2OH$ (6)

However, lactate is detected among the final products only if the DF process is carried out with short contact times. Otherwise, it can be further transformed into other metabolites such as acetic and propionic acids, according to the following reaction (Alexandropoulou et al. 2018):

$3\ CH_3CHOHCOOH \rightarrow CH_3COOH + 2\ CH_3CH_2COOH + CO_2 + H_2O$ (7)

So, lactic acid is generally considered an intermediate metabolic product in DF, but its formation is in any case not associated to H_2 production. Lactic acid bacteria (LAB) are responsible for these pathways and they were found to partially or even completely inhibiting H_2 production (Elbeshbishy et al. 2017). While some attempts to inhibit LAB, such as thermal pre-treatment of the inoculum (Noike et al. 2002) have been effective, limitation of LAB pathway is still one of the major challenges for those systems that involve naturally LAB-rich substrates such as lactose-based residues (Gomes et al. 2015; Castelló et al. 2018; Asunis et al. 2019).

In the Pfor pathway, the pyruvate, together with coenzyme A and ferrodioxin-oxidase (Fd_{ox}), is converted into acetyl-CoA, ferredioxin reductase (Fd_{red}) and CO_2:

$CH_3COCOO^- + CoA + 2\ Fd_{ox} \rightarrow \text{acetyl-CoA} + 2\ Fd_{red} + CO_2$ (8)

Thus, Fd_{red} can produce H_2 through protons reduction, with the catalytic action of [Fe-Fe] hydrogenases and Fd_{ox} generation:

$Fd_{red} + 2H^+ \rightarrow Fd_{ox} + H_2$ (9)

Both Pfor and Pfl routes can be performed, depending on the microorganisms involved and the medium conditions, in order to produce acetyl-CoA. The acetyl-CoA is in the branch point position as well as NADH: from that stage, it can be transformed through many different pathways, but only a few involve H_2 production. The most stoichiometrically effective reaction for H_2 production is the acetic route, that involves the following step:

$\text{Acetyl-CoA} + H_2O \rightarrow CH_3COO^- + H^+ + \text{CoA-H}$ (10)

The complete reaction of the acetic pathway shows that it is stoichiometrically possible to achieve 4 moles of H_2 per mole of hexose consumed:

$C_6H_{12}O_6 + 2H_2O \rightarrow 2CH_3COOH + 2CO_2 + 4H_2$ (11)

This amount is an upper threshold known as the Thauer limit (Thauer et al. 1977b). This limitation results from the fact that, compared to a theoretical amount of 12 H_2 moles available from the complete hexose transformation:

$C_6H_{12}O_6 + 6\ H_2O \rightarrow 12\ H_2 + 6\ CO_2$ (12)

additional organic metabolites are formed; among these, acetic acid allows the highest substrate conversion into H_2.

The more by-products are accumulated in the medium, the harder the theoretical yield is approached. Moreover, competing reaction such as homoacetogenesis can further reduce the net H_2 yield (Saady 2013):

$$4H_2 + 2CO_2 \rightarrow CH_3COOH + 2H_2O \quad (13)$$

This means that acetic acid among the end-products is not necessarily correlated with high H_2 yield as it has been observed in different experimental studies (Castelló et al. 2018; Montiel-Corona et al. 2020). Montecchio et al. (2018) identified the role played by homoacetogenesis in H_2 consumption during cheese whey DF. While the authors modelled theoretical yields of 1.33 – 1.84 mol H_2/mol lactose in absence of homoacetogenesis, the experimentally observed yield was as low as 0.18 mol H_2/mol lactose. This indicates a H_2 consumption rate of approximately 90%. Similar values were stoichiometrically calculated by Dinamarca et al. (2011) under different conditions.

Homoacetogens are recognized to play a critical role in H_2 consumption and its recognition and inhibition are challenging issues (Saady 2013). It is worth noting that the Clostridia sp., which are most widely recognized as H_2-producers, can play the dual behaviour of H_2 producers and H_2 consumers depending on the environmental conditions.

Concerning acetyl-CoA transformation depending on the operating conditions it can also be used in other pathways, including the ethanol route, which involves NADH that has not been oxidized in the previous phase:

$$\text{Acetyl-CoA} + 2NADH + 2H^+ \rightarrow CH_3CH_2OH + CoA\text{-}H + 2NAD^+ \quad (14)$$

As can be seen, the ethanol pathway is H_2 neutral:

$$C_6H_{12}O_6 \rightarrow 2CH_3CH_2OH + 2CO_2 \quad (15)$$

From the acetyl-CoA, another possible route is the butyric fermentation, that leads to 2 moles of H_2 and 1 mole of butyric acid per mole of hexose consumed, using NADH as in the ethanol route.

$$C_6H_{12}O_6 \rightarrow CH_3CH_2CH_2COOH + 2CO_2 + 2H_2 \quad (16)$$

This is the most common pathway along with the acetate route during fermentative H_2 production, so that acetate and butyrate are usually the most abundant metabolites of DF.

Propionic acid is another metabolite that can be formed and involves a H_2-consuming reaction:

$$C_6H_{12}O_6 + 2H_2 \rightarrow 2CH_3CH_2COOH + 2H_2O \quad (17)$$

The most relevant biochemical transformations from pyruvate involved in DF are schematically illustrated in Figure 2-1.

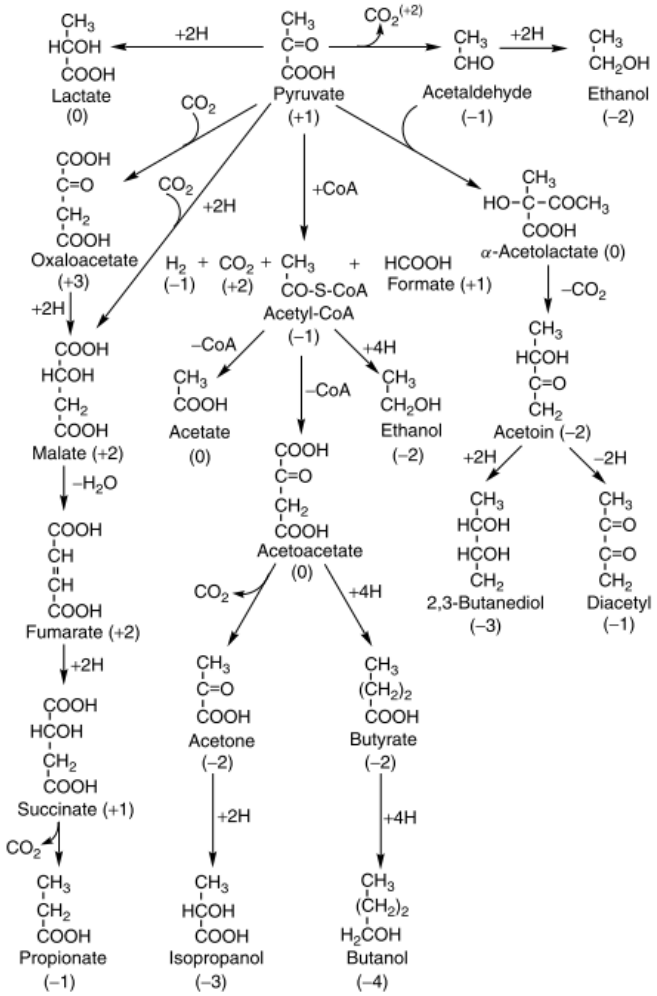

Figure 2-1. Several possible biochemical transformations of pyruvate producing different metabolites in DF (Moat et al. 2003)

Several other reactions can take place concomitantly with the pyruvate transformations depending on various factors such as environmental and operating conditions. The overview provided some of the main routes, but it is not exhaustive of all possible pathways, so other VFAs and solvents may be produced albeit at lower extents. Table 2.1 summarises the most common reactions that may be encountered during the process.

As a consequence of the coexistence of multiple biochemical reactions, H_2 yields typically observed in fermentative studies are generally lower compared to the threshold given by Thauer's theoretical prediction, commonly by a factor of 2 – 3 (Lee and Rittmann 2009). Therefore, one of the main goals of the studies related to the fermentative H_2 production was to investigate the influence of the key factors on H_2 yields and how to promote hydrogenogenic pathways by acting on the operating

conditions. Considerable advancements have been reported, especially by studies under batch mode (Ghimire et al. 2015; Akhlaghi et al. 2017b; Lopez-Hidalgo et al. 2018; Rao and Basak 2021), on correlating process parameters and metabolic routes with the aim of improving the energy recovery from the organic substrate. Nevertheless, some issues remain concerning the evolution of the process under continuous mode, where the existence of competitive metabolic routes may on the one hand limit the yield and the rate of H_2 production, and on the other hand also compromise the long-term process stability. From the perspective of the future industrial implementation of DF, it is essential to ensure the stability of the H_2 production as much as high substrate conversion. The factors contributing to unstable conditions are clearly related to the complex network of biochemical pathways involved in the fermentation process; investigating this aspect is supposed to be one of the fundamental aims of the studies involving a continuous mode for DF, although to date there is no adequate common method.

Table 2.1 Main biochemical reactions involved in DF showing H_2 production, consumption and competitive routes

Hydrogenogenic pathways	
Acetate	$C_6H_{12}O_6 + 2H_2O \rightarrow 2CH_3COOH + 2CO_2 + 4H_2$
Butyrate	$C_6H_{12}O_6 \rightarrow CH_3CH_2CH_2COOH + 2CO_2 + 2H_2$
H_2-neutral pathways	
Alcoholic fermentation	$C_6H_{12}O_6 \rightarrow 2CH_3CH_2OH + 2CO_2$
Homolactic fermentation	$C_6H_{12}O_6 \rightarrow 2CH_3CHOHCOOH$
Heterolactic fermentation	$C_6H_{12}O_6 \rightarrow CH_3CHOHCOOH + CO_2 + CH_3COOH$ $C_6H_{12}O_6 \rightarrow CH_3CHOHCOOH + CO_2 + CH_3CH_2OH$
Lactate utilization	$3\ CH_3CHOHCOOH \rightarrow CH_3COOH + 2\ CH_3CH_2COOH + CO_2 + H_2O$
Hydrogenotrophic pathways	
Propionate	$C_6H_{12}O_6 + 2H_2 \rightarrow 2CH_3CH_2COOH + 2H_2O$
Valerate	$CH_3CH_2COO^- + 2CO_2 + 6H_2 \rightarrow CH_3(CH_2)_3COO^- + 4H_2O$ $3CH_3COO^- + 3H_2 + 2H^+ \rightarrow CH_3(CH_2)_4COO^- + 4H_2O$ $CH_3(CH_2)_2COO^- + CH_3COO^- + 2H_2 + H^+ \rightarrow CH_3(CH_2)_4COO^- + 2H_2O$
Caproate	$CH_3(CH_2)_2COO^- + 2CO_2 + 6H_2 \rightarrow CH_3(CH_2)_4COO^- + 4H_2O$
Homoacetogenesis	$4H_2 + 2CO_2 \rightarrow CH_3COOH + 2H_2O$
Methanogenesis	$4H_2 + CO_2 \rightarrow CH_4 + 2H_2O$

2.2 Operating parameters

A significant challenge for biochemical H_2 production is the process stability performance, as H_2 is an intermediate product of fermentation and is thus often preferably reused in further metabolic routes. In conventional anaerobic digestion, methanogenic bacteria generally drive the fermentation through the utilization of H_2 to produce CH_4. Methanogens include both hydrogenotrophic bacteria, which can transform H_2 and CO_2 in CH_4, and acetoclastic bacteria, which use acetate produced from the previous stage to generate CH_4 and CO_2. Several strategies have been investigated and successfully implemented to suppress the latter biochemical phase, which include inhibition of methanogens by inoculum pre-treatment and/or adjustment of operating conditions unfavourable to methanogenesis. However, the stability of H_2 production may still be counteracted by several other competing and overlapping microbial pathways, as shown in the previous section.

In the literature studies, there is no agreement concerning the stability definition in DF. From the experience gathered with anaerobic digestion treatments, the stability can be conceptually interpreted as a result of the fermentation system operated at the steady state, that means at or near its controlled and fixed-variable design levels, providing relatively constant biogas quality and production rates (Kroeker et al. 1979). Among DF studies, a common approach is to consider the stability achieved when the H_2 production fluctuations are below 10% for a specific time range (Kyazze et al. 2006; Tapia-Venegas et al. 2015; Alexandropoulou et al. 2018; Ramos and Silva 2018). A more accurate and quantitative criterion has been newly adopted by defining the H_2 production stability index (HPSI), which takes into account the ratio between the standard deviation and the average of the production rate over a defined time span (Tenca et al. 2011; Ghimire et al. 2017; Muñoz-Páez et al. 2020). Therefore, different authors assess the process stability based on different definitions. As a result, there are often large inhomogeneities in the time range considered as well as the frequency and number of measured data points used to calculate the HPSI. This obviously impairs the comparability between processes under different conditions. In addition, whatever approach is adopted, the selection of the appropriate design parameters and the consequent achievement of stability are current research challenges that have not yet gained unanimous agreement. The fluctuating behavior usually reported in the literature data is partly due to the numerous features differentiating DF systems and is also evidently related to the different operating conditions adopted, that were observed to produce changes in the microbial community composition (Jia et al. 2019). Indeed, several microbial species are involved in fermentative H_2 production where mixed microbial cultures are used as inocula. To date, a number of studies points out that the use of mixed microbial cultures is nonetheless preferred to pure cultures, since the latter require sterile substrates and restrictive conditions for use, which are not sustainable for full-scale implementation. Mixed cultures, thanks to their biodiversity, are suitable for

the treatment of substrates with very different characteristics such as organic waste, which may also contain indigenous biomass. At the same time, this biodiversity makes them able to tolerate system fluctuations and potential toxic conditions, but is also at the origin of process instability, since the biomass is not static and undergoes transformations during the process.

In the following sections, some of the relevant parameters and their influence on process stability and performance are illustrated.

2.2.1 Reactor configuration

System configuration affects physical issues, such as fluid dynamics and mass transfer among the different phases, but it can also influence the characteristics of the microbial community. A major distinction lies in reactors based on suspended biomass and reactors using granular/attached biomass. Among the continuous systems, the continuous stirred tank reactor (CSTR) is certainly the most widespread due to its simple design and large cost-effectiveness, that allows for easy control of parameters such as pH and hydraulic retention time (HRT). In a CSTR without recycle, the HRT corresponds to the sludge residence time (SRT). On one side, this can be a limiting factor since it is not possible to operate with too low HRT because of the risk of biomass washout. Retention times generally reported in the literature for H_2 production start from 6 hours. Arooj et al. (2008a) adopted HRT = 4 h in continuous H_2 production from starch in a CSTR, even though with low H_2 yield (HY) and H_2 production rate (HPR), and observed biomass washout decreasing HRT to 3 h. Davila-Vazquez et al. (2009) results on cheese whey fermentation showed biomass washout for HRT = 4 h. At the same time, this feature in CSTR can be useful in manipulating biomass behavior specifically by means of adjustment in the HRT value. As will be discussed below, adjusting the HRT is one of the main drivers of the microbial community that results in different effects.

Sequencing batch reactors (SBRs) can be used to decouple HRT from SRT, and have also been tested for fermentative H_2 production (Arooj et al. 2008b; Carrillo-Reyes et al. 2016; Muñoz-Páez et al. 2020). Although substrate type, inoculum source and pre-treatment play a major role in determining the pattern of microbial communities, it was observed that the reactor configuration can also produce some differences. Etchebehere et al. (2016) analyzed the microbial community in 20 different DF reactors and reported that there was less variability among biomass and more active H_2 producers due to the lower solid retention time in a CSTR than in attached biomass reactors.

Reactors based on granular and attached biomass are considered viable options to achieve high HPR due to the feasibility to maintain high biomass concentration during low HRT. Bio-granules formation is a relatively long process during which microorganisms self-aggregate under the influence of electrostatic, van der Waals and repulsive forces resulting from cell-to-cell interactions. The key

properties of density and structural stability of the bio-granules are particularly influenced by extracellular polymeric substances (EPS) (Liu et al. 2004). Thus, the evolution of bio-granules depends both on factors specifically related to the reactor (flow velocity and fluid dynamics), and on microbial composition (ability to generate EPS), which are in turn dependent on specific environmental conditions. Hydrogen-producing microorganisms can be immobilized through different methods, mainly adsorption, entrapment and encapsulation, after which microorganisms are attached to inert and insoluble particles (Banu et al. 2018). These are the most effective methods to prevent biomass washout and in particular entrapment was observed to minimize the microorganisms loss during high flow due to shorter HRT (Banu et al. 2018). Moreover, this protection can be useful in enhancing the resistance of the biomass to toxic or inhibiting agents. At the same time, some limitations can occur such as inefficient supply of nutrients to the microorganisms as well as reduced efficiency of inoculum pre-treatments for methanogens inhibition (Carrillo-Reyes et al. 2012).

The upflow anaerobic sludge blanket (UASB) has also been used for H_2 production. Sivagurunathan et al. (2016) investigated H_2 production from galactose in a UASB reactor, showing a stable H_2 production at HRTs down to 2 h. They obtained a maximum HPR of 56.8 L H_2/L·d with a HY of 2.25 mol H_2/mol galactose-added at HRT of 2 h and showed that further shortening of HRT to 1.5 h led to instability and significantly reduced the HPR and HY. In a previous study by the same authors (Kumar et al. 2016), granular biomass in CSTR was found to produce unstable H_2 performance due to the washout of the granular biomass for HRTs < 3 h. Microbial community analysis indicated a change in the microbial community at high dilution rates.

Some studies mention difficulties in suppressing the methanogenic activity in reactors involving bio-granules and attached biomass, since inhibition by heat and chemical treatments is not completely effective on the microorganisms in the granules core. In this case, suggested options include using more aggressive pretreatments of the granular inoculum and manipulating the control parameters. An effective solution was found in the study from Si et al. (2015) by lowering HRT to enhance the H_2 yield and avoid its further conversion through methanogenesis. The HRT was decreased from 24 h to 4 h in a UASB reactor and the maximum HY was observed at 8 h HRT along with a significant reduction in methanogenesis and completely inhibition of the homoacetogenic pathway. Biomass washout was observed at HRT = 4 h.

FBRs (fixed bed reactors), such as packed bed reactor (PBR), operate with biomass immobilized on carriers to maximize microorganisms retention. Despite the advantages offered by this configuration, some instability issues in H_2 production were reported in literature. In the previously mentioned study by Si et al. (2015) a PBR was also investigated. The inhibition of H_2-consuming pathways was found to be more difficult to obtain for the attached-biomass system. In the UASB reactor, H_2 consumption

due to methanogenesis varied from 12.1 to 3.1% (as a consequence of the HRT variation from 24 h to 4 h), while for the PBR higher percentages of H_2-consumption were observed, where the values ranged from 66.9 to 31.4% (values corresponding to the lowering of HRT from 24 h to 2 h). In the latter case, inhibition of methanogenesis and homoacetogenesis was achieved at HRT = 4 h, whereas washout of the attached biomass was observed at HRT = 2 h. Del Pilar Anzola-Rojas et al. (2015) found that the instability in H_2 production in the FBR was directly related to long cell retention times. Biomass accumulation in the FBR caused the proliferation of H_2-consuming microorganisms, such as homoacetogens, which were observed in the microbial analyses. They also reported that organic loading rate (OLR) control was an effective method to address instability. Similar findings were reported by Ferraz Júnior et al. (2015) in thermophilic H_2 production in PBR from raw sugarcane vinasse, where the authors also observed that thermophilic conditions were more effective than mesophilic regime in limiting non-hydrogenogenic biomass in PBR treating sugarcane vinasse.

Other widely used reactor configurations for continuous DF are expanded granular sludge bed reactors (EGSBs) (Liu et al. 2011; Muñoz-Páez et al. 2020; Ramos et al. 2020) and fluidized bed reactors (Ferreira Rosa et al. 2014a; Ottaviano et al. 2017; Ramos and Silva 2018; Silva et al. 2019). These reactors address some of the limitations related to UASB reactors and FBRs. Relatively high up-flow velocities are applied in order to expand the granular biomass in the EGSB as well as the carriers in the fluidized bed reactor. In these configurations, the up-flow velocity is controlled not only by the inlet flow but also by recirculation of the effluent. Therefore, the primary advantage obtained is more enhanced mass transfer compared to UASB reactors and FBRs. Mikheeva et al. (2021) tested continuous H_2 production from cheese whey both in fixed and fluidized bed reactors equipped with polyurethane carriers. In this study it was noted that the fluidized bed reactor performed better than the FBR. The authors attribute this to the better mass transfer and the absence of stagnant zones within the fluidized bed reactor, which may have contributed to the improved results in terms of H_2 production compared to the conventional FBR. In this case, HRT values were high (2 – 14.5 days); the methanogenic activity was inhibited through control of different pretreatments that had been previously tested in a batch mode. They also employed two different types of inoculum (thermophilic anaerobic sludge from a CSTR and mesophilic anaerobic sludge from an industrial UASB) finding that acid pretreatment failed to inactivate methanogens in mesophilic sludge, while heat pretreament was effective. On the contrary, the acid pretreatment successfully inactivated the methanogens in thermophilic sludge. Thus, the continuous experimental tests were performed through heat-pretreated mesophilic inoculum because of the relative simplicity of the thermal pretreatment involved, moreover the authors considered the mesophilic more stable than the thermophilic regime. On the other hand, during continuous operation, they observed methane formation in both reactor configurations,

suggesting that the pretreatment was not suitable to obtain full inactivation of methanogens and HRT control is recommended.

Table 2.2 Different reactor configurations for continuous H_2 production under mesophilic conditions

Reactor configuration	Substrate	Inoculum	T	pH	HRT	OLR	Maximum HY	Maximum HPR	References
-	-	-	°C	-	h	g COD/Ld	mol H_2/mol hexose	L H_2/Ld	-
CSTR	Starch	HT AS	35	5.3	18, 15, 12, 9, 6, 4	26.7, 32, 40, 53.3, 80, 120	0.92 (at HRT 12; OLR 40)	5.59 (at HRT 6; OLR 80)	(Arooj et al. 2008a)
SBR	Starch	HT AS	35	5.3	18, 15, 12, 9, 6, 4	26.7, 32, 40, 53.3, 80, 120	0.51 (at HRT 12; OLR 40)	4.12 (at HRT 6; OLR 80)	(Arooj et al. 2008b)
CSTR	Cheese whey powder	HT granular AS	37	7.5	10, 6, 4	103.7, 129.6, 155.5, 206.9	1.40 (at HRT 6; OLR 155.5)	25.07 (at HRT 6; OLR 155.5)	(Davila-Vazquez et al. 2009)
SBR	Lactose	HT AS	37	5.5	34, 12, 8, 6, 3, 1	10, 12.6, 15, 20, 40, 120	1.39 (at HRT 3; OLR 40)	6.43 (at HRT 3; OLR 40 gCOD/Ld)	(Carrillo-Reyes et al. 2016)
SBR	Acid agave bagasse hydrolyzates	HT AS	35	5.5	48	8.5, 12, 15.2	-	0.23 (at HRT 48; OLR 8.5)	(Muñoz-Páez et al. 2020)
EGSB	Acid agave bagasse hydrolyzates	HT granular AS	35	4.5	11	19.7	-	0.36 (at HRT 11; OLR 19.7)	
CSTR	Galactose	HT granular AS	35	5.5	6, 3, 2	64, 127.9, 191.9	2.21 (at HRT 6; OLR 64)	25.9 (at HRT 3; OLR 127.9)	(Kumar et al. 2016)
UASB	Galactose	Enriched mixed cultures from UASB	37	5.5 - 6.2	3, 2, 1.5	127.9, 191.9, 255.8	2.25 (at HRT 2; OLR 191.9)	56.8 (at HRT 2; OLR 191.9)	(Sivagurunathan et al. 2016)
UASB	Glucose	HT AS	35	5.7 initial	24, 12, 8, 4	8.5, 17.1, 25.6, 51.2	1.47 (at HRT 8; OLR 25.6)	4.38 (at HRT 8; OLR 25.6)	(Si et al. 2015)
PBR	Glucose	HT AS	35	5.7 initial	24, 12, 8, 4, 2	8.5, 17.1, 25.6, 51.2, 102.3	0.89 (at HRT 2 h; 102.3)	10.66 (at HRT 2; OLR 102.3)	

FBR	Cheese whey	HT AS	37	6.5	348, 218.4, 134.4, 108, 86.4, 48.5	2.07, 3.31, 5.37, 6.61, 8.26, 14.88	1.28 (at HRT 108; OLR 6.61)	1.28 (at HRT 48.5; OLR 14.88)	(Mikheeva et al. 2021)
Fluidized bed reactor	Cheese whey	HT AS	37	6.5	348, 218.4, 134.4, 108, 86.4, 48.5	2.07, 3.31, 5.37, 6.61, 8.26, 14.88	1.53 (at HRT 108; OLR 6.61)	1.9 (at HRT 48.5; OLR 14.88)	

Abbreviations:

AS – anaerobic sludge; CSTR ─ continuous stirred-tank reactor; EGSB ─ expanded granular sludge bed reactor; FBR ─ fixed bed reactor; HPR ─ hydrogen production rate; HRT ─ hydraulic retention time; HT ─ heat-treated; HY ─ hydrogen yield; OLR ─ organic loading rate; PBR ─ packed bed reactor; SBR ─ sequencing batch reactor; T ─ temperature; UASB ─ upflow anaerobic sludge blanket.

2.2.2 Temperature

The operating temperature is one of the factors influencing the fermentation process, since at given temperatures different bacterial species can prevail, thus shifting the metabolic pathways. Temperature also influences the activity of hydrogenases, promoting hydrolysis. Literature studies show a wide range of temperatures suitable for DF. The most common are mesophilic (25 – 40 °C) and thermophilic (40 – 65 °C) conditions, with the mesophilic microbial utilization representing around 70% of the studies (Shao et al. 2020). Generally, the optimal values are identified between 37 – 40 °C and 55 – 60 °C to achieve H_2 production with no inhibition (Elbeshbishy et al. 2017). In a few cases extreme thermophilic (65 – 80 °C) and hyperthermophilic conditions (> 80 °C), have been studied as a means to enhance hydrolysis and improve substrate utilization, especially for refractory feedstock such as lignocellulosic materials. Among other reported advantages of high temperatures, the reduced chance of contamination by other microorganisms and higher pathogenic destruction have been reported (Shao et al. 2020). On the other hand, temperatures above 60 °C may inhibit H_2-producing microorganisms too, because of the inactivation of essential enzymes for cell growth as well as denaturation of some cell proteins (Schut and Adams 2009; Pawar and Van Niel 2013; Shao et al. 2020). In general, increased temperatures favor the process from both the kinetic and thermodynamic viewpoint. However, in certain cases, thermophilic bacteria display lower volumetric HPRs compared to mesophilic bacteria, despite the higher HY. Pakarinen et al. (2008) investigated the effect of temperature on fermentative H_2 production from grass silage in a batch mode. They observed that production increased from 3.2 to 7.2 and 16.0 mL H_2/gVS when temperature was increased from 35 to 55 and 70 °C, respectively. On the other hand, they also found that the maximum HY was achieved after 25 days at 70 °C, 10 days at 55 °C and 3–4 days at 35 °C. Although the high temperature promoted substrate utilization, the authors suggested that efficient substrate pretreatments or two-stage systems are recommended to enhance the overall energy recovery from grass silage since, based on their results, the HY was moderate and the energy value of H_2 is not comparable to CH_4 yield. Gokfiliz-Yildiz and Karapinar (2018) tested different temperatures (35, 39, 45, 55 °C) through an immobilized cell bioreactor operated in a batch mode for H_2 generation from acid-hydrolyzed waste wheat powder. They identified the lowest HY at 35 °C and the highest at 45 °C. Kumar et al. (2015) studied the optimization of fermentative H_2 production from de-oiled Jatropha waste via the response surface methodology and investigated temperatures of 38, 45, 55, 65 and 72 °C. Under such conditions, they found the optimal temperature at 55.1 °C. Azbar et al. (2009) compared H_2 production from cheese whey wastewater under thermophilic (55 °C) and mesophilic (36 °C) conditions, in a batch mode, testing different starting pH values between 4.5 and 7.5. The HY reached the highest values at an initial pH of 4.5 in thermophilic

conditions (8.1 mmol H_2/g COD) and pH 5.5 in mesophilic conditions (9.2 mmol H_2/g COD), but the highest substrate conversion took place at an initial pH of 5.5 for thermophilic conditions and 6.5 for mesophilic conditions. Dessì et al. (2017) compared fresh activated and digested sludge as the inoculum after heat treatment for H_2 production at mesophilic (37 °C), thermophilic (55 °C) and hyperthermophilic (70 °C) conditions using xylose as the substrate in a batch mode. They observed that both under mesophilic and thermophilic conditions the fresh activated sludge yielded more H_2 than the digested sludge, whereas at 70 °C neither inoculum produced H_2 effectively. In particular, the maximum HY (1.85 mol H_2/mol xylose-consumed) was achieved with fresh sludge under thermophilic conditions. With the same inoculum, at 37 °C, H_2 consumption was observed, and this was mainly attributed to homoacetogenesis, since no CH_4 was detected. Therefore, it was concluded that some spore-forming homoacetogenic microorganisms can survive heat treatment, as also observed in other studies (Slobodkin et al. 1997). Furthermore, at low pH (where homoacetogens growth is inhibited) Clostridium acetobutylicum was found to be present at 37 °C, which was considered responsible for H_2 consumption at pH < 4.5. Lastly, the authors suggested that the lower H_2 production at 70 °C was possibly caused by the pH that was below the optimum for the detected hyperthermophiles present in both inocula.

It is evident that the optimal operating temperature in DF may differ depending on the system, as it is also affected by the other variables, particularly the substrate characteristics, the type of microbial species in the inoculum and the applied pretreatments. Moreover, high-temperature operation would imply high energy consumption and cost. Perera et al. (2010) assessed the net energy gain of the processes comparing literature studies on DF of different substrates. They found that the improvement in HY at higher temperatures did not imply higher energy gains.

2.2.3 pH

pH is a crucial parameter in any biological process. The effects on fermentative H_2 production are manifold and there is a wide variety of information available throughout the literature, although the results are often conflicting. It is known that pH influences the metabolic pathways, the activity of hydrogenase enzymes, substrate hydrolysis as well as microbial community structure, thus indirectly affecting the yield and process stability. The optimal value is generally identified within a quite wide range (5 – 7) (Guo et al. 2010). Differences are mainly due to the large variety of substrates, inocula and pretreatments adopted. Furthermore, many studies differ in the way in which pH is controlled. In some cases, just the initial pH is fixed, and the process is carried on without further pH control,

especially when working in a batch mode. On the contrary, mostly in continuous systems, pH is maintained constant throughout the whole process.

From a biochemical perspective, the optimal pH range for H_2 production is associated to the fact that the acetate and butyrate pathways are favored in the pH range 4.5 – 6.0, while neutral or higher pHs promote propionate accumulation and alcoholic fermentation (Guo et al. 2010; Elbeshbishy et al. 2017). Moreover, low pHs (generally < 5) are able to inhibit the methanogenic activity (Kim et al. 2004). Solventogenesis is considered as a detoxification method harnessed by the biomass to avoid inhibitory effects caused by high acid concentrations (De Gioannis et al. 2013). The shift to solventogenesis was found to occur below pH 4.5 (Khanal et al. 2004), even if the specific threshold could change under different conditions. The mechanism responsible for the inhibition caused by high level of acids is mainly associated to the microbial cell equilibrium and the presence of undissociated acids. Indeed, at low pHs, the latter preferentially cross the cell membrane, and dissociate afterwards within the cell due to its higher pH, releasing protons inside the cell. This behavior results in an unbalance in the proton motive force, which causes an increase in energy requirements for cell maintenance, thereby forcing ATP to being used to maintain the intracellular pH near neutrality rather than to produce H_2 (Jones and Woods 1986).

The enzymatic activity is also affected by pH. It was observed that the hydrogenase activity measured in whole cells from acid-producing cultures maintained at pH 5.8 was about 2.2 times higher than that measured in solvent-producing cultures maintained at pH 4.5 (Jones and Woods 1986). Van Ginkel and Logan (2005) examined the inhibitory effect of acetic and butyric acids on continuous fermentative H_2 production by either adding external acids to the feed as well as increasing the inlet glucose concentrations. They found that 19 mM of total self-produced acids was the specific threshold concentration above which solventogenesis was detected with an associated decrease in the HY, although the literature reports values in the range 2 – 50 mM (Wang et al. 2008). An interesting aspect is that they observed higher inhibition caused by self-produced acids (with butyrate to a higher degree than acetate) than externally added acids.

It is evident that, during DF, manipulation of the operational pH it is certainly required in order to drive the metabolic pathways towards H_2 production and avoid competitive and inhibitory biochemical reactions. However, pH adjustment via external chemical agents is one of the significant constraints to large-scale DF implementation due to the related chemical consumption and costs. Concerning this issue, some efforts have been made towards replacing pH adjustment by alternative strategies. Examples can be found in literature studies (De Gioannis et al. 2013) on DF for continuous H_2 production, where pH control is performed: 1) by adjusting operating parameters, such as the organic

load; 2) by using a suitable co-substrate with sufficient alkalinity or, 3) (in the case of a two-stage process) by recirculation of the effluent from the methanogenic phase to the acidogenic reactor.

2.2.4 Hydraulic retention time and organic loading rate

As described in the previous paragraphs, HRT control plays a key role in DF. This is particularly relevant in systems without biomass recirculation, as most of the reactors used in research for fermentative H_2 production. Moreover, the importance of HRT is not only a process management concern but is also related to construction. A common consensus is that higher HRTs are required by more complex substrates, to ensure adequate hydrolysis and efficient organic matter degradation, and in general to avoid washout of the H_2-producing biomass. Therefore, in some cases HRTs above 48 h are documented in the literature on H_2 production from biodegradable municipal waste (De Gioannis et al. 2013) and HRTs of 2 – 3 d are frequently used in DF of lignocellulosic waste, but it can even reach 5 d (Soares et al. 2020). On the other hand, beneficial effects of low HRTs have been extensively reported, primarily involving effects on the proliferation time of hydrogenotrophs. Indeed, low HRTs were found to avoid methanogens formation (Yun and Cho 2016), and can promote H_2 production in those microbial cultures where inoculum pretreatment techniques are not completely successful (Hernández-Mendoza and Buitrón 2014). Methanogens control by low HRTs also offers the prospect of reducing inoculum pretreatments giving clear benefits in terms of operating costs.

The influence of HRT on homoacetogenic microorganisms has also been extensively explored, although often with often conflicting results. One of the reasons may be that the doubling time of homoacetogens can fall into a wide time span, from 1.75 to 29 h (Saady 2013), overlapping with the optimal HRT for H_2 producers. It can be noted that decreasing HRT seems to exert a favorable effect on homoacetogens washout (consequently lowering H_2 consumption) as well as on LAB inhibition. Dinamarca and Bakke (2009) assessed H_2 consumption in various operating conditions, investigating HRTs from 6 to 40 h. They observed that longer HRTs leads to higher H_2 consumption. The authors also suggest that high biomass retention times could result in higher H_2 consumption. Similar findings were proposed by Gavala et al. (2006), who compared UASB and CSTR system, using glucose as the model substrate and heat treated anaerobic sludge. The UASB reactor configuration was found to be more stable than the CSTR with HRTs of 12, 6 and 2 h. Moreover, the HPR in the UASB was significantly higher compared to the CSTR, achieving the maximum at 2h. However, the HY was higher in the CSTR reactor at all HRTs tested. They suggested that H_2-consumption due to homoacetogenesis and LAB, took place preferably in the attached biomass reactor and especially at increasing HRTs. The results achieved by Palomo-Briones et al. (2017) on continuous H_2 production

from lactose and anaerobic sludge in a CSTR showed that at higher HRTs (18 – 24 h) HPR was affected by the presence of LAB. On the contrary, short HRTs (6 – 12 h) are identified to effectively drive the process towards acetate and butyrate fermentation, leading to the maximum HPR at 6 h.

Nevertheless, some studies reported the presence of homoacetogenic activity even at short HRTs. This is the case of Arooj et al. (2008b), where continuous H_2 production from corn starch in an SBR at various HRTs from 4 to 18 h was investigated. Through an homoacetogenesis prediction model they assumed that acetate from this pathway accounted for almost 45% of the total acetate produced at 18, 15, 12, 9 and 4 h HRT and homoacetogenism was found significant at 6 h. Wu et al. (2009) investigated HRTs from 8 to 24 h in an SBR for fermentative H_2 production from liquid swine manure and glucose. They reported H_2 consumption at high HRTs where the H_2 content of biogas was 33.7% at an HRT of 24 h and increased to over 38 – 44% for HRTs of 8–20 h. They obtained the highest HPR at 8 h HRT, while the HY displayed the highest value at 16 h HRT. Therefore, they assumed that the optimal trade-off for the system might be achieved at an HRT of 12 h. Moreover, it was suggested that H_2 consumption was to be ascribed to other species than methanogens which were effectively inhibited by combining heating and acidic pretreatment of inocula and operating at pH 5.0, unlike a previous study (Zhu et al. 2007) where pH 5.3 and HRTs between 16 and 24 h led to CH_4 production, increasingly as the HRT increased.

The performance of continuous fermentative H_2 production has been widely explored in relation to the OLR. Depending on the type of substrate used, the influence of the OLR can be extremely different. From a full-scale implementation point of view, high substrate concentrations are to be preferred since they potentially lead to high volumetric production rates (Kraemer and Bagley 2007). Also considering the minimization of the heating energy required and in order to achieve a net positive energy gain, the use of highly concentrated feeds is attractive (Kyazze et al. 2006). On the other hand, experimental evidence can be somewhat contradictory especially in mixed microbial cultures and complex substrates, moreover, issues related to process inhibition above a certain threshold are frequently reported. The study by Palomo-Briones et al. (2018) on cheese whey powder and anaerobic granular sludge fermentation was carried out at an HRT of 6 h varying the OLR from 15 to 88 g lactose/L·d; they observed that system operation at OLR above 58.8 g lactose/L·d caused a significant decline in the HPY, while at 29.4 g lactose/L·d the maximum HPY of 2.14 mol H_2/mol hexose was obtained with HPR in the range 3.2 – 11.6 L H_2/L·d; in that case, the microbial community analysis showed that low OLRs (14.7 – 44.1 g lactose/L·d) are more effective in Clostridia selection. Unlike the HPY, they observed an increase in the HPR at OLRs ≥ 58.8 g lactose/L·d, that reached 14.5 L H_2/L·d, but was also accompanied by a drop in the HY down to 0.74 mol H_2/mol hexose. They suggested that at high OLRs, H_2 production is limited by mass transfer, thus alternative pathways to dispose of the

electrons generated by substrate consumption are pursued and the microorganisms tend to produce less H_2. In the mentioned study the alternative routes were observed to involve lactate and formate production. Davila-Vazquez et al. (2009) adopted high OLRs (92.4, 115.5, 138.6 and 184.4 g lactose/L·d at a fixed HRT of 6 h) with the aim to enhance the HPR in fermentation of cheese whey powder in a CSTR inoculated with anaerobic granular sludge. The highest HPR of 25.1 L H_2/L·d) with a corresponding HY of 1.4 mol H_2/mol hexose was found at an OLR of 138.6 g lactose/L·d; a sharp decrease in the HPR when rising the OLR from 138.6 to 184.4 g lactose/L·d. The reason was mainly identified in the excessive metabolites accumulation inside the fermentation medium as well as a shift towards the propionic route. The authors suggest that the use of higher OLRs in order to increase the HPR is desirable although this reduces the HY. A pilot-scale DF reactor (400 L) was operated by Lin et al. (2011) with sucrose by progressively increasing the OLR from 60 to 160 g COD/L·d by adjusting the HRT and/or the substrate concentration. The optimal condition (HPR = 1.18 mol H_2/L·d and HY of 1.92 mol H_2/mol hexose) was at an HRT of 6 h and an OLR of 120 g COD/L·d. They also observed an increase in lactate and ethanol production when the reactor was operated at a higher OLR (160 g COD/L·d).

2.3 Experimental part: continuous fermentative hydrogen production from synthetic cheese whey

2.3.1 Research objectives

An experimental campaign of fermentative H_2 production from synthetic cheese whey, with wastewater sludge as inoculum, was performed in automated lab-scale CSTRs operated under continuous mode.

The use of cheese whey was motivated by the fact that is an excellent candidate as substrate for DF due to its organic content (ranging largely between 0.8 and 102 g COD/L (Carvalho et al., 2013)) as well as the large availability considering that, among dairy residues, the cheese whey production is estimated to reach ~9-10 L per kg of cheese manufactured (Carvalho et al., 2013).

The research aim was to investigate the effect of several combinations of the main process parameters, OLR and HRT, on the fermentation outcomes. In total, 17 runs under different combinations of HRTs and OLRs were carried out respectively in the ranges 6 – 20 h and 16 – 129 g TOC/(L·d). More details can be found in the following research paper (section 2.4).

The results were evaluated both in terms of H_2 production yield, H_2 production rate and long-term stability. Particular attention was paid to the definition of a quantitative criterion for the stability assessment (named *dynamic stability index*) in order to address the lack of consistency mentioned in

section 2.2. Moreover, it was investigated the effect that a modification of the adopted method might have on the evaluation of the process.

An assessment of the main metabolic pathways occurred during the fermentative H_2 production was also performed. To this aim, a predictive model was built, including six of the reactions that are considered to be among the major contributors to DF (see section **Errore. L'origine riferimento non è stata trovata.**). The model demonstrated to fit at high degree the experimental data concerning the metabolic products obtained during the tests, allowing for a deeper understanding of the metabolic routes occurred under the different conditions investigated.

2.3.2 Summary of the results

According to the definition adopted, 10 combinations of operating parameters were found to guarantee stable conditions, while the higher production yield and rate were found at HRTs 6 and 8 h respectively combined with OLRs of 97.5 and 65 g TOC/(L·d), with a yield in the range 42–50 L H_2/kg TOC, corresponding to a rate of 2.7–4.8 L H_2/(L·d). The experimental results also suggested that there was an interaction effect of the two investigated operating parameters, so that in general terms lower HRTs required comparatively higher OLRs to sustain the hydrogenogenic process. Moreover, the upper value adopted (129 g TOC/(L·d)) appeared to be excessive for the metabolic requirements of the biomass.

In general, carbohydrates removal was observed to be higher than 96%. Acetate and butyrate were in all cases the predominant metabolic products, albeit their relative proportions varied with the fermentation conditions. The other organic acids with ≥5 C atoms (i.e., valerate, hexanoate and heptanoate) were found to be present at detectable concentrations only in a few tests (with HRT > 12 h).

In the present research, hydrogenogenic acetate and butyrate production were found to be the most important driving pattern towards H_2 generation. The results also clearly outlined that homoacetogenesis was the dominant H_2 consuming pathway under all the conditions tested. Conversely, in the present tests the propionic route proved to be less relevant. Therefore, the research underlined that a proper control against the formation of homoacetogenic biomass is mandatory to enhance the net H_2 yield.

2.4 Research paper: continuous fermentative hydrogen production from cheese whey – new insights into process stability

The present section has been accepted for publication in the
International Journal of Hydrogen Energy
https://www.journals.elsevier.com/international-journal-of-hydrogen-energy

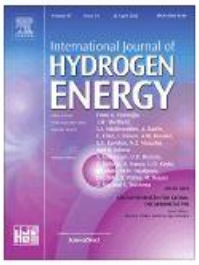

Title: "Continuous fermentative hydrogen production from cheese whey – new insights into process stability"

Authors: A. Polettini[(1)], R. Pomi[(1)], A. Rossi[(1)], T. Zonfa[(1)], G. De Gioannis[(2)], A. Muntoni[(2)]

[(1)] Department of Civil and Environmental Engineering, Sapienza University of Rome (Italy)

[(2)] Department of Civil and Environmental Engineering and Architecture, University of Cagliari (Italy)

Acceptance date: 23rd April 2022

The content of this section is available at the following link:

https://doi.org/10.1016/j.ijhydene.2022.04.229

The content of this section is available at the following link:

https://doi.org/10.1016/j.ijhydene.2022.04.229

The content of this section is available at the following link:

https://doi.org/10.1016/j.ijhydene.2022.04.229

The content of this section is available at the following link:

https://doi.org/10.1016/j.ijhydene.2022.04.229

The content of this section is available at the following link:

https://doi.org/10.1016/j.ijhydene.2022.04.229

The content of this section is available at the following link:

https://doi.org/10.1016/j.ijhydene.2022.04.229

The content of this section is available at the following link:

https://doi.org/10.1016/j.ijhydene.2022.04.229

The content of this section is available at the following link:

https://doi.org/10.1016/j.ijhydene.2022.04.229

The content of this section is available at the following link:

https://doi.org/10.1016/j.ijhydene.2022.04.229

The content of this section is available at the following link:

https://doi.org/10.1016/j.ijhydene.2022.04.229

The content of this section is available at the following link:

https://doi.org/10.1016/j.ijhydene.2022.04.229

The content of this section is available at the following link:

https://doi.org/10.1016/j.ijhydene.2022.04.229

The content of this section is available at the following link:

https://doi.org/10.1016/j.ijhydene.2022.04.229

The content of this section is available at the following link:

https://doi.org/10.1016/j.ijhydene.2022.04.229

The content of this section is available at the following link:

https://doi.org/10.1016/j.ijhydene.2022.04.229

The content of this section is available at the following link:

https://doi.org/10.1016/j.ijhydene.2022.04.229

The content of this section is available at the following link:

https://doi.org/10.1016/j.ijhydene.2022.04.229

The content of this section is available at the following link:

https://doi.org/10.1016/j.ijhydene.2022.04.229

The content of this section is available at the following link:

https://doi.org/10.1016/j.ijhydene.2022.04.229

The content of this section is available at the following link:

https://doi.org/10.1016/j.ijhydene.2022.04.229

The content of this section is available at the following link:

https://doi.org/10.1016/j.ijhydene.2022.04.229

The content of this section is available at the following link:

https://doi.org/10.1016/j.ijhydene.2022.04.229

The content of this section is available at the following link:

https://doi.org/10.1016/j.ijhydene.2022.04.229

The content of this section is available at the following link:

https://doi.org/10.1016/j.ijhydene.2022.04.229

The content of this section is available at the following link:

https://doi.org/10.1016/j.ijhydene.2022.04.229

The content of this section is available at the following link:

https://doi.org/10.1016/j.ijhydene.2022.04.229

The content of this section is available at the following link:

https://doi.org/10.1016/j.ijhydene.2022.04.229

The content of this section is available at the following link:

https://doi.org/10.1016/j.ijhydene.2022.04.229

3 Integrated bio-electrochemical system for simultaneous production of hydrogen and electricity

3.1 Research objectives

The possibility of enhancing biochemical H_2 yield of DF was assessed through an innovative approach consisting of a beneficial combination of the biochemical and electrochemical processes. To this aim, an integrated bio-electrochemical system (IBES) was devised, which attempts to overcome the biological constraint that DF presents in achieving H_2 yields close to the theoretical ones, as discussed in chapter 2.

The operating principle of the IBES is based on the electrochemical conversion of protons released upon dissociation of the acid metabolites of the biological process and is mediated by the electron flow from the galvanic cell, coupling biochemical and electrochemical H_2 production. Accordingly, the galvanic compartment also generates electricity thanks to the oxidation of a metallic element in the anodic chamber. Moreover, the conversion of protons to H_2 may offer the additional benefit of contrasting the acidification of the fermentation medium. The theory underlying the process and the experimental setup are explained in more detail in the following publication (section 3.3).

The first experimental phase was intended to provide a preliminary assessment of the integrated bio-electrochemical process and identify the optimal configuration for further tests. Four different experimental setups (named A, B, C, D) were designed, which differed for the compartment volume, the type of separation between the cathodic and anodic solutions (involving either a salt bridge or an anion exchange membrane, AEM) and the AEM surface to volume ratio (S/V). In the preliminary electrochemical tests, diluted acetic or butyric acid was used as the model substrate to simulate the metabolic products of DF. System A and B were employed for testing different cathode materials and the type of separation between compartments, evaluating the process in terms of pH change and voltage generated. On the basis of the preliminary results, systems C and D were designed with also the possibility of gas collection, measurement and sampling. The main difference between the two latter systems is the S/V ratio, which has been increased in the configuration D.

The aim of the second experimental phase was to investigate the performance of the IBES during the evolution of the fermentative process and compared the results to the conventional DF. In this phase, the optimized configuration D was employed in a batch mode using CW as the substrate, without inoculum, and a stand-alone batch DF reactor fed with CW was employed as a reference.

3.2 Summary of the results

Preliminary tests in system A and B showed the influence of the cathode characteristics on the electrochemical profile of the process and led to the selection of titanium mesh as the cathodic material. Moreover, system A displayed the presence of a high overpotential, likely due to the use of a salt bridge as connection between the chambers instead of the AEM, that was used in systems B, C and D.

The electrical characteristics of the systems equipped with the AEM were then compared performing the power curves. The results show that the S/V ratio played a key role in determining the power efficiency of the electrochemical cell. System D, where the geometrical configuration was arranged to maximize the S/V ratio, indeed proved to have been optimized with regard to the electrical performance. Moreover, the higher S/V ratio resulted in a considerably faster current evolution over time and remarkably higher current intensities, resulting in higher H_2 generation rate.

Throughout the electrochemical tests, the electric current flow was observed to recover upon renewed addition of the proton source (acetic or butyric acid), suggesting the feasibility of preserving cell operation during a continuous acid generation process as in the case of continuous fermentation.

The total volume of H_2 produced and the theoretical H_2 yield (expected on the basis of the overall amount of electric charge generated) was compared to the H_2 yield deriving from a complete dissociation of the acid. The results showed that the released protons from acetic acid appear to be totally reduced to H_2 both in system C and D, albeit at a considerably slower rate in the former case, while the conversion reached 90% in the experiment with butyric acid.

The bio-electrochemical experimental section illustrates the comparison between the results from DF of CW implemented in the IBES (with system D) and in the stand-alone DF reactor. The IBES achieved a H_2 yield in the range 75.5 – 78.8 N LH_2/kg TOC, showing a 3 times improvement over the stand-alone biochemical process which reached 22.4 NL H_2/kg TOC. In order to clearly appreciate the nature of the advantage provided by the integrated system over conventional DF, an attempt was made to separate the different contributions. It was found that the contribution of the electrochemical conversion of protons does not display an exclusively additive role with regard to the biological process, since, in that hypothetical case, the H_2 yield produced by the IBES would be ~ 22% lower. Therefore, it was suggested that the electrochemical process exerted a synergistic effect on the fermentation reactions, enhancing also H_2 generation associated to the biochemical metabolic pathways. Such an effect could in principle be related to a pH buffering effect caused by the conversion of protons to H_2; on the other hand, this was found to be relatively minor. Other effects, presumably related to changes in the redox potential of the fermentation medium, may be presumed to exert influence over the process. The synergistic effect deriving from the integration of the biochemical and electrochemical processes was

also consistent with the higher amounts of metabolic products measured in the IBES compared to the stand-alone DF.

The buffering effect expected from proton consumption in the IBES was mainly visible during the first stages of the process. As acid accumulation proceeds during DF in the cathodic compartment, the buffer effect was found to be not capable of contrasting the progressive acidification. In addition, towards the end of the test an unexpected decline in current intensity was observed despite protons availability. The reason was presumed to be ascribed to a passivation effect of the anode likely caused by the precipitation of $Zn(OH)_2$ onto its surface. Thus, future aspects to investigate will certainly include strategies to prevent the passivation of the anode in order to provide the complete exploitation of available protons as well as a better understanding of the potential electrochemical stimulation effects that there might have been on biomass.

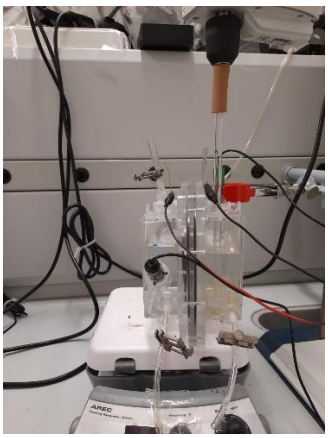

Figure 3-1 The integrated bio-electrochemical system in configuration D

3.3 Research paper: bio-electrochemical production of hydrogen and electricity from organic waste: preliminary assessment

The present section has been published in
Clean Technologies and Environmental Policy
https://doi.org/10.1007/s10098-022-02305-1

Title: "Bio-electrochemical production of hydrogen and electricity from organic waste: preliminary assessment"

Authors: G. De Gioannis[(1)],A. Dell'Era[(2)], A. Muntoni[(1)], M. Pasquali[(2)], A. Polettini[(3)], R. Pomi[(3)], A. Rossi[(3)], T. Zonfa[(3)]

[(1)] Department of Civil and Environmental Engineering and Architecture, University of Cagliari (Italy)

[(2)] Department of Basic and Applied Sciences for Engineering, Sapienza University of Rome (Italy)

[(3)] Department of Civil and Environmental Engineering, Sapienza University of Rome (Italy)

Clean Technologies and Environmental Policy
https://doi.org/10.1007/s10098-022-02305-1

ORIGINAL PAPER

Bio-electrochemical production of hydrogen and electricity from organic waste: preliminary assessment

Giorgia De Gioannis[1] · Alessandro Dell'Era[2] · Aldo Muntoni[1] · Mauro Pasquali[2] · Alessandra Polettini[3] · Raffaella Pomi[3] · Andreina Rossi[3] · Tatiana Zonfa[3]

Received: 29 October 2021 / Accepted: 7 March 2022

Abstract
This study investigated the performance of a novel integrated bio-electrochemical system for synergistic hydrogen production from a process combining a dark fermentation reactor and a galvanic cell. The operating principle of the system is based on the electrochemical conversion of protons released upon dissociation of the acid metabolites of the biological process and is mediated by the electron flow from the galvanic cell, coupling biochemical and electrochemical hydrogen production. Accordingly, the galvanic compartment also generates electricity. Four different experimental setups were designed to provide a preliminary assessment of the integrated bio-electrochemical process and identify the optimal configuration for further tests. Subsequently, dark fermentation of cheese whey was implemented both in a stand-alone biochemical reactor and in the integrated bio-electrochemical process. The integrated system achieved a hydrogen yield in the range 75.5–78.8 N LH_2/kg TOC, showing a 3 times improvement over the biochemical process.

Graphical abstract

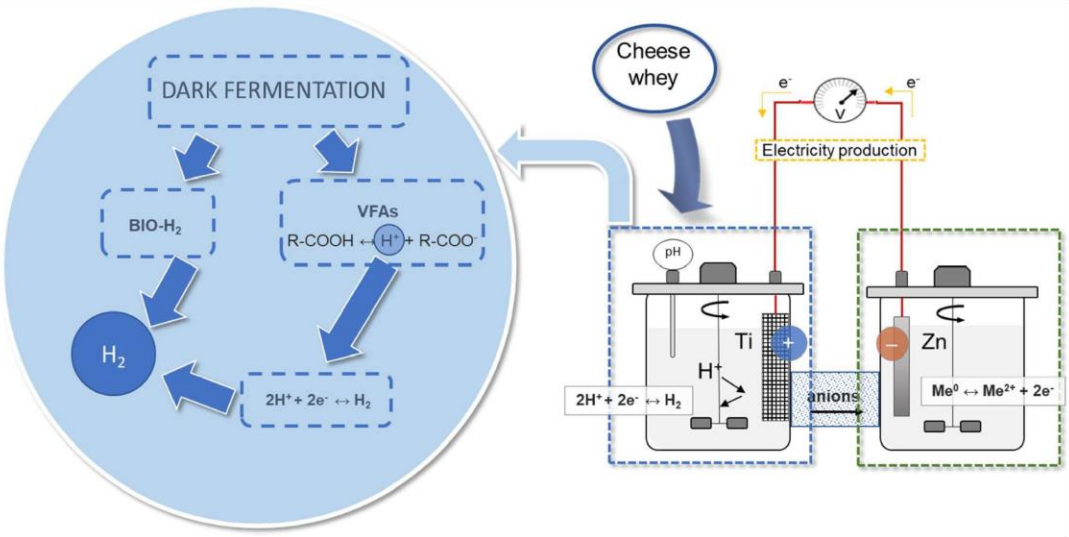

Keywords Cheese whey · Dark fermentation · Hydrogen · Bio-electrochemical process

✉ Tatiana Zonfa
tatiana.zonfa@uniroma1.it

Extended author information available on the last page of the article

Published online: 10 April 2022

Introduction

Hydrogen can be used in both power generation systems and direct combustion processes, providing the great advantage of clean combustion. Moreover, H_2 is considered a very competitive energy carrier compared to other fuels, thanks to its high net heating value per unit volume. Nowadays, its use as a clean energy source is yet uncommon, while its main use is in ammonia production and hydrogenation of coal and petroleum during hydrocracking of traditional fuels (IEA 2019). However, the good environmental profile of H_2 is commonly counteracted by the fact that it is still primarily derived from non-renewable sources, with a high associated energy consumption and relevant related CO_2 emissions, posing an urgent need for sustainable production methods.

Several bioprocesses have been investigated over the last decades to produce H_2 through sustainable methods (Hallenbeck et al. 2012). Among them, dark fermentation (DF) is considered one of the most promising options. The main reason is that DF averts the major drawbacks of other biological processes (including direct or indirect photolysis and photo-fermentation), related to the intermittent production of H_2 and the need of a light source to support the process. Compared to the other biological processes, dark fermentative H_2 production has the additional advantages of higher production rate, flexibility of operation under different temperature and pressure conditions, lower net energy input and, noteworthy, applicability to a range of renewable organic sources including organic residues and carbohydrate-based wastewaters (Ghimire et al. 2015; Silva et al. 2017; Park et al. 2021).

While DF of organic residues has been widely investigated over the past decades, the major current challenges include the poor stability of the biochemical process and the thermodynamic/biochemical limitations to the actual H_2 production yield attainable. To this regard, when acetate is the final metabolic product of fermentation, a production of 4 mol of H_2 per mole of hexose consumed is expected, which is regarded as an upper threshold for the H_2 yield, known as the Thauer limit (Thauer et al.1977). Therefore, of the potential 12 mol of H_2 that may be produced by one mole of glucose, only a third can be obtained biochemically. The actual H_2 yield can even be lower than the mentioned limit if other more reduced metabolic products (e.g., butyrate, ethanol) are formed or additional competing metabolic pathways occur (e.g. propionic fermentation, homoacetogenesis).

Bioelectrochemical processes (BESs) have been proposed for a variety of applications aimed at improving the performance of biological systems. Their operating principle is based on the ability of specific microorganisms defined as electroactive bacteria (EAB) to interact with solid electrodes by forming a biofilm and catalyse the oxidation of organic matter by generating an electric potential. Microbial fuel cells (MFCs) are among the most widely investigated BESs, due to their capability of producing an electric power while simultaneously degrading an organic substrate. Generally, in the anodic chamber, where the EAB are attached to dedicated inert electrodes, the oxidation of organic substances takes place generating CO_2 and protons, which migrate into the cathodic chamber through ion exchange membranes. The cathodic chamber is maintained under aerobic conditions, so that, in the presence of electrons, protons react with oxygen to produce water, resulting in the spontaneous production of electricity, the intensity and flow of which are functions of the construction features of the cell, the substrate characteristics, the inoculum and the operating conditions adopted.

A modified type of MFC, the microbial electrolysis cell (MEC), has been studied since 2005 (Liu et al. 2005b), and its scientific interest has strongly increased in recent years (Santoro et al. 2017). In that case, unlike the MFC, the cathodic chamber is maintained under anaerobic conditions; consequently, protons are reduced to H_2, since there are no other electronegative species to intercept electrons. This process requires the supply of an electric current, since the electric potential naturally generated by microorganisms is not enough to reduce H^+ to H_2. Assuming acetate as a model organic source, the electrode reactions involve oxidation to CO_2 at the anode and H^+ reduction to H_2 at the cathode (see Eqs. 1 and 2). Assuming that the open-circuit potential at the anode in an MFC is generally about $E^0 \sim -300$ mV (Liu et al. 2005b) and the minimum standard redox potential required for the cathodic reaction is $E^0 = -410$ mV (NHE) at pH 7.0, H_2 can theoretically be obtained by applying a higher than 110 mV circuit voltage (typically 410–300 mV to overcome internal electric resistances). However, the voltage required is significantly lower than that used for conventional water electrolysis (1.21 V at neutral pH, which can increase up to 1.8–2.0 V under alkaline conditions due to electrode overpotentials), since the chemical energy extracted from organic substrates oxidized at the anode supplies most of the potential needed.

$$\text{Anode}: \quad CH_3COOH + 2H_2O \rightarrow 2CO_2 + 8e^- + 8H^+ \tag{1}$$

$$\text{Cathode}: \quad 8H^+ + 8e^- \rightarrow 4H_2 \tag{2}$$

Some studies have successfully investigated BESs for the exploitation of volatile fatty acids (VFAs) or DF effluents into electricity or H_2. Liu et al. (2005b) obtained 2.9 mol H_2/mol acetate applying an additional voltage

of 0.250 V in a MEC. Through optimization of materials and reactor configuration, Cheng and Logan (2007) achieved H_2 yields between 2.0 and 3.9 mol H_2/mol acetate at applied voltages of 0.2–0.8 V. Chae et al. (2008) showed that H_2 production gradually increases as the applied voltage is increased from 0.1 to 1 V, reaching 2.1 mol H_2/mol acetate. Liu et al. (2005a) tested power generation from acetate and butyrate in a MFC and observed that acetate is preferred over butyrate as the substrate, producing respectively 506 mW/m^2 and 305 mW/m^2.

The treatment of a real DF effluent was investigated by Chookaew et al. (2014) using both a MEC and a MFC. A power density of 92 mW/m^2 in the MFC was achieved along with 50% COD removal. When treated in the MEC, the same substrate yielded 106 mL H_2/g COD. Rivera et al. (2015) evaluated DF effluent exploitation as a substrate for a MEC. The highest production rate (81 mL H_2/L/day) was obtained at a 550 mV voltage and was accompanied by 85% COD removal. Wang et al. (2011) performed a multistage process using a DF reactor for cellulose degradation, followed by two MFCs that were used as power sources for a subsequent MEC. The MFCs produced a maximum of 0.43 V using the fermentation effluent that induced H_2 production in the MEC at a rate of 0.48 m^3 H_2/m^3/d and with a yield of 33.2 mmol H_2/g COD removed in the MEC. The authors observed a 41% overall improvement in H_2 production for the integrated process compared with fermentation alone.

The integration of fermentation and electrochemical processes in the same unit has been the focus of specific studies on electro-fermentation (Moscoviz et al. 2016; Schievano et al. 2016; Yu et al. 2018). The fundamental concept is based on driving the fermentation process by modifying the redox potential through polarized electrodes placed in the reactor, which can either supply electrons or act as a sink under certain conditions. This could allow overcoming the metabolic limitations through direct electricity supply to the fermentation medium. Potential inocula include both electroactive and fermentative bacteria that can produce value-added organic acids and alcohols (Xue et al. 2018; Paiano et al. 2019), sometimes with concomitant production of H_2 and/or CH_4 (Nelabhotla and Dinamarca 2019; Toledo-Alarcón et al. 2019). Electro-fermentation has been rapidly gaining attention given the successful results. To date, the study of the process is still in a preliminary stage and future developments include the orientation of the metabolic pathways towards specific end products, the selection of efficient redox mediators, the application to complex substrates or suspended biomass configurations.

In the present work, an attempt was made at developing an innovative BES coupling DF with an electrochemical process, with the multiple aims of enhancing H_2 generation, exploiting the fermentation products, produce electricity and provide an internal pH buffering effect. To the best of the authors' knowledge, the concept behind the proposed process is novel and the BES developed has not been documented in other literature studies so far.

Materials and methods

Integrated bio-electrochemical system; principle and setup

The integrated bio-electrochemical system (IBES) proposed here is based (see Fig. 1) on the electrochemical reduction of the protons released from the dissociation of the VFAs produced during the fermentation process, leading to additional H_2 generation. The reduction reaction is mediated by the electrons released by the oxidation of a metallic element in the anodic chamber, which generates an electric current. An inert electrode, which does not take direct part in the reaction but rather plays the role of electron carrier, is placed in the fermentation medium, which is connected through an external electric circuit to the reducing electrode (anode) placed in an electrolytic solution in a dedicated chamber. The ion flow required to maintain the electroneutrality of the two electrolytes is attained through an appropriate connection between the two compartments. The reactions that occur in the cathodic (1) and anodic (2) compartments are shown below, along with the corresponding reduction potentials (E^0) in accordance with the IUPAC standard potentials convention (298 K, 1 bar, 1 M), assuming metallic Zn as the anode:

$$2H^+ + 2e^- \leftrightarrow H_2 \quad E^0(2H^+/H_2) = 0.000\text{V} \tag{1}$$

$$Zn \leftrightarrow Zn^{2+} + 2e^- \quad E^0(Zn_2^+/Zn) = -0.762\text{V} \tag{2}$$

The overall cell electromotive force under standard conditions (ΔE^0), defined as the potential difference between the cathode and the anode, for this system is as follows:

$$\Delta E^0 = E^0(2H^+/H_2) - E^0(Zn^{2+}/Zn) = 0.762\text{V} \tag{3}$$

The fact that the Gibbs free energy $\Delta G^0 = -nF\Delta E^0$ (with n = number of electrons exchanged in the reaction and F = Faraday's constant = 9.64853×10^4 C mol^{-1}) is negative (− 147 kJ) ensures that the redox reaction can take place spontaneously, as the reduction potential of the anode is adequately low.

Consequently, the IBES provides, compared to the biochemical process, an additional electrochemical generation of H_2, exploiting the protons from the metabolic products. Moreover, since the system is designed as a galvanic cell, the process is energetically self-sufficient. Finally, the

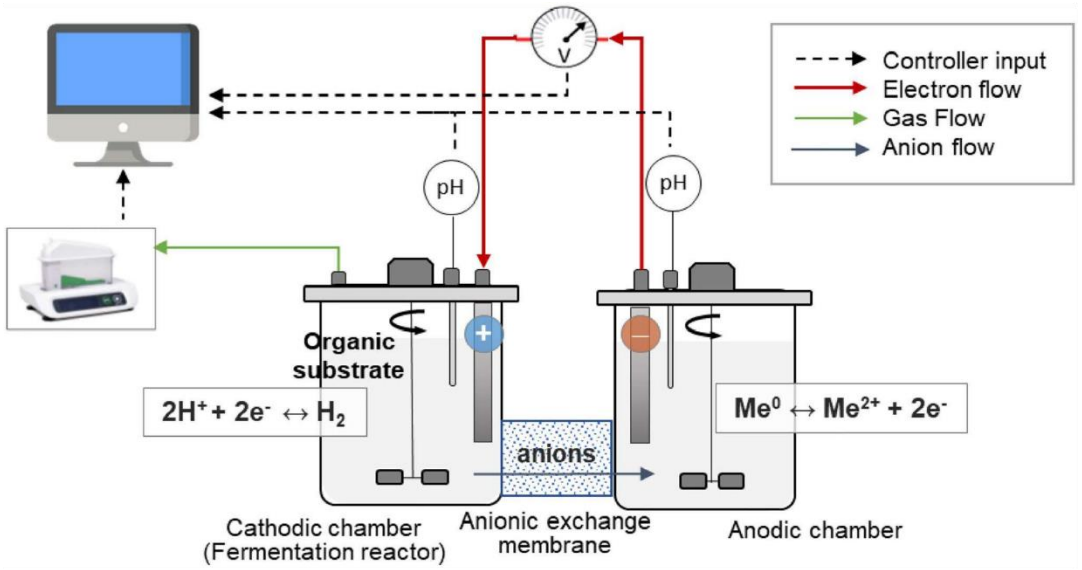

Fig. 1 Layout of the IBES

conversion of protons to H_2 may offer the additional benefit of contrasting the acidification of the fermentation medium, which would otherwise require the external addition of buffering agents to maintain adequate pH levels for the microbial system.

In the present work, four different experimental setups (named A, B, C, D) were designed in order to identify the most suitable materials and configuration for the IBES (Fig. 2). The anode and cathode were mutually connected through an external electric circuit equipped with a system for continuous measurement and recording of electric current and cell potential produced under an electric load (resistor). As detailed in Table 1, the four systems differed for the compartment volume, the type of separation between the cathodic and anodic solutions (involving either a salt bridge or an anion exchange membrane, AEM) and (when applicable) the AEM surface-to-volume ratio (S/V). Both the salt bridge and the AEM served the purpose of allowing the ionic flow between the two compartments required to ensure the electroneutrality of the catholyte and anolyte. The AEM was specifically selected because of its recognized acid/proton blocking capability (Xu 2005; Guo et al. 2017).

While in systems A and B the gas produced was allowed to evolve outside the system and therefore was not directly measured, systems C and D were gas-tight and also included collection, measurement and sampling of the gas generated. Dedicated H_2 leakage tests were conducted for systems C and D in order to quantify potential gas losses during the tests due to the high fugacity of H_2. The measured loss was found to lie in the range 0.12–0.16 mL/h for system C and 0.64–0.95 mL/h for system D (likely due to some minor gas leakage through the AEM), which was accounted for to quantify the amount of gas produced.

In systems A and B, the following cathode materials were selected for the tests on the basis of electrical conductivity, recognized inert redox behaviour and absence of potential toxic effects on microorganisms: graphite sheet (15 cm^2), Pt sheet (2 cm^2), Ti grid (2 mm wire with mesh of 0.16 mm^2) and Ni mesh (60 mesh with 0.18 mm wire).

In all systems, the anolyte was 0.5 M Zn sulphate, while a metallic Zn plate was used as the anode.

Materials and electrochemical/bio-electrochemical tests

CW was collected at an Italian dairy industry producing mozzarella cheese from a mixture of cow and buffalo milk. The characteristics of CW are reported in Table 2. The samples were stored at − 18 °C and thawed at room temperature for approximately 24 h before use. The pH of CW was adjusted to 7.5 at the beginning of the DF experiments using 2 M NaOH, while no further pH control was performed during the tests. The indigenous microorganisms in CW were the only active biomass source in the system, as it was previously demonstrated (Asunis et al. 2019) that it

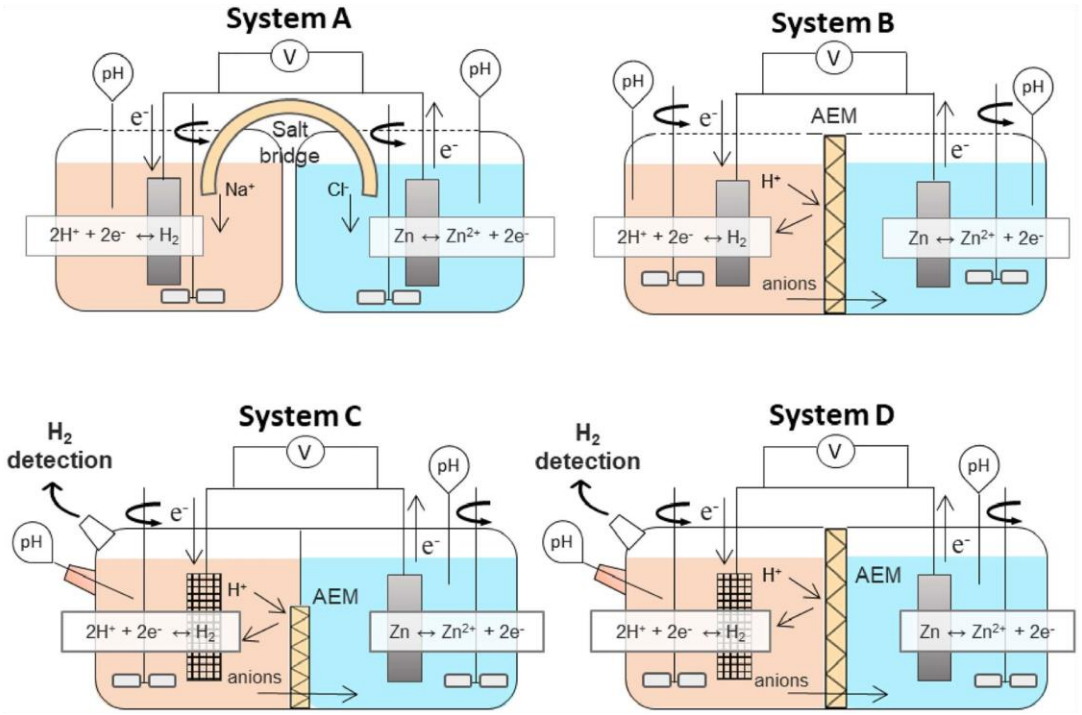

Fig. 2 Schematics of the IBES experimental setups

Table 1 Summary of the key features of system configuration (synthetic model solution used)

	System A	System B	System C	System D
Compartment separation	Sodium chloride salt bridge	24 cm^2 AEM	11.3 cm^2 AEM	67.5 cm^2 AEM
AEM surface to volume ratio (S/V)	–	120 cm^2/L	23 cm^2/L	135 cm^2/L
Catholyte volume	0.2 L	0.2 L	0.5 L	0.5 L
Catholyte	HAc	HAc	HAc	HAc HBu
Anolyte volume	0.2 L	0.4 L	0.5 L	0.5 L
Anolyte	Zn sulphate	Zn sulphate	Zn sulphate	Zn sulphate
Cathode material	15 cm^2 Graphite sheet 2 cm^2 Pt sheet 15 cm^2 Ni mesh 15 cm^2 Ti grid	15 cm^2 Ni mesh 15 cm^2 Ti grid	10 cm^2 Ti grid	66 cm^2 Ti grid
Anode material	15 cm^2 Zn plate	15 cm^2 Zn plate	43 cm^2 Zn plate	53 cm^2 Zn plate

can successfully produce H_2 through dark fermentation with no need of an external inoculum. The DF tests were operated under mesophilic conditions (38 ± 1 °C).

In the preliminary electrochemical tests, conducted in systems A, B and C, either diluted acetic (HAc) or butyric acid (HBu) was used as the model substrate to simulate the metabolic products of DF. The IBES was then tested in a batch mode using the optimized configuration D with cheese whey (CW) as the substrate; in this case, a stand-alone batch DF reactor fed with CW was employed as a reference. All tests were performed in duplicate. A summary of the experiments is reported in Table 3.

Table 2 Characterization parameters of CW used for IBES in system D and stand-alone DF

Parameter	Unit of measure	
Total solids	% wet weight	7.4 ± 0.3
Volatile solids	% wet weight	6.4 ± 0.3
Carbohydrates	g glucose-C/L	38.5 ± 3.8
Total Organic Carbon	g C/L	39.3 ± 3.7
pH	–	3.6 ± 1
Acetic acid	mg HAc/L	364 ± 71
Butyric acid	mg HBu/L	< DL
Ethanol	mg EtOH/L	3360 ± 82

Table 3 Experimental design

Run no	Run code	System configuration	Cathode type	Catholyte solution
1	A-G-HAc	A	Graphite sheet	HAc
2	A-Pt-HAc	A	Pt sheet	HAc
3	A-Ti-HAc	A	Ti grid	HAc
4	A-Ni-HAc	A	Ni mesh	HAc
5	B-Ti-HAc	B	Ti grid	HAc
6	B-Ni-HAc	B	Ni mesh	HAc
7	C-Ti-HAc	C	Ti grid	HAc
8	D-Ti-HAc	D	Ti grid	HAc
9	D-Ti-HBu	D	Ti grid	HBu
10	D-Ti-CW	D	Ti grid	CW

DL detection limit

Analytical methods

In systems C and D, a volumetric gas counter with a 2 mL capacity was used for gas volume measurement, while a gas bag was employed for gas storage. In all cases the measured volume was converted under standard pressure and temperature conditions ($T = 273.15$ K, $P = 10^5$ Pa).

The biogas was periodically sampled from the gas bag with a 25-mL gastight syringe and analysed through a gas chromatograph (Model 3600 CX, VARIAN) equipped with a thermal conductivity detector and 2-m stainless-steel packed column (ShinCarbon ST) with an inner diameter of 1 mm. The operating temperatures of the injector and detector were 100 and 130 °C, respectively, with He as the carrier gas. The oven temperature was initially set at 80 °C and subsequently increased to 100 °C at 2 °C/min.

The VFAs (acetate, butyrate, propionate, valerate, caproate, heptanoate) and ethanol concentrations were determined in 0.2-µm filtered and HCl acidified (pH = 2) liquid effluent (1 µl) with a gas chromatograph equipped with a flame ionization detector (FID) and a 30-m capillary column (TRB-WAX) with an inner diameter of 0.53 mm. The temperatures of the detector and the injector were 270 and 250 °C, respectively. The oven temperature was initially set at 60 °C, held for 3 min at this value, subsequently increased to 180 °C at a rate of 10 °C/min and finally increased to 220 °C at a rate of 30 °C/min and held for 2 min.

Sulphates, total and volatile solids were measured according to the Standard Methods for the Examination of Water and Wastewater (APHA AWWA and WEF 2005).

Total organic carbon (TOC) was measured using a Shimadzu TOC analyser (TOC-VCHS and SSM-5000 module, Shimadzu, Japan).

Carbohydrates were analysed through the colorimetric phenol–sulfuric acid method using glucose as the standard (Dubois et al. 1956).

The electrochemical process was monitored through cell voltage (ΔV) and electric current intensity (I) measurements. The acquisition system NI cDAQ-9174 was used for this purpose, and a potentiometer with a resistive load ranging from 500 Ω to 1.3 Ω was used to obtain the power curves for each system configuration. The cell voltage was measured continuously for a few minutes following each resistance variation, in order to avoid significant changes in the electrolyte solutions, at the same time ensuring the achievement of equilibrium conditions. The measurement system was combined with LabVIEW as the data acquisition software.

The total amount of electric charge, Q, generated during the electrochemical process was calculated as the integral of the measured electric current, and the related theoretical amount of H_2 produced was also derived.

Results and discussion

Electrochemical tests

A summary of the preliminary tests using systems A and B is provided in Table 4. The cathode characteristics were found to affect the electrochemical profile of the process, with the highest (2.2 mA) and lowest (0.77 mA) current intensities in system A being obtained with the Ti grid (run A-Ti-HAc) and graphite sheet (run A-G-HAc) electrodes, respectively. However, system A also showed the presence of a high overpotential, likely due to the fact that salt bridges are known to generate high internal resistances (Logan et al. 2006). When the salt bridge was replaced by the AEM (system B) using a Ti cathode, the cell voltage and the current intensity increased from 0.20 (run A-Ti-HAc) to 0.43 V (run B-Ti-HAc) and from 2.2 to 4.7 mA (average of the values measured during the first hour of the tests at 90 Ω as the external load), respectively.

Figure 3 depicts the power curves derived to describe the electrical characteristics of the optimized systems (runs B-Ti-HAc, C-Ti-HAc and D-Ti-HAc). The maximum power,

Table 4 Main results for systems A and B (average values during the first hour with a fixed external resistive load of 90 Ω)

Parameters	Unit of measure	Run					
		A-G-HAc	A-Pt-HAc	A-Ti-HAc	A-Ni-HAc	B-Ti-HAc	B-Ni-HAc
Cell voltage, ΔV	mV	70	80	200	100	430	350
Current intensity, I	mA	0.77	0.93	2.20	1.07	4.68	3.70

P, observed was 5.1 mW for D-Ti-HAc (at $I=9$ mA and $R=62$ Ω), 2.5 mW for B-Ti-HAc (at $I=8.5$ mA and $R=33.5$ Ω) and 0.6 mW for C-Ti-HAc (at $I=2.1$ mA and $R=110$ Ω). Since the experimental conditions of the three systems were the same apart from the S/V ratio of the AEM, the results show that this parameter played a key role in determining the power efficiency of the electrochemical cell. Run D-Ti-HAc, where the geometrical configuration was arranged to maximize the S/V ratio, indeed showed to have been improved with regard to the electrical performance.

The process evolution over time displayed a similar profile in all the investigated systems, although with different absolute values and rates of variation of the investigated parameters. In particular, as shown in Fig. 4 for C-Ti-HAc and D-Ti-HAc, the catholyte pH displayed an increasing trend as a result of proton conversion into H_2, with the typical shape of an acid–base titration curve that reached a final plateau as soon as the acid dissociation was complete. The current intensity mirrored the pH evolution, decreasing to almost zero as pH levelled off at the plateau. When comparing C-Ti-HAc and D-Ti-HAc, it is clear that the lower S/V ratio of the former resulted in a considerably slower current evolution and remarkably lower current intensities.

It is also worth mentioning that in all systems the electric current flow was observed to recover upon renewed addition of the proton source (data not shown), as would happen during continuous fermentation.

The anolyte pH was found to slightly increase within the first 5−6 h of the test from an initial value of ~ 4.3 to a value of ~ 5.7, likely due to the migration of hydroxide ions from the catholyte through the AEM. The final constant pH value achieved is in good agreement with that expected in a solution in equilibrium with a $Zn(OH)_2$ precipitate ($K_s = 2 \times 10^{-17} - 4 \times 10^{-17}$). Acetate and butyrate were also clearly observed to migrate (most likely in the dissociated form, given the nature of the AEM used) to the anodic chamber over time, in compliance with electroneutrality constraints, and virtually fully transferred to this compartment at the end of the test (see the values of the percent partitioning of acetate at the anode shown in Fig. 4c) for D-Ti-HAc and Fig. 5b) for D-Ti-HBu).

For D-Ti-HBu, the observed trends (see Fig. 5) of the electric current, pH of the cathodic and anodic solutions as well as the acid dissociation behaviour and migration of anionic species through the AEM were identical to run D-Ti-HAc. This prospectively indicates that the electrochemical process investigated can be applied to a fermentation system where an array of organic acids is generated.

A summary of the assessment of the process performance of C-Ti-HAc, D-Ti-HAc and C-Ti-HBu is provided in Table 5. The reported data provide a comparison between the observed cumulative H_2 production and the total theoretical H_2 yield expected based on either the overall amount of electric charge generated or the overall amount of protons derived from acid dissociation.

Taking into account the potential gas losses (see Sect. 2.1), the data in Table 5 show that the total volume of H_2 produced is consistent with the total theoretical volume of H_2 calculated from the mobilized electrons. The released protons, assuming complete dissociation of the acid, appear to have been totally reduced to H_2 for C-Ti-HAc ($V_{H2,th}/V_{H2,max}$=99%), albeit at a slower production rate, and for D-Ti-HAc ($V_{H2,th}/V_{H2,max}$=102%) , while for D-Ti-HBu the conversion was slightly lower (90%).

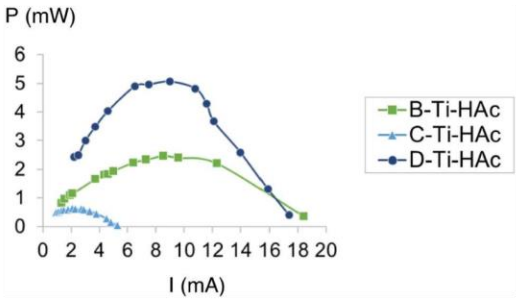

Fig. 3 Power curves for B-Ti-HAc, C-Ti-HAc and D-Ti-HAc showing the influence of the S/V ratio

Bio-electrochemical tests

Figure 6a shows the evolution of the cumulative H_2 production for the stand-alone DF reactor and the IBES, while the profiles of pH of the biological compartment and current intensity are reported in Fig. 6b. The experimental

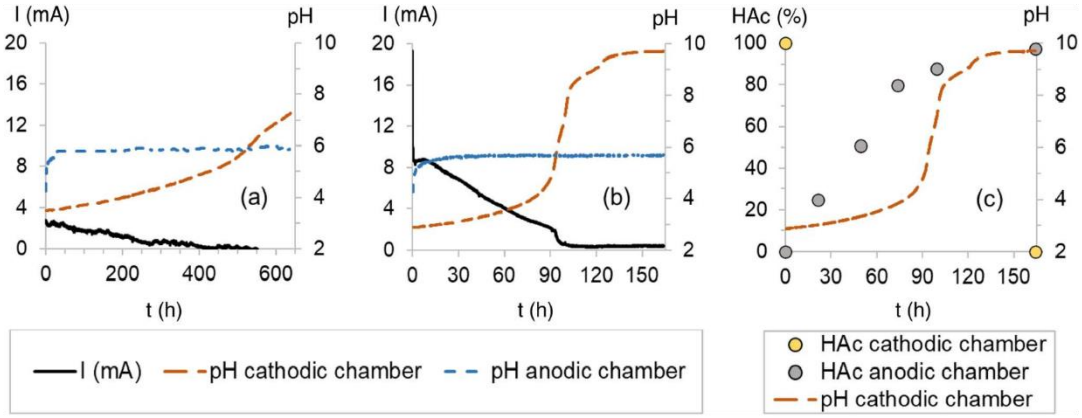

Fig. 4 Time evolution of catholyte and anolyte pH and current intensity for **a** C-Ti-HAc and **b** D-Ti-HAc; **c** catholyte pH and acetate partitioning among the two chambers for D-Ti-HAc

data indicate a final yield of, respectively 22.4 NL H_2/kg TOC and 68.7 NL H_2/kg TOC (the latter corresponding to 75.5–78.8 NL H_2/kg TOC considering the H_2 leakage through the AEM), and a total duration of H_2 production of 32 and 44 h. As observed in our previous experiments on dark fermentation of various organic substrates, the biological process stopped as soon as the degradation of carbohydrates, which are the preferred substrate for H_2 generation, was complete. The generation of organic acids as the metabolic products of fermentation was therefore virtually complete after 32 h (DF alone) and 44 h (IBES) from the start of the experiments, concomitantly with the pH plateau at 5–5.5.

From the data in Fig. 6a, it is therefore evident that the IBES attained a significant improvement in H_2 production (by 3 times) over stand-alone DF. In order to assess the advantages of the IBES over the conventional DF process, an attempt was made at separating the contributions of the biological and the electrochemical processes to the total H_2 yield. The green dashed curve in Fig. 6a represents the theoretical volume of H_2 that would be expected from the electrochemical reactions on the basis of the electric charge mobilized. If the biological and the electrochemical processes were additive, such a volume would add up to the volume generated by the biochemical process alone. According to such hypotheses, a total yield of 63.4 NL H_2/

Table 5 Summary of preliminary results for systems C and D

	Unit of measure	C-Ti-HAc	D-Ti-HAc	D-Ti-HBu
Initial amount of acid at the cathode	mol	0.0197	0.0196	0.0134
Time to the pH/current plateau	h	645	100	74
Mobilized electrons [(a)]	mol e^-	0.0196	0.0174	0.0120
Total theoretical volume of electrochemical H_2 produced, $V_{H2,th}$ [(b)]	NL H_2	0.220	0.223	0.135
Total measured volume of H_2, $V_{H2,meas}$	NL H_2	0.127	0.092	0.053
Expected H_2 losses, $V_{H2,loss}$	NL H_2	0.077–0.103	0.105–0.156	0.064–0.095
Total volume of H_2 produced, $V_{H2,pr}$ [(c)]	NL H_2	0.205–0.230	0.197–0.249	0.117–0.149
Maximum theoretical volume of electrochemical H_2, $V_{H2,max}$ [(d)]	NL H_2	0.221	0.219	0.150
$V_{H2,pr}/V_{H2,th}$	%	93–105	88–112	87–111
$V_{H2,pr}/V_{H2,max}$	%	93–104	90–113	78–99
$V_{H2,th}/V_{H2,max}$	%	99	102	90

[(a)] Calculated from the measured total amount of electric charge

[(b)] Calculated from mobilized electrons

[(c)] $V_{H2,meas} + V_{H2,loss}$

[(d)] Calculated from the released protons assuming complete dissociation of the acid

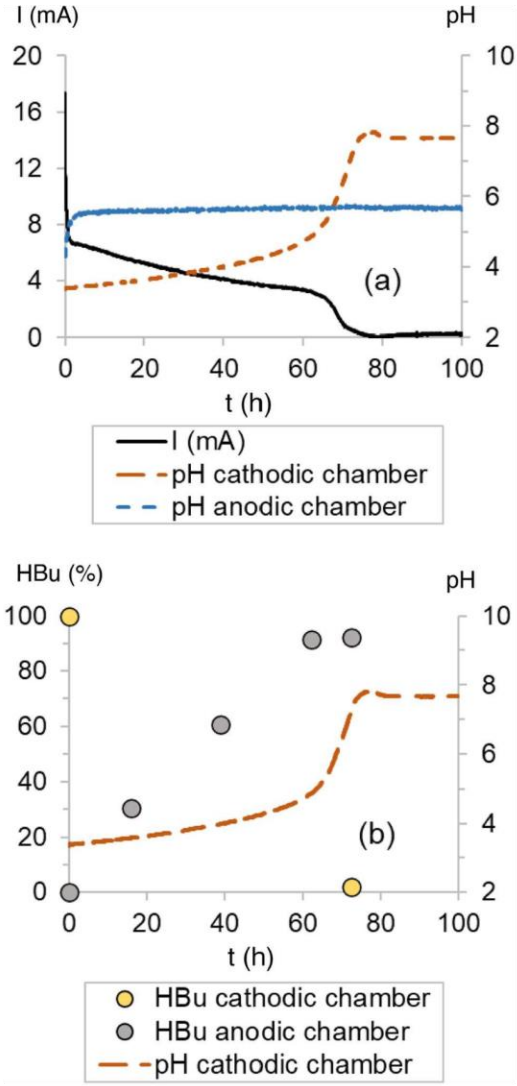

Fig. 5 Time evolution of catholyte and anolyte pH and current intensity for D-Ti-HBu (**a**); (**b**) catholyte pH and butyrate partitioning among the two chambers for D-Ti-HBu

kg TOC would be expected, that is 19–24% lower than the actual value obtained for the IBES. It is thus tempting to hypothesize that, further to the additional volume of H_2 produced by chemical reduction of protons, the electrochemical process exerted a synergistic effect on the fermentation reactions, enhancing H_2 generation associated to the biochemical metabolic pathways. While such a result could in principle be related to a pH buffering effect caused by the conversion of protons to H_2, this was in fact found to be relatively minor (see the pH profiles in Fig. 6b). Other mechanisms are thus claimed to have played a role during the process, including changes in the redox potential of the fermentation medium caused by the electricity flow. Concerning this, several studies on BESs, and more specifically on electro-fermentation, have demonstrated that fermentation pathways can be electrically enhanced if improved electron transport routes and energy conservation mechanisms in biomass take place. It is recognized that changes in the extracellular redox potential (ORP) may affect the intracellular redox homeostasis and metabolism of microbial cells. As a consequence, changes in fermentation metabolites (Liu et al. 2013) can occur. This concept can be advantageously exploited in anaerobic processes, because the standard ORP for the redox pair O_2/H_2O ($E^0 = +820$ mV) is the highest among the other pairs associated with intracellular metabolism (i.e., H^+/H $E^0 = -420$ mV; $NAD^+/NADH$ $E^0 = -320$ mV; $NADP^+/NADPH = -315$ mV). Therefore, with no O_2 in the system, electrons can be more easily accepted by intermediate metabolites. Possible ways through which electron supply may affect the fermentation process include NADH reduction and may also promote the production of additional ATP (Schievano et al. 2016). Toledo-Alarcón et al. (2019) showed that even a small amount of electrons can have a significant effect on the metabolic pathways, affecting H_2 production (with an improvement in H_2 yield by 1.8–2.5 times compared to conventional DF), almost irrespective of the applied potential. The authors suggested that small changes in ORP can affect the regulation of hydrogenase involved in H_2 production, due to its high sensitivity to ORP variations.

The enhancement of the fermentation reactions when coupling the biological process with an electrochemical system was also reported by Paiano et al. (2019), who observed an increased amount of metabolic products when exogenous redox mediators were used.

Table 6 shows the concentration of the metabolic products in the cathodic and anodic compartments of the IBES and the stand-alone DF reactor. These mainly included HAc, HBu and EtOH, although EtOH concentration did not differ considerably from the initial value. It can be observed that the concentrations of HBu and the total metabolic products were higher in the IBES than in the stand-alone DF. The higher amounts of metabolic products measured in the IBES are consistent with its larger observed H_2 generation. While clarifying the electro-stimulation of the fermentation pathways was beyond the scope of the present study, the results yet show that the integration of the biochemical and electrochemical processes produced larger than additive effects on H_2 generation.

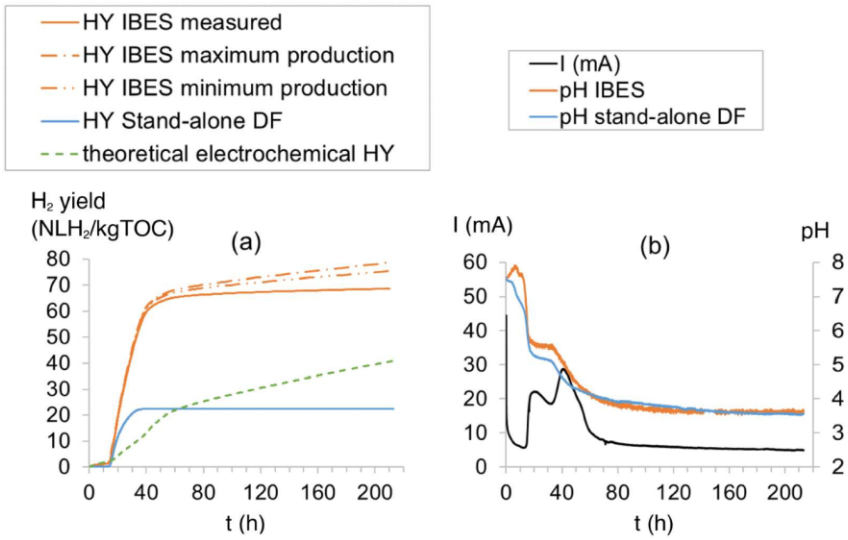

Fig. 6 **a** Comparison between the stand-alone DF and IBES in terms of H_2 yield and theoretical electrochemical H_2 yield calculated from charge (green dashed line); **b** pH evolution over time in both systems and electricity production in the IBES.

The data in Table 6 also show that unlike the tests with the model acid solutions, the extent of migration of the organic metabolites towards the anode was only minor. This was due to the larger complexity of the chemical composition of CW compared to the model solutions used in the previous tests, with other anionic species (presumably with smaller ionic radiuses) being likely responsible for ensuring the electroneutrality balance.

As mentioned above, the buffering effect associated with proton consumption in the IBES was mainly visible during the first stages of the process (see pH profiles in Fig. 6b), but was not capable of contrasting the progressive acidification of the cathode solution caused by the accumulation of volatile fatty acids produced during fermentation. Towards the end of the test, pH approached a value of ~ 3.5 for both tests, which was mirrored by a drop in the current flow. The unexpected decline in current intensity after ~ 45 h was probably related to a passivation effect of the anode likely caused by the precipitation of $Zn(OH)_2$ onto its surface (also evident upon visual inspection).

Conclusions

The purpose of this preliminary work was exploring the feasibility and performance of a novel IBES which is aimed at improving the H_2 yield during DF through protons reduction into H_2 mediated by a self-generated electron flow, with no need for external energy supply (as otherwise required by other conventional systems such as MECs) and taking advantage from the coupling of the biochemical and electrochemical components of the system.

Preliminary tests were carried out through different configurations using a model solution to assess the electrochemical process. They highlighted the importance of optimizing the reactor design in order to reduce internal resistances and provide an appropriate H_2 generation rate along with electricity production. According to the electric current production that was measured and the flow of dissociated organic acid through the AEM, it was concluded that the model

Table 6 Metabolic products at the end of IBES (run D-Ti-CW) and stand-alone DF

		IBES catholyte	IBES anolyte	Stand-alone DF
Acetic acid	mg HAc/L	1188 ± 333	454 ± 26	1247 ± 235
Butyric acid	mg HBu/L	3493 ± 293	746 ± 266	1756 ± 110
Ethanol	mg EtOH/L	2428 ± 192	< DL	3505 ± 12
Total metabolites (as C)	mg $C_{VFAs+EtOH}$/L	3643 ± 73	588 ± 155	3281 ± 160

DL Detection limit

solution was almost completely (90–100%) dissociated and the protons were virtually fully converted into H_2.

The experimental tests on the bio-electrochemical integration were performed through DF of CW, without inoculum, in the optimized reactor configuration. Under this condition, IBES achieved a H_2 yield of 75.5–78.8 NL H_2/kg TOC that, compared to the stand-alone DF (22.4 NL H_2/kg TOC) shows a 3-times improvement. When converted into an energy yield assuming a heating value of ~ 140 kJ/g H_2, these figures correspond to an energetic equivalent of ~ 940–1000 kJ/kg TOC; conversely, the energy associated with the amount of electrons mobilized during the process represents a minor additional contribution (~ 6.6 kJ/kg TOC) to the total energy output of the process. The scale at which the process was tested in the present study does not allow deriving energetic/economic considerations about the industrial-scale implementation of the IBES. However, it can be inferred that, for the process to be energetically sustainable, the additional energy requirements associated with the electrochemical compartment (i.e. mixing of the anodic chamber, indirect energy consumption for the electrodes manufacturing, energy demand for treatment of the final $ZnSO_4$ solution) must be well below the above-mentioned gross energy gain of 940–1000 kJ/kg TOC. While a comprehensive assessment of the energetic profile of the IBES was beyond the scope of the work, this issue is certainly of extreme relevance in view of a thorough assessment of the feasibility of the process.

Based on the discussion provided about the IBES, the results appear to be promising. However, to derive a better understanding of the process, future aspects need to be investigated in further detail; these include the potential electrochemical stimulation effects on biomass and the strategies to prevent the passivation of the anode, as such phenomena likely played a role in the experiments performed.

Funding The research was funded by the University of Rome "La Sapienza" in the framework of the call for scientific research projects (years 2019 and 2020).

Data availability The authors state that the data generated during this study are mostly included in this published article in graphic form. The complete datasets generated during the current study are also available from the corresponding author on reasonable request.

Declarations

Conflict of interest The authors declare they have no known competing financial interests or personal relationships that could have appeared to influence the work reported in this paper.

References

APHA, Awwa, WEF, (2005) Standard methods for the examination of water and wastewater, 21st edn. American Public Health Association, Baltimore

Asunis F, De Gioannis G, Isipato M et al (2019) Control of fermentation duration and pH to orient biochemicals and biofuels production from cheese whey. Bioresour Technol. https://doi.org/10.1016/j.biortech.2019.121722

Chae K-J, Choi M-J, Lee J et al (2008) Biohydrogen production via biocatalyzed electrolysis in acetate-fed bioelectrochemical cells and microbial community analysis. Int J Hydrogen Energy 33:5184–5192. https://doi.org/10.1016/J.IJHYDENE.2008.05.013

Cheng S, Logan BE (2007) Sustainable and efficient biohydrogen production via electrohydrogenesis. PNAS. https://doi.org/10.1111/j.1365

Chookaew T, Prasertsan P, Ren ZJ (2014) Two-stage conversion of crude glycerol to energy using dark fermentation linked with microbial fuel cell or microbial electrolysis cell. N Biotechnol 31:179–184. https://doi.org/10.1016/J.NBT.2013.12.004

Da Silva VT, Mozer TS, da Costa Rubim Messeder dos Santos D, da Silva César A, (2017) Hydrogen: Trends, production and characterization of the main process worldwide. Int J Hydrogen Energy 42:2018–2033

Dubois M, Gilles KA, Hamilton JK et al (1956) Colorimetric method for determination of sugars and related substances. Anal Chem 28:350–356. https://doi.org/10.1021/ac60111a017

Ghimire A, Frunzo L, Pirozzi F et al (2015) A review on dark fermentative biohydrogen production from organic biomass: Process parameters and use of by-products. Appl Energy 144:73–95. https://doi.org/10.1016/j.apenergy.2015.01.045

Guo R, Wang B, Jia Y, Wang M (2017) Development of acid block anion exchange membrane by structure design and its possible application in waste acid recovery. Sep Purif Technol 186:188–196. https://doi.org/10.1016/J.SEPPUR.2017.06.006

Hallenbeck PC, Abo-Hashesh M, Ghosh D (2012) Strategies for improving biological hydrogen production. Bioresour. Technol.

IEA (2019) World Energy Outlook 2019 – Analysis - IEA

Liu H, Cheng S, Logan BE (2005a) Production of electricity from acetate or butyrate using a single-chamber microbial fuel cell. Environ Sci Technol 39:658–662. https://doi.org/10.1021/es048927c

Liu H, Grot S, Logan BE (2005b) Electrochemically assisted microbial production of hydrogen from acetate. Environ Sci Technol. https://doi.org/10.1021/ES050244P

Liu C-G, Xue C, Lin Y-H, Bai F-W (2013) Redox potential control and applications in microaerobic and anaerobic fermentations. Biotechnol Adv 31:257–265. https://doi.org/10.1016/J.BIOTECHADV.2012.11.005

Logan B, Hamelers B, Rozendal R et al (2006) Microbial fuel cells: methodology and technology. Environ Sci Technol 40:5181–5192. https://doi.org/10.1021/es0605016

Moscoviz R, Toledo-Alarcón J, Trably E, Bernet N (2016) Electro-fermentation: how to drive fermentation using electrochemical systems. Trends Biotechnol 34:856–865

Nelabhotla ABT, Dinamarca C (2019) Bioelectrochemical CO 2 reduction to methane: MES integration in biogas production processes. Appl Sci 9:16–18. https://doi.org/10.3390/app9061056

Paiano P, Menini M, Zeppilli M et al (2019) Electro-fermentation and redox mediators enhance glucose conversion into butyric acid with mixed microbial cultures. Bioelectrochemistry. https://doi.org/10.1016/j.bioelechem.2019.107333

Park JH, Chandrasekhar K, Jeon BH et al (2021) State-of-the-art technologies for continuous high-rate biohydrogen production. Bioresour Technol 320:124304. https://doi.org/10.1016/j.biortech.2020.124304

Rivera I, Buitrón G, Bakonyi P et al (2015) Hydrogen production in a microbial electrolysis cell fed with a dark fermentation effluent. J Appl Electrochem 45:1223–1229. https://doi.org/10.1007/s10800-015-0864-6

Santoro C, Arbizzani C, Erable B, Ieropoulos I (2017) Microbial fuel cells: From fundamentals to applications. A review. J Power Sources. https://doi.org/10.1016/j.jpowsour.2017.03.109

Schievano A, Pepé Sciarria T, Vanbroekhoven K et al (2016) Electro-fermentation—merging electrochemistry with fermentation in industrial applications. Trends Biotechnol 34:866–878

Thauer RK, Jungermann K, Decker K (1977) Energy conservation in chemotrophic anaerobic bacteria. Bacteriol Rev 41:100–180

Toledo-Alarcón J, Moscoviz R, Trably E, Bernet N (2019) Glucose electro-fermentation as main driver for efficient H2-producing bacteria selection in mixed cultures. Int J Hydrogen Energy 4:2230–2238. https://doi.org/10.1016/j.ijhydene.2018.07.091

Wang A, Sun D, Cao G et al (2011) Integrated hydrogen production process from cellulose by combining dark fermentation, microbial fuel cells, and a microbial electrolysis cell. Bioresour Technol 102:4137–4143. https://doi.org/10.1016/j.biortech.2010.10.137

Xu T (2005) Ion exchange membranes: State of their development and perspective. J Memb Sci 263:1–29. https://doi.org/10.1016/j.memsci.2005.05.002

Xue G, Lai S, Li X et al (2018) Efficient bioconversion of organic wastes to high optical activity of L-lactic acid stimulated by cathode in mixed microbial consortium. Water Res 131:1–10. https://doi.org/10.1016/j.watres.2017.12.024

Yu Z, Leng X, Zhao S et al (2018) A review on the applications of microbial electrolysis cells in anaerobic digestion. Bioresour Technol 255:340–348. https://doi.org/10.1016/j.biortech.2018.02.003

Authors and Affiliations

Giorgia De Gioannis[1] · Alessandro Dell'Era[2] · Aldo Muntoni[1] · Mauro Pasquali[2] · Alessandra Polettini[3] · Raffaella Pomi[3] · Andreina Rossi[3] · Tatiana Zonfa[3]

[1] Department of Civil and Environmental Engineering and Architecture, University of Cagliari, Cagliari, Italy

[2] Department of Basic and Applied Sciences for Engineering, University of Rome "La Sapienza", Via del Castro Laurenziano 7, 00161 Rome, Italy

[3] Department of Civil and Environmental Engineering, University of Rome "La Sapienza", Via Eudossiana 18, 00184 Rome, Italy

4 Bio-electrochemical systems as post-treatment for additional exploitation of the organic matter

4.1 Introduction

The previous chapters pointed out that in the course of DF large part of the carbon associated to the initial substrate, and therefore the potential energy content of the organic waste, remains in the digestate at the end of the process in the form of metabolites, such as VFAs and/or alcohols. This suggests that energy recovery through reuse of the DF end-products is further achievable. Therefore, further treatment of the DF effluent should not only aim at reducing the residual organic content, but also at recovering energy in order to increase the net gain of the whole multistage process (De Gioannis et al. 2013; Ghimire et al. 2015; Moscoviz et al. 2018). In the present study, different bio-electrochemical systems (BESs) were investigated as possible subsequent stages downstream of bio-electrochemical H_2 production from CW.

The BESs are based on the ability of specific microorganisms defined as electroactive bacteria (EAB) to interact with solid electrodes by forming a biofilm and catalyze the oxidation of organic matter by generating an electrical potential. The first evidence of microorganisms interacting with solids dates back to a century ago, when specific bacteria were found to interact electrically with a platinum electrode (Potter 1911). Since then, a number of processes have been explored to exploit the electrical potential generated by the EAB, through different systems configurations. These include mainly electricity production from wastewater in microbial fuel cells (MFCs), microbial electrolysis cells (MECs) for H_2 or CH_4 production, elongation of CO_2 to VFAs in microbial electrosynthesis cells (MES) and low-cost desalinization in microbial desalination cells (MDC) (Sánchez et al. 2020).

MFCs are the first and the most widely investigated BESs, due to their capability of producing an electric power while simultaneously degrading an organic substrate such as diluted waste and wastewater. The recognized benefits include also the operating conditions close to ambient levels, with temperature ranging between 15 and 45 °C (most commonly 20 – 30 °C) and around neutral pHs. Generally, in the anodic chamber, where the EAB are attached to dedicated inert electrodes, the oxidation of the organic substances takes place by generating CO_2 and protons, which migrate into the cathodic chamber through ion exchange membranes (Figure 4-1 - a). The cathodic chamber is maintained under aerobic conditions, so that in the presence of electrons, the protons react with oxygen to produce water, resulting in the spontaneous production of electricity.

Therefore, voltage generation in an MFC is the consequence of a thermodynamically favorable reaction, that can be evaluated in terms of Gibbs free energy (J), defined as follows (1):

$$\Delta G = - n F EMF \quad (1)$$

with n = number of electrons exchanged in the reaction, F = Faraday's constant = 9.64853 x 10^4 C mol^{-1} and EMF = overall electromotive force.

The reactions that potentially occur in the cathodic and anodic compartments are shown, along with the corresponding reduction potentials (E^0) under standard condition defined as IUPAC convention (temperature = 298 K, pressure = 1 bar, concentration of each species = 1 M), considering O_2 as the electron acceptor (2) and acetate (3) as the electron donor (Logan et al. 2006; Seelajaroen et al. 2020):

$$O_2 + 4H^+ + 4e^- \leftrightarrow 2H_2O \qquad E^0_{cat} = 1.229 \text{ V (vs. NHE)} \quad (2)$$

$$CH_3COO^- + 4H_2O \leftrightarrow 2\ HCO_3^- + 9H^+ + 8e^- \qquad E^0_{an} = 0.187 \text{ V (vs. NHE)} \quad (3)$$

The overall electromotive force developed by the cell (EMF = $E_{cat} - E_{an}$) can be calculated assuming the common conditions usually found in the MFC systems (Yasri et al. 2019), i.e. pH = 7, acetate concentration at the anode of 1 g/L (16.9 mM) and 5 mM of HCO_3^-, with the assumption of O_2 partial pressure of 0.21 atm. The calculation through the Nernst equation (4) provides electrode potentials under such conditions of E_{cat} = 0.805 V and E_{an} = – 0.300 V.

$$E = E^0 + \frac{R\,T}{n\,F}\ \ln\left[\frac{\pi\,(a,ox)^{\vartheta ox}}{\pi\,(a,red)^{\vartheta red}}\right] \quad (4)$$

With E = half-cell potential, E^0 = standard reduction potential, R = universal gas constant, T = temperature, n = number of electrons exchanged in the reaction, F = Faraday's constant and Π = activities (assumed identical to the concentrations) of the species involved.

Thus, the EMF is generally about = 0.805 V – (– 0.300 V) = 1.105 V; this result underlines that, in an MFC, the Gibbs free energy is negative (equation 1), leading to a thermodynamically spontaneous redox reaction. However, this value does not correspond to the actual voltage produce by a real MFC (ΔV), but it represents an upper threshold because real systems are affected by various types of losses that the Nernst potential does not consider. The contributions of the different voltage losses can be schematically summarized as follows:

$$\Delta V = EMF - \eta_a - \eta_c - IR_\Omega \quad (5)$$

where η_a and η_c are, respectively, the anodic and cathodic overpotentials, and IR_Ω represents the contribution of the ohmic losses. The extent of η_a and η_c are generally dependent on various factors

including mainly activation losses, metabolic losses and mass transport/concentration losses. Activation losses are related to the activation energy needed for the redox reaction and occur during the electrons transfer between microorganisms/mediators and the electrodes. Metabolic losses depend on bacterial behaviour and the level of complexity that they encounter in the use of the substrate. Concentration losses occur when mass transfer of chemical species to the electrode surface is limited. This is the case when the released or supply of oxidized or reduced species from/towards the electrodes surface is poor, leading to an increase in the anodic potential or a reduction in the cathodic potential. Moreover, typical concentration losses can be found in poorly mixed systems where diffusional gradients may also arise in the bulk liquid. On the other hand, ohmic losses are mainly caused by the constructional features of the cell; they concern the resistance encountered by the electrons in flowing through the interconnections and the electrodes as well as the resistance of the ions in flow through the membrane and the electrolyte solutions.

Therefore, in an MFC, in several cases the measured voltage is reported as follows (Logan et al. 2006; Sánchez et al. 2020):

$$\Delta V = OCV - IR_{int} \quad (6)$$

where OCV is the open circuit voltage, which can be considered as the overall EMF of the cell reduced by the electrode overpotentials occurring under open circuit conditions, while IR_{int} represents the internal losses of the cell that depend on the electric current generated and the internal resistances and also includes the ohmic losses.

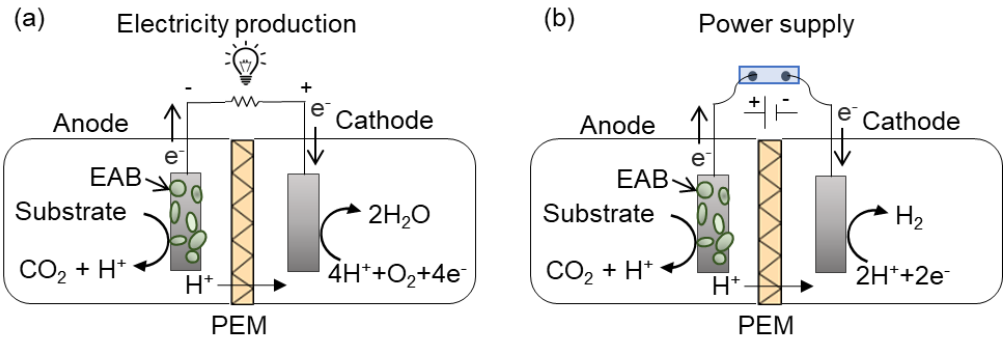

Figure 4-1 Schematic representation of a MFC (a) and a MEC for H_2 production (b) consisting of two chambers separated by a proton exchange membrane (PEM). In the MFC, a redox reaction takes place which results in electricity production through degradation of the of the organic substrate in the anodic chamber, whereas the MEC system allows the H_2 production by applying a low potential

To date, research efforts in this field are focused on the identification and adjustment of factors affecting the maximum achievable voltage, the use of materials compatible with environmental sustainability and cost-effectiveness. Indeed, the intensity and flow of the electron transport are

functions of the construction features of the cell as well as of substrate and inoculum characteristics and the operating conditions adopted, that govern system performance. The conventional lab-scale MFC reactor consists of two chambers connected by a tube containing the membrane able to provide the protons or cations passage (proton/cation exchange membrane, PEM/CEM) (Oh et al. 2004; Kim et al. 2007a; Rozenfeld et al. 2017). This type of configuration is commonly used for basic research such as investigating the microbial behaviour, testing new materials, compare diverse types of membranes and/or different substrates, but it was found to be generally characterised by high ohmic resistances that result in low power densities (Antonopoulou et al. 2010; Tremouli et al. 2013). Therefore, several configurations were employed among the numerous studies with the aim of enhancing the performance. A simple alternative involves eliminating the tube by using cubic chambers separated by the membrane and held together by screws, that allows for larger membrane surface areas. Generally, conventional MFC employed aqueous cathode where dissolved oxygen is provided by aeration with bubbles. However, it was observed that using oxygen as the electron acceptor with an air-cathode can provide higher power densities than typical cathodes submerged in water. In addition to that, the air-cathode is placed in direct contact with the air and allows for a more simplified and cost-effective configuration by eliminating the second chamber and possibly the membrane (Serra et al. 2020). Liu and Logan (2004) tested an air-cathode MFC both in the presence and absence of PEM. Their results showed a maximum power density of 494 mW/m^2 without the PEM compared to 262 mW/m^2 obtained with the membrane. However, a disadvantage using a MFC without a PEM can be the probable losses of substrate due to oxygen diffusion into the anodic chamber that leads to aerobic oxidation by bacteria. Indeed, the authors observed a coulombic efficiency reduction from 40-55% with the PEM to 9-12% without the PEM, that indicates oxygen presence in the anodic compartment. So that in some air-cathode MFCs, the membrane is still used to prevent both solution leakage through the cathode and oxygen diffusion into the anodic chamber. But a number of other possibilities can be considered for the MFC design. An alternative to the membrane was found in a proton-permeable porcelain layer combined with a graphite cathode in order to obtain a single separator-cathode structure by Park and Zeikus (2003). The authors showed that the single-chamber design was less expensive and more practical than the conventional two-chamber system, which requires aeration and a catalyst solution in the cathodic compartment. Finally, with a view to scalability, experiments were carried out on a large-scale MFC by Rossi et al. (2019), where a maximum power density of 0.101 W/m^2 (or 0.74 W/m^3) was obtained in an 85-L MFC with graphite fiber brushes in the anodic chamber and flat air cathode in batch mode. Under continuous flow, the performance improved by 17% at HRT of 22 min. The results also demonstrated the importance of electrode spacing and hydraulic flow on large-scale

MFC performance. Although the most promising approach appears to be the connection of multiple MFC units in series or parallel in order to increase the overall voltage and current produced by the system (Aelterman et al. 2006; Tremouli et al. 2019b).

A further opportunity to exploit the catalytic activity of EAB is given by MECs, that can be considered as modified MFC (Figure 4-1 - b)). MECs have been studied since 2005 (Liu et al. 2005b), and their scientific interest have strongly increased in recent years (Santoro et al. 2017). The main difference is due to the cathodic chamber that is maintained under anaerobic conditions; consequently, protons are reduced to H_2, as there are no other electronegative species that can be a sink of electrons. This process requires the supply of an electric current, since the electric potential naturally generated by microorganisms is not high enough to reduce H^+ to H_2. However, the voltage required is significantly lower than that used for conventional water electrolysis, since the chemical energy extracted from organic substrates oxidized at the anode supplies most of the potential needed.

To date, the need of expensive materials such as platinum as cathodic catalysts for H_2 production is one of the main drawbacks encountered in MECs. Therefore, research is currently being directed towards alternative materials, both cheaper and more sustainable but equally effective (Selembo et al. 2010; Rozenfeld et al. 2018; Son et al. 2021). Particular attention, in this context, is directed towards the so-called full-biological cells, which exploit microbial catalysis also at the cathode (Jeremiasse et al. 2010; Jafary et al. 2018).

A special type of MEC is the case of a modified cell in order to produce CH_4 rather than H_2, exploiting CO_2 as the carbon source. The capture and possible recycling of CO_2 produced during substrate oxidation by the biological reactions is indeed another aspect that deserves further attention. In this context, the use of CO_2 in a modified MEC for CH_4 production is worth considering. The reduction of CO_2 to CH_4 by means of a MEC offers the advantage of a method for CO_2 removal and simultaneously a source for CH_4 production under mild conditions, that are typical in BESs operations.

In a CH_4-producing MEC, microorganisms are attached on the cathode thus forming the biocathode that catalyses the conversion of CO_2, while the anode compartment provides protons and part of the electrons required.

In the cathodic compartment, CH_4 production can follow two possible options, namely direct (7) and indirect (8, 9) electron transfer (Zhang et al. 2019):

$$CO_2 + 8H^+ + 8e^- \rightarrow CH_4 + 2H_2O \quad (7)$$

$$8H^+ + 8e^- \rightarrow 4H_2 \quad (8)$$

$$CO_2 + 4H_2 \rightarrow CH_4 + 2H_2O \quad (9)$$

Although the indirect conversion of H_2 (or even acetate) to CH_4 is thermodynamically favorable, as shown by acetoclastic and hydrogenotrophic methanogenesis spontaneously occurring during anaerobic digestion, the bio-electrochemical production of CH_4 requires an auxiliary applied potential because it is necessary to overcome the overvoltage and the ohmic losses associated to the two-chamber configuration. Nevertheless, the implementation of organic substrate oxidation in a separate compartment from CH_4 conversion provides some advantages, including the independence of CH_4-producing bacteria from syntrophic reactions such as organic acids utilization, which prompts the CO_2 consumption and results in a biogas at the cathode with a higher percentage of CH_4. Moreover, methanogens are preserved from any possible inhibiting agents coming from the substrate. The whole cell potential is often controlled by decreasing the cathode voltage, but it is also possible to increase the anodic potential (Villano et al. 2013) or to apply an overall potential difference to the cell (Seelajaroen et al. 2020). Nevertheless, these overpotentials can be reduced by improving the configuration and implementing a well-performing biocathode with the overall aim of limiting the power supply required by the system.

Cheng et al. (2009) reported the first results concerning CO_2 utilization in MECs for CH_4 production. A two-chamber reactor was used, with carbon clothes coated with a carbon layer inoculated with a pure culture as the biocathode, without any precious metal as the catalyst, combined with an abiotic anode and acetate solution. By applying a set voltage range of – 0.7 to – 1.0 V vs. Ag/AgCl (that corresponds respectively to – 0.5 and – 0.8 vs. the SHE, Standard Hydrogen Electrode) to the cathode, the authors reported CH_4 production, with a current capture efficiency of 96% at – 1.0 V. On the basis of the electrochemical analysis, they also suggested that CH_4 production was mainly performed via direct transformation from current and not with H_2 as an intermediate. Villano et al. (2010) observed both direct and indirect reduction of CO_2 to CH_4, which means by directly accepting electrons from the surface of the electrode and by converting the abiotically produced H_2 into CH_4. The experiments were performed in a two-chamber MEC using a hydrogenophilic methanogenic culture at the biocathode. CH_4 production was found to proceed at potentials between – 0.65 V and – 0.90 V (vs. SHE). In the whole range of cathode potentials investigated, only a fraction of CH_4 was produced via direct extracellular electron transfer processes; the other contribution was biologically produced via H_2 consumption by hydrogenophilic methanogenesis. They observed that the relative contribution of these routes was highly dependent on the set cathode potential, and the relative contribution of extracellular electron transfer showed a maximum at – 0.75 V. Van Eerten-Jansen et al. (2015) analyzed the mechanisms of electron transfer during CH_4 production in a MEC employing mixed cultures coming from anaerobic sludge at an applied cathode potential of − 0.7 V and – 0.9 V vs. NHE (Normal

Hydrogen Electrode, that can be assumed to correspond to SHE). They observed that CH_4 was predominantly produced through indirectly routes such as H_2 and acetate utilization, while CH_4 production via direct electron transfer hardly occurred. They also showed that, among the various electron transfer mechanisms that can occur in a bio-electrochemical CH_4-producing system, the direct electron transfer requires the lowest minimum energy input, that is 11.0 kWh/m^3-CH_4 at standard temperature and pressure, catholyte pH at 7, anolyte pH at 2. Bio-electrochemical production of acetate requires a minimum electrical energy input of 11.3 kWh/m^3-CH_4 while the bio-electrochemical production of H_2 requires the highest energy input of 12.5 kWh/m^3-CH_4. Therefore, under these conditions, CH_4 production via direct electron transfer seems to be energetically favorable. However, they stated that the energy input is highly dependent on catholyte pH and H_2 partial pressure, thus changing these parameters could be a strategy to decrease the energy requirements when other routes than direct electron transfer are performed.

Some studies have successfully investigated different BESs for exploitation of VFAs or DF effluents into electricity and H_2. Liu et al. (2005b) obtained 2.9 mol H_2/mol acetate applying an additional voltage of 0.250 V in a H_2-producing MEC. Through optimization of materials and reactor configuration, Cheng and Logan (2007) achieved H_2 yields between 2.0 and 3.9 mol H_2/mol acetate at applied voltages of 0.2 to 0.8 V. Chae et al. (2008) showed that H_2 production gradually increases as the applied voltage is increased from 0.1 to 1 V, reaching 2.1 mol H_2/mol acetate. Liu et al. (2005a) tested power generation from acetate and butyrate in a MFC and observed that acetate is preferred over butyrate as the substrate, producing respectively 506 mW/m^2 and 305 mW/m^2.

The treatment of a real DF effluent was investigated by Chookaew et al. (2014) using both a MEC and a MFC. A power density of 92 mW/m^2 in the MFC was achieved along with 50% COD removal. When treated in the MEC, the same substrate yielded 106 mL H_2/g COD. Rivera et al. (2015) evaluated DF effluent exploitation as a substrate for a MEC. The highest production rate (81 mL H_2/Ld) was obtained at a 550 mV voltage and was accompanied by 85% COD removal. Wang et al. (2011) performed a multi-stage process using a DF reactor for cellulose degradation followed by two MFCs that were used as power sources for a subsequent MEC stage. The MFCs produced a maximum of 0.43 V using the fermentation effluent that induced H_2 production in the MEC at a rate of 0.48 m^3 H_2/m^3d and with a yield of 33.2 mmol H_2/g COD removed in the MEC. The authors observed an overall improvement in H_2 production for the integrated process by 41% compared with fermentation alone.

The evidence from the research studies reveals that BESs are effective tools in enabling a maximization of the energy recovery from the organic substrate for fermentative H_2 production processes. In the present work, a single-chambered MFC, with an innovative configuration consisting of 4 air-cathodes

connected in series (modified from Tremouli et al. 2021), was tested for the removal of the residual organic matter contained in the IBES effluent and the contextual power generation. Moreover, a dual-chamber MEC, equipped with both a bioanode and a biocathode, was investigated for CO_2 reduction to CH_4 in the cathodic compartment using the IBES effluent as the electron donor in the anodic chamber.

4.2 Materials and methods

4.2.1 MFC experimental setup

A four-air cathode single-chamber MFC was tested for the exploitation of the VFAs effluent from the cathodic chamber of the IBES (see chapter 3), with the aim of producing additional electricity (a schematization is shown in Figure 4-2). The reactor consists of a single Plexiglas chamber (11.8 cm x 9.6 cm x 9.6 cm; 1.6 cm wall thickness) equipped with four cathode tubes (2-cm diameter and 15-cm length) made of mullite, which is permeable to protons. The interior of the mullite tubes was coated through the brush coat technique with a paste containing the oxygen reduction catalyst. The internal paste consists of graphite paint, and fly ash was used as a substitute of MnO_2 typically used as the catalyst, while a stainless-steel mesh was employed for connection. No forced O_2 aeration was used since the cathodes were in direct contact with the atmosphere, and the four air cathodes were connected in series to each other through a copper wire. The anode compartment was made of 250 g of graphite granules (type 00514, Le Carbone, Belgium), with diameters ranging between 1.5 and 5 mm, employed as biofilm support and conducting material, while a graphite rod (13-cm length and 7-mm diameter) was embedded into the packed bed of granules for the external connection as well as the electron transfer. Prior to use, the granules were washed in 32 % HCl for 24 h and the process was repeated four times with the aim of removing the metals from the surface and the inner pores (Tremouli et al. 2019a). An external resistance of 100 Ω was applied between the electrodes in order to reproduce a closed electrical circuit and the reactor was maintained at a temperature of 30 °C.

The anolyte solution, having a volume of 150 mL, was added directly onto the packed bed in order to completely submerge it. After the enrichment phase (described in paragraph 4.2.3), nine consecutive batch cycles (MFC-S1 – MFC-S9) were performed using a synthetic anolyte solution composed of VFAs (HAc, HBu) and EtOH, with concentrations that simulate the proportions at which they were detected in the IBES effluent (HAc:HBu:EtOH = 1:3:2), at different dilutions. The corresponding

soluble COD values of the starting solution in each cycle are displayed in Table 4.1. Subsequently, three cycles (MFC-R10 – MFC-R12) were carried out employing the IBES effluent, diluted with deionized water. The real effluent was previously filtered in order to remove any competitive biomass, as suggested by the study of Antonopoulou et al. (2010) which involved an MFC run with diluted raw CW; the authors demonstrated that indigenous non-electrogenic microbial community, that is contained in that kind of substrate, caused the biochemical oxidation of the organic substrate, depleting COD instead of the attached electrogenic biomass and drastically reducing the cell columbic efficiency. The initial pH of the synthetic and the real solutions varied in the range 3.0 – 3.9, so it was increased by adding 2M NaOH with the aim of providing a more suitable environment for the microorganisms, reaching a starting pH in the range 5.6 – 6.5. Table 4.1 shows the experimental design for MFC operation and the main characteristics of each cycle after NaOH addition.

Table 4.1 Experimental design for the MFC

Cycle number	**MFC cycle code**	**Substrate**	**Concentration**	**Initial pH**	**Initial conductivity**
-	-	-	mg sCOD/L	-	mS/cm
1	S1	Synthetic	4458	6.37	1.24
2	S2	Synthetic	8802	5.60	2.73
3	S3	Synthetic	5665	6.12	1.20
4	S4	Synthetic	5688	5.50	2.08
5	S5	Synthetic	3342	6.50	1.27
6	S6	Synthetic	3249	6.21	1.24
7	S7	Synthetic	5070	6.12	1.76
8	S8	Synthetic	5084	6.12	1.76
9	S9	Synthetic	5014	6.12	1.76
10	R10	Real effluent dil 1:10	6268	6.45	3.94
11	R11	Real effluent dil 1:10	6083	6.37	3.82
12	R12	Real effluent dil 1:2	32279	6.12	14.95

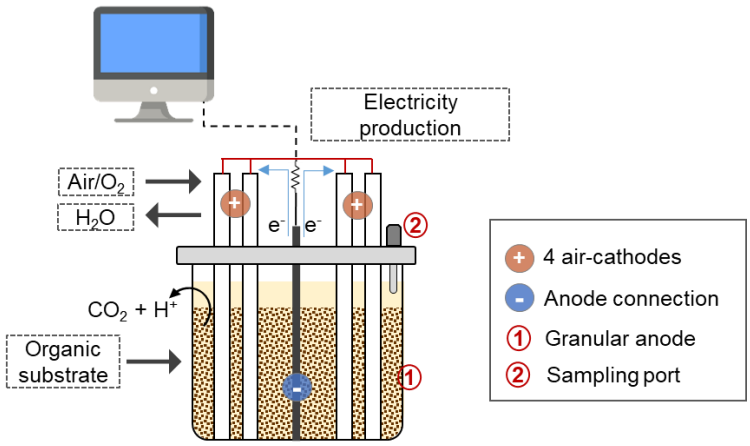

Figure 4-2 Single-chamber MFC layout composed of 4 air-cathodes submerged in the anodic compartment which contains the graphite granules with attached biomass and the organic substrate

4.2.2 MEC experimental setup

A dual-chamber MEC equipped with both a bioanode and a biocathode was designed to exploit biological processes in both compartments. The aim of the tests was the simultaneous treatment of the two effluent streams of the fermentation process. In particular, the upgrading of CO_2 to CH_4 at the cathode and the use of the VFA-rich fermentate from the IBES as the electron supplier at the anode were investigated. Therefore, while in the anodic compartment the oxidation of organic substrate catalyzed by microorganisms takes place, in the cathodic compartment the autotrophic bacteria utilize HCO_3^-/CO_2 as the carbon source and result in CH_4 production.

The CH_4-producing MEC used for the experimental tests is outlined in Figure 4-3. The reactor was composed of two square-shaped chambers made of PTFE and kept separated by a pre-treated PEM (Nafion 117) with a surface area of 5 x 5 cm^2 that allows for proton passage between the chambers. Each compartment was equipped with carbon felt electrodes that provide biomass support and electron transfer. The anodic carbon felt had a surface area of 5 x 5 cm^2, while the cathodic carbon felt was made of 3 carbon felts connected together, with dimensions of 5 x 5 x 2 cm^3, in order to increase the effective surface available to methanogens. The bio-electrodes were connected through an external circuit by means of Ti wires and linked to both the measuring system and the power supplier, through which a constant total potential difference of 0.5 V was applied to the whole cell for the entire duration of each cycle. The reactor was maintained at 30 °C.

A synthetic anolyte solution (working volume of 80 mL) composed of VFAs (HAc, HBu) and EtOH in proportions that simulate the IBES effluent, was first used at different dilutions for four consecutive

batch cycles after the enrichment phase (MEC-S1 – MEC-S4). Subsequently, three cycles were operated with the IBES effluent that was previously filtered as described for the MFC (MEC-R5 – MEC-R7). Since the initial pH of the synthetic and the real solutions varied in the range 3.0 – 3.9, pH was adjusted with 2M NaOH to a suitable range for the microbial processes (see below). Table 4.2 summarizes the experimental design for MEC operation and the main characteristics of each cycle after NaOH addition.

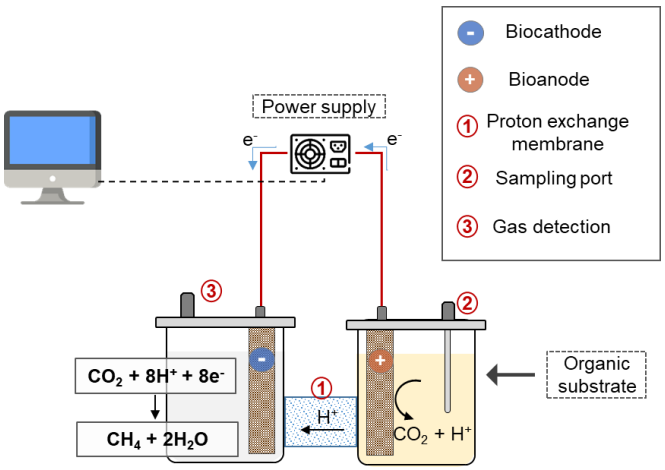

Figure 4-3 Dual-chamber MEC layout for CH_4 production via CO_2 conversion in the cathodic chamber. Organic substrate utilization takes place in the anodic chamber that is separated through a proton exchange membrane

Table 4.2 Experimental conditions for the CH_4-producing MEC

Cycle number	MEC cycle code	Substrate	Concentration	Anode initial pH	Anode initial conductivity	Cathode initial pH	Cathode initial conductivity
-	-	-	mg COD/L	-	mS/cm	-	mS/cm
1	S1	Synthetic	6616	6.31	2.43	6.90	9.93
2	S2	Synthetic	6384	6.13	2.48	6.85	7.92
3	S3	Synthetic	5016	6.12	1.76	6.80	10.01
4	S4	Synthetic	6480	6.25	2.15	6.77	9.78
5	R5	Real effluent dil 1:10	6131	6.50	3.74	6.75	10.15
6	R6	Real effluent dil 1:10	6310	6.21	4.00	6.95	10.01
7	R7	Real effluent dil 1:2	30193	6.12	14.50	6.60	9.90

4.2.3 Substrate and inoculum

Wastewater sludge (WWS), provided by a Wastewater Treatment Plant in Athens, Greece, was employed as the inoculum for the enrichment procedure of the electrochemically active bacteria in the anodic chambers of both the MFC and the MEC.

At the beginning of the MFC operation, three acclimation cycles were performed using fresh anaerobic sludge. In each cycle the inoculum concentration was 10 % v/v, whereas glucose was used as the substrate with a concentration of 1.5 g COD/L. The buffer and nutrients solution contained 5 g/L $NaHCO_3$, 0.16 g/L KCl, 4.8 g/L NaH_2PO_4, 3.44 g/L Na_2HPO_4 and trace metals.

After acclimation of the electroactive bacteria on the graphite granules, few cycles were performed without WWS using the same synthetic glucose feed of the enrichment phase, then the MFC operation was switched using the synthetic substrate simulating the IBES effluent.

An identical acclimation procedure was used for the MEC bioanode, where three cycles were performed using the glucose solution as the substrate at a concentration of 1.5 gCOD/L and fresh sludge addition, then two cycles without WWS with the same glucose feeding were run before switching to the feeding with the synthetic solution of VFAs and EtOH. In the second chamber of the MEC, the biocathode was acclimatized using 10 % v/v WWS for three cycles with the same buffer solution as the anode. In the cathodic compartment, in the enrichment phase CO_2 was sparged at the outset of each batch, in order to acclimate the autotrophic biomass to CO_2 uptake.

In both the MFC and the MEC, when the biomass was assumed to have adapted to the synthetic solution simulating the IBES effluent, the real IBES effluent was used as the substrate. Table 4.3 provides the main characteristics of the IBES effluent.

Table 4.3 Characterization of the IBES effluent used as the substrate for the microbial systems

Parameter	Unit of measure	
Total solids	g/L	59.44
Volatile solids	g/L	41.08
Total suspended solids	g/L	6.96
Volatile suspended solids	g/L	0.95
Carbohydrates	g glucose/L	18.0±0.1
Total Organic Carbon	g C/kg	26.7±0.1
Soluble COD	mgO_2/L	67267±329
Total COD	mgO_2/L	80106±572
pH	-	3.56
Conductivity	mS/cm	15.36
Acetic acid	mg HAc/L	1188±333

Butyric acid	mg HBu/L	3493±293
Ethanol	mg EtOH/L	2428±192

4.2.4 Analytical methods

The chemical analyses of chemical oxygen demand (COD) and solids were conducted according to standard methods (APHA et al. 2017). The soluble COD was determined in all the samples after filtration at 1.2 μm. Total organic carbon (TOC), carbohydrates and VFAs (acetate, butyrate, propionate, valerate, caproate, heptanoate) and ethanol concentrations in the IBES real effluent were determined through the same methods described in section 3.3.

Conductivity and pH were measured through WTW INOLAB PH720 probes.

In the cathodic chamber of the MEC, the biogas composition was analyzed through a gas chromatograph by periodically sampling with a 1 mL gastight syringe.

The electrical parameters including voltage (V) and electric current intensity (I) were continuously recorded every 2 minutes. A potentiostat–galvanostat (AUTOLAB) with NOVA software was used to perform the linear sweep voltammetry (LSV) from open circuit voltage (OCV) to zero voltage with a step of 5 – 10 mV/s.

4.2.5 Evaluation parameters and calculation

In both microbial cells, the organic matter utilization in the anodic compartment was evaluated for each cycle in terms of COD removal efficiency (COD_{re}), as follows:

$$COD_{re}\,(\%) = \frac{\Delta COD}{COD\ in} \cdot 100$$

Where ΔCOD is the COD variation over a cycle and COD_{in} is the starting value. The COD was evaluated on the soluble fraction of the samples.

The conversion of COD into electricity was assessed through the coulombic efficiency (ε_{ce}), defined as the ratio between the total charge actually transferred to the anode from the substrate (C experimental, C_{ex}) and the maximum charge attainable on the basis of the total amount of electrons potentially mobilized by the removed substrate (C theoretical, C_{theo}) (Logan et al. 2006):

$$\varepsilon_{ce}\,(\%) = \frac{Cex}{Ctheo} = \frac{M \int_0^t I\,dt}{F\ b\ v\ \Delta COD}$$

where C_{ex} is derived from the integration of the electric current intensity produced by the cell over a cycle, M is the molar weight of O_2, F is the Faraday's constant, b is the number of electrons exchanged per mole of O_2, and v is the anolyte volume.

The power output (P) was calculated as P = I×V and expressed in mW/m^3 for the single chamber MFC (where the anodic solution volume is 150 cm^3) or in mW/m^2 for the dual chamber MEC (considering an anodic surface area of 25 cm^2).

In the CH_4-producing MEC, the charge conversion into CH_4 was evaluated through the faradaic efficiency (FE) (Seelajaroen et al. 2020):

$$FE\,(\%) = \frac{8\,F\,n_{CH_4}}{\int_0^t I\,dt} \cdot 100$$

where n_{CH4} is the number of CH_4 moles produced in the system, 8 is the number of electrons stoichiometrically needed for the reduction of CO_2 to CH_4 (eq. 7) and F is Faraday's constant.

4.3 Results and discussion

4.3.1 MFC operation

Twelve consecutive batch cycles were carried out in the MFC after the acclimation cycles with the glucose feeding. The voltage output (see Figure 4-4) displayed some fluctuations in the early stages of operation when testing the synthetic VFAs+EtOH solution. These were presumably the consequence of the acclimation requirements of the biomass to the new, more complex substrate. The first cycle (S1) reached an initial voltage of 180 mV that was close to the value obtained in the last cycle run with glucose feeding, as shown in Figure 4-6. It is likely that operation during cycle S1 was positively influenced by the energy reserves accumulated by the electrogenic biomass in the previous cycles and the residual availability of mineral salts and buffer solution in the reactor. The process duration was instead a function of the higher COD concentration supplied in the case of S1, which led to a total amount of charge transferred (C_{ex}) of 511 C for S1 and 82 C for the cycle with glucose feeding. On the contrary, run S2, which had a two times higher COD than S1, displayed the lowest initial voltage and also the lowest charge transferred compared to all cycles (C_{ex} = 151 C) as well as the lowest COD removal (see Table 4.4). This outcome may be explained by the influence of adaptation requirements of the biomass to the new substrate. This was also reflected in the pH profile; in general, during cell operation, the pH is self-adjusted to a value of 6 –7 through to the transport of protons in the cathodic compartments, but this phenomenon appeared to be reduced in this cycle.

The third cycle (S3) showed a recovery in efficiency with a high COD removal (95.9%) and total charge transferred of 431 C. However, a slight decrease in the voltage output was observed in the subsequent cycles; therefore, feeding with the real IBES effluent started only once reactor operation

showed adequate repeatability. In order to avoid substrate overloading, the IBES effluent was diluted ten times in the case of R10 and R11 and two times for R12. The system displayed an increase in voltage compared to the previous cycles, even when COD concentration was increased, demonstrating that the biomass was finally adapted to the use of the substrate. Moreover, it was noticed that from S8 the voltage trend inside the cycle, after the initial decrease, raised again. This increasing trend was also shown by runs R10 and R11 and was particularly evident in R12. This phenomenon may be explained considering that likely the components of the IBES effluent have different biodegradation kinetics and show different affinities with the electroactive biomass. This performance is consistent with literature findings. Liu et al. (2005a) demonstrated the feasibility of electricity production in a single-chambered MFC, with a platinum-catalysed cathode, from acetate or alternatively butyrate as substrates. They obtained a maximum power density of 12700 mW/m^3 using 800 mg/L of acetate, and the ε_{ce} varied between 28.3 % and 13.2 % changing the substrate concentration respectively from 80 to 800 mg HAc/L. On the other hand, the efficiency of the cell with butyrate was lower, underlying that acetate is a preferred substrate for the electroactive bacteria. The maximum power density was 7600 mW/m^3 with 1000 mg/L of butyrate, while ε_{ce} varied in the range 15 – 7.8 % with a concentration of 75 – 1000 mg HBu/L. The authors also observed low concentrations of acetate during butyrate tests, indicating that butyrate may first be converted into acetate by acetogenic bacteria typically present in mixed microbial communities. In the study by Kim et al. (2007b) it was also observed that the ethanol was first fermented to acetate and H_2 in the anodic chamber before transferring electrons to the electrode in a MFC.

Figure 4-7 shows the power density curves that were derived at the beginning of the testing period through LSV analysis. The results are consistent with the above observations, showing the lowest and highest power densities reached by S2 and S3, respectively. Some good performance was also obtained for R11 and R12 with P = 1104 and 1180 mW/m^3, respectively. It is worth noting that the internal cell resistance (see

Table 4.5) appeared to increase when feeding with the synthetic solution. However, this decreased for R11 and R12, probably due to the slightly higher conductivity of the real effluent. Nevertheless, power outputs were in general much lower than the value of 4507 mW/m^3 obtained in the last cycle of glucose feeding.

The modest power outputs obtained could be partly explained by limitations to substrate utilization. Choi et al. (2011) observed that the co-existence of different VFAs slowed the removal of the individual species, which indicated that anodic microbes were competing for different substrates. Moreover, the authors stated that acetate can be directly consumed for electricity production while other VFAs must

first be converted into acetate. In their experiments, a maximum power density of 240 mW/m^2 was obtained in a dual-chamber MFC, with platinum as the catalyst, after acetate and propionate addition, while the use of a mixture of VFAs (acetate, propionate, butyrate and valerate in the ratio of 2:1:6:1.5) and EtOH resulted in 175 mW/m^2 in the same dual-chamber MFC and 140 mW/m^2 (or 1120 mW/m^3) in a single-chamber air cathode MFC.

Thus, it is possible that in the present experimental work, the electrogenic biomass encountered limitations in the use of the synthetic substrate and of the real effluent from the IBES. Nevertheless, the tests that used the real effluent displayed higher maximum power outputs and better voltage production in comparison with the tests fed with the synthetic solution (excluding S3). This could be the result of the presence of various mineral salts and nutrients in IBES that could have improved the electrolytic properties of the anolyte and supported the microbial activity. Therefore, the use of the real effluent as substrate for the MFC is considered promising, and a future objective will be to identify the appropriate concentration and experimental conditions in order to obtain the maximum energy yield.

A similar MFC configuration was experimented by Tremouli et al. (2021) which investigated a four air–cathode MFC, with MnO_2 as the cathodic catalyst, fed with the effluents from a thermophilic and a mesophilic anaerobic digester of fermentable household food waste. The mesophilic digestate turned out to be more hardly degradable compared with the thermophilic one, probably due to the presence of more complex organic compounds in the mesophilic effluent, that are more difficult to decompose and be consumed by electrogenic bacteria. Nevertheless, the system was characterized by low internal resistances in both cases (10–50 Ω) and proved to reach higher power densities compared to the present experimental setup, which were 2000 mW/m^3 with the mesophilic effluent and 3500 mW/m^3 with the thermophilic digestate.

In the present experiments, the COD removal ranged between 76.8% (S2) and 99.8% (R12) with an average of 88.3%. On the other hand, the columbic efficiencies displayed quite low values. This suggests that, although substrate consumption took place, it did not result in the generation of an electric current, thus limiting the performance of the MFC. Several factors could produce low electron and energy recoveries in MFC. First, a fraction of the substrate is clearly used for bacterial growth and production of biomass; Freguia et al. (2007) also documented the temporary storage of electrons in form of polymers (in particular poly-β-hydroxyalkanoates (PHAs) and glycogen) inside the microbial biomass of an MFC in an excess of substrate. However, in the present case, this is not the only possible explanation for the discrepancy between the COD consumed and the electrons actually transferred. Indeed, oxygen infiltration in the anode compartment may have limited the electron transfer to the cathodes in the membrane-less reactor. Such a negative effect could be related to the inhibition of the

obligate anaerobic EAB or to the loss of electrons from aerobic respiration by facultative or other aerobic bacteria present in the inoculum (Antonopoulou et al. 2010). In the present MFC, the anodic chamber was protected by a coating inside the cathodes which prevented oxygen diffusion. Nevertheless, the MFC reactor did not prove particularly effective in preventing gas transfer during the tests, resulting in some cases in the evaporation of the anolyte solution, which may have affected the process and could also have allowed oxygen to reach the anodic compartment. Therefore, it may be hypothesized that an improvement in gas tightness to prevent air from entering the system may enhance the process performance. Lastly, the anaerobic conditions at the anode and the presence of acetate could also have prompted CH_4 production with a consequent diversion of part of the substrate from the intended reactions. Parameswaran et al. (2009) extensively investigated the syntrophic interactions among different microorganisms that could co-exist in the anodic biofilm of a MEC fed with EtOH. They firstly observed that EtOH was not consumed directly by EAB but need to be previous transformed into acetate and H_2. Subsequently, H_2 was transformed by hydrogenotrophic bacteria into CH_4 causing a large reduction in ε_{ce} in addition to the acetoclastic methanogenesis. The authors concluded that inhibition of methanogenesis is a prerequisite for driving substrate conversion into electricity.

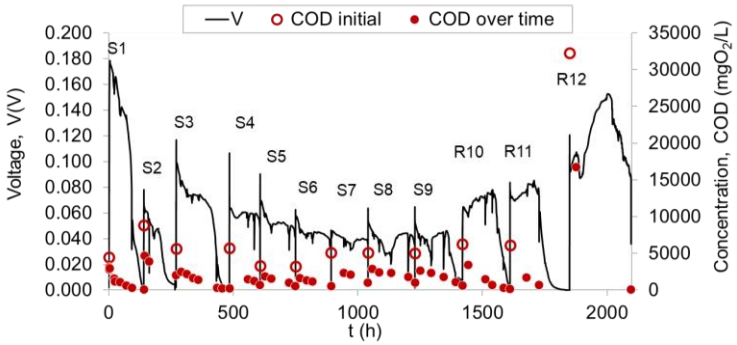

Figure 4-4 Voltage production and COD consumption over time in the MFC fed with the synthetic VFA+EtOH solution (cycles S1 - S9) and the IBES effluent (cycles R10 - R12)

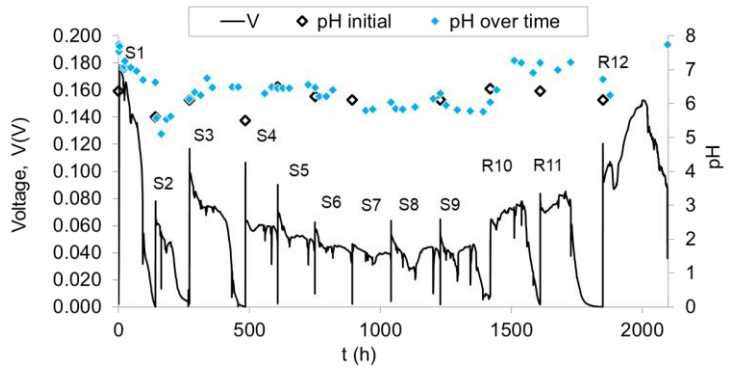

Figure 4-5 Voltage production over time and pH evolution in the MFC

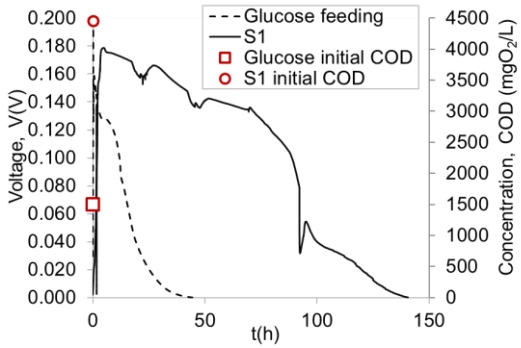

Figure 4-6 Voltage production over time during the last acclimation cycle with glucose feeding compared to the first cycle with synthetic solution (S1)

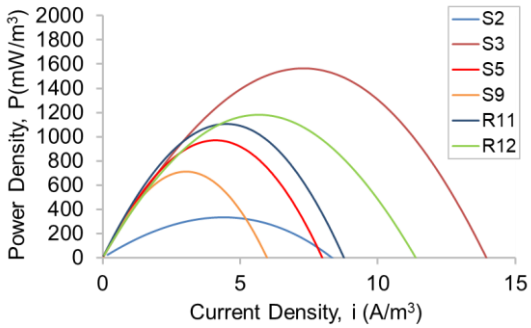

Figure 4-7 Power curves in the MFC at the beginning of each cycle with power and current density normalized to the volume of the anolyte

Table 4.4 Summary of the results in the MFC

MFC cycle code	Δt	ΔCOD	COD_{re}	C_{ex}	C_{theo}	ε_{ce}
	h	mgO_2/L	%	C	C	%
S1	140.6	4396	98.6	511	7952	6.4
S2	125.3	6758	76.8	151	12226	1.2
S3	213.8	5432	95.9	431	9828	4.4
S4	123.3	5002	87.9	259	9048	2.9
S5	142.1	2836	84.9	269	5130	5.2
S6	142.9	2678	82.4	229	4844	4.7
S7	147.9	4027	79.4	210	7286	2.9
S8	188.1	4067	80.0	263	7357	3.6
S9	191.0	4387	87.5	229	7937	2.9
R10	190.8	6146	98.0	389	11118	3.5
R11	238.8	5352	88.0	369	9682	3.8
R12	247.0	32221	99.8	1062	58291	1.8

Table 4.5 Summary of the results from LSV analysis

MFC cycle code	OCV	Max power density	Internal resistance
	V	mW/m^3	Ω
Glucose	0.422	4507	85
S2	0.140	333	118
S3	0.388	1565	202
S5	0.434	970	384
S6	0.435	742	485
S8	0.425	649	531
S9	0.443	710	520
R11	0.457	1104	369
R12	0.388	1180	248

4.3.2 MEC operation

After the acclimation cycles with the glucose feeding in the anodic compartment and the CO_2 feeding in the cathodic chamber, seven consecutive batch cycles were carried out in the MEC. The anodic chamber was filled with the synthetic solution for four cycles (S1 – S4) and with the real IBES effluent for the last three runs (R5 – R7); an external potential of 0.5 V was applied to the cell for the entire duration of the experiments. Figure 4-8 shows the electric current outputs recorded during the tests and the COD removal, while in Figure 4-9 the pH variation in both the chambers is reported. A summary of the main results is provided in Table 4.6. The electricity fluctuation observed in S1 was not related to the process but was caused by instability issues of the external applied voltage that were fixed in the subsequent runs. The process performance during cycles S2, S3 and S4 displayed a good repeatability over time and a high COD removal (~ 98%).

The electric current flow, although assisted by the application of the external potential, appeared to be correlated with COD consumption, showing a sharp decline when the latter was depleted. This was also the explanation for the slightly lower duration displayed by S3 compared to S2 and S4. In contrast to the MFC, no noticeable differences were observed in the MEC when the real effluent was used with the same influent COD (R5), probably due to the fact that the electron flow in this case was mainly supported by the applied voltage. On the other hand, the increased initial COD in R7 led to a higher overall amount of charge transferred and a longer operation time. Nevertheless, the tests displayed ε_{ce} values ranging between 9.0 and 13.7%, which proves that a large fraction of the electrons produced by COD consumption were not transferred to the electrode. As already discussed for the MFC (see section 4.3.1), many factors can contribute significantly to reducing the coulombic efficiency. In particular, oxygen infiltration in the anodic chamber could have resulted in COD consumption by facultative

bacteria rather than EAB; thus, one option to enhance the efficiency of the MEC would be to drive off air from the anodic compartment prior to the start up of the tests. Moreover, even when anaerobic conditions are fully established, the COD consumption could be operated by the methanogens potentially present in the inoculum. Lastly, it is possible that a small contribution to the carbon source depletion was due to biomass growth and also temporarily retention inside the microbial cell as energy storage.

Figure 4.10 shows the result of the LSV analysis carried out at the beginning of S3; the maximum power density was 176 mW/m^2 achieved at a 0.5 V applied potential, that corresponds to 5490 mW/m3 considering the anolyte volume.

The conversion of CO_2 to CH_4 was examined in the cathodic chamber during cycles S3, R5, and R7; Figure 4-11 shows the change in the headspace composition while Figure 4-12 displays the amount of CH_4 produced. The transition from the synthetic (S3) to the real solution (R5) with a similar influent COD concentrations did not cause considerable differences, generating CH_4 yields respectively of 0.81 and 0.76 mmol CH_4/g COD. The recovery of CH_4 compared to the expected values on the basis of the transferred charge was 49.7 % for S3 and 43.9 % for R5. A possible limitation to the achievement of the theoretical value could be given by a sub-optimal mass transfer rate considering that the chamber is not mixed. The slow dissolution of CO_2 in the medium and, after the conversion, the slow release of CH_4 into the headspace could also explain the slight delay observed in S3 between the current flow and the detection of CH_4. On the other hand, the use of a higher influent COD concentration in R7 prompted the CO_2 to CH_4 conversion thanks to the higher electron flow rate, resulting in a final FE of 74 % and an overall CH_4 yield of 0.94 mmol CH_4/g COD. In this case, the largest deviation from the theoretical production appeared after 200 hours, when the current value decreased to 1 mA. Other factors that may contribute to reducing FE include the diffusion of CH_4 through the PEM (and also H_2, if the indirect CH_4 transformation is considered) and electrons subtraction for cathodic biomass growth. Although the results of the present study suggest that the process performance may be increased by properly adjusting the system configuration, the FE values obtained are yet comparable to the cathodic efficiencies reported in the literature: 24.2±4.7% (Zhen et al. 2015), 35±6 – 55±18% (Seelajaroen et al. 2020), 65±8% and 79±17% (Cerrillo et al. 2017), 73% (van Eerten-Jansen et al. 2015), 76±7% (Villano et al. 2010), 79±2% (Villano et al. 2013), 80% (Cheng et al. 2011).

R7 displayed promising results in terms of CO_2 conversion into CH_4 with the IBES effluent as the electron donor and reached a COD removal of 99.4 %, however, further investigation on driving the electrons towards the electric circuit is needed.

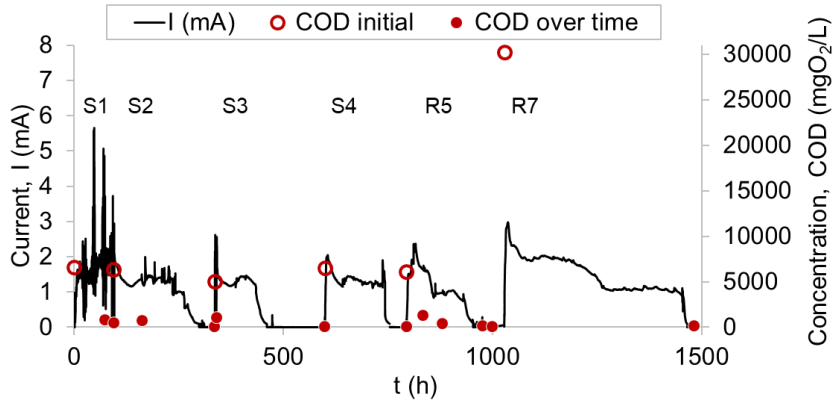

Figure 4-8 Electric current evolution and COD consumption over time in the MEC fed with the synthetic VFA+EtOH solution (cycles S1 – S4) and the IBES effluent (cycles R5 and R7)

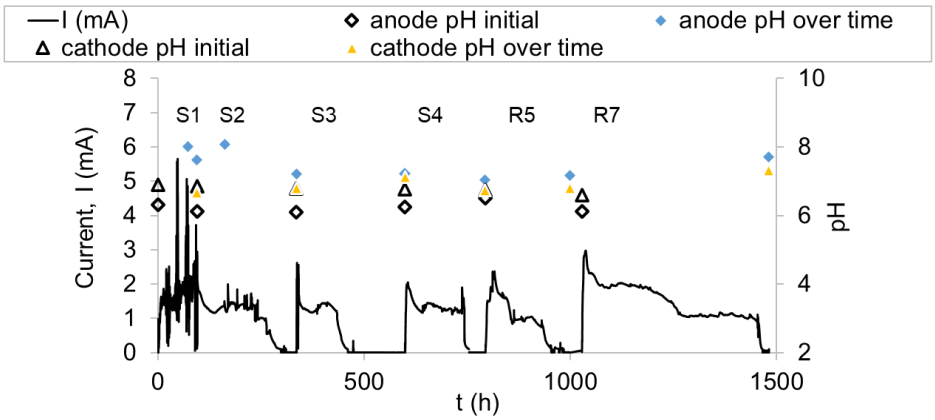

Figure 4-9 Electric current evolution and pH variation over time in the MEC fed with the synthetic VFA+EtOH solution (cycles S1 – S4) and IBES effluent (cycles R5 and R7)

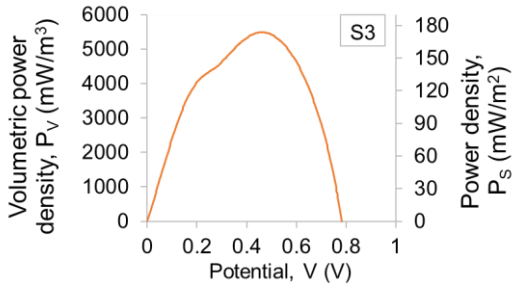

Figure 4-10 Power curve derived at the beginning of cycle S3

Table 4.6 Summary of the results in the MEC

MEC cycle code	Δt	ΔCOD	COD_{re}	C_{ex}	C_{theo}	ε_{ce}
-	h	mgO_2/L	%	C	C	%
S1	94.6	6092	92.1	531	5877	9.0
S2	241.3	6300	98.7	831	6079	13.7
S3	263.2	4915	98.0	507	4742	10.7
S4	194.6	6372*	-	711	6149*	11.6*
R5	205.2	6018	98.2	657	5806	11.3
R7	453.7	30025	99.4	2364	28969	8.2

*Final COD value for S4 is not available. Thus, it was reported ε_{ce} as a hypothetical value calculated assuming a COD_{re} of 98.3% as the average of observed values in the similar cycles S2 and S3.

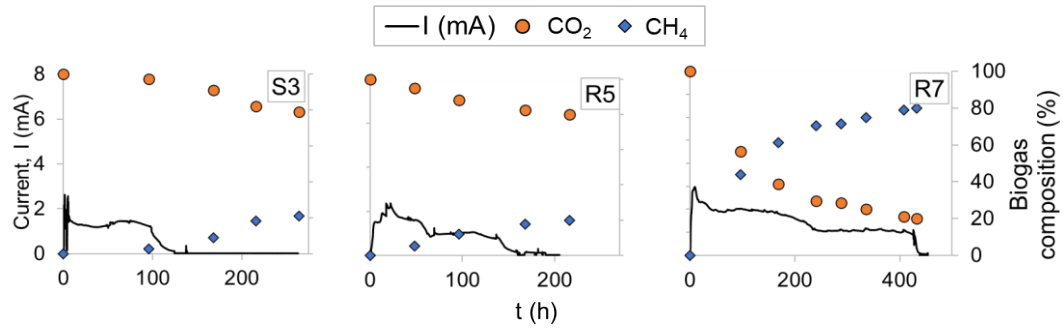

Figure 4-11 Electric current evolution over time in the MEC (cycles S3, R5, R7) and biogas composition of the cathodic headspace

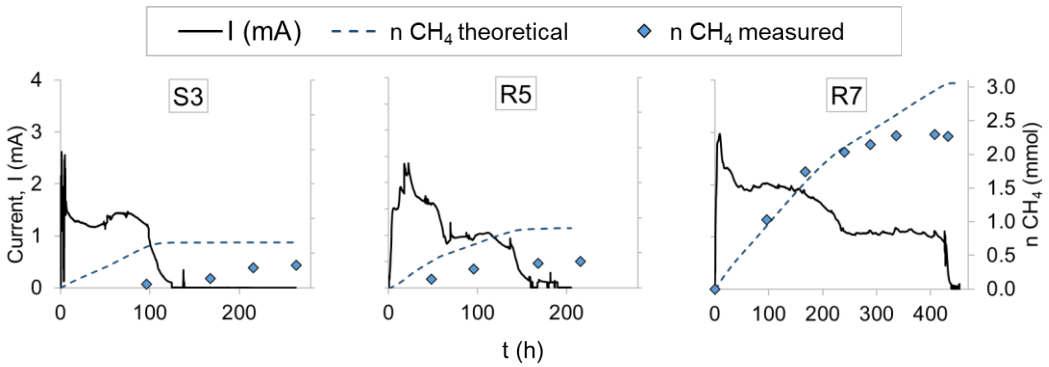

Figure 4-12 Electric current evolution over time in the MEC (cycles S3, R5, R7) and CH_4 production; the dashed lines represent the theoretical amount of CH_4 produced based on the transferred charge

Table 4.7 Main results of CO_2 conversion in the cathodic chamber of the MEC for tests S3, R5 and R7.

MEC cycle code	CH_4 theoretical	CH_4 measured	FE	CH_4 yield measured
-	mmol CH_4	mmol CH_4	%	mmol CH_4/g COD
S3	0.656	0.326	49.7	0.812
R5	0.851	0.374	43.9	0.763
R7	3.062	2.266	74.0	0.938

4.4 Conclusions

Both bio-electrochemical reactors that were tested in this phase proved to be suitable for the exploitation of the effluent deriving from the IBES of the previously experimentation.

An MFC was tested for electricity production through VFAs and ethanol consumption, which were found to be the main constituents of the IBES effluent. The MFC used also presented an innovative configuration consisting of four mullite air-cathodes connected in series, where fly-ash was the catalyst for the cathodic reaction without any necessity of oxygen supply, allowing for an attempt at containing the constructional and operative costs of this kind of reactors. The cathodes were inserted in the anodic chamber that was filled with graphite granules, serving as supporting material for the electroactive inoculum, thus forming a membrane-less single-chamber reactor. The results revealed that, after a few batch tests, the biomass was adapted to the consumption of organic acids and ethanol, although it was initially acclimatized with glucose. Furthermore, the last cycle fed with IBES effluent diluted twice (rather than ten times as in the previous cycles) showed that it is possible to use high strength substrates such as IBES effluent. The last cycle displayed a voltage output of 0.160 mV (external resistance of 100 Ω) and a maximum power density of 1180 mW/m^3. This result opens up the possibility of attempting to apply directly the undiluted effluent in future investigations.

A second option to harness the residual energy content in the IBES effluent involved a dual-chamber MEC equipped with bioanode and biocathode aimed at CO_2 upgrade to bio-methane. In the anodic chamber, the residual VFAs and ethanol served as electron and proton donors, while in the cathodic chamber the latter were used by the biomass to provide the CO_2 conversion. This type of MEC offers a considerable benefit when considering the opportunity to recirculate the CO_2 produced by the inoculum during the degradation of the substrate, thus maximizing the total energy recovery and limiting the CO_2 emission. The best result was achieved in the last cycle when the IBES effluent diluted

twice as well as in the MFC was applied, where the prolonged electron flow resulted in the conversion to methane by 80% of the starting CO_2 and 74% of the electrons recovery.

On the other hand, both MFC and MEC displayed extremely low coulombic efficiencies despite the high COD removal (higher than 76% for the MFC and 98% for the MEC). The reason might imply several factors. First of all, the energy gained from the substrate is used for biomass growth and this kind of microbial biomass also presents the possibility of temporary energy storage inside the bacteria. Moreover, oxygen infiltrations in the anodic compartments may have limited electron transfer to the cathodes. Another possible explanation may also include the use of substrate by competitive bacteria that co-exist with the electroactive microorganisms in the inoculum. Therefore, it is concluded that there is potential for further studies to clarify the dynamics involved in order to improve the processes investigated, which, in this preliminary research, have proved to be successful post-treatment options for energy recovery from the complex substrate tested.

5 Concluding remarks

The present thesis explored several aspects related to the energy recovery from organic waste, focusing on H_2 production through dark fermentation of dairy-industry residues.

In view of the full-scale application, the assessment of process stability is certainly one of the major concerns. The considerations previously mentioned extensively outlined that the criterion selected for stability evaluation may affect the interpretation of the process outcomes. The novelty underlying the first phase of this work consisted in the formulation of a quantitative criterion for the stability assessment, which was capable to recognized in detail the temporal fluctuations during biochemical H_2 production under continuous-flow conditions. In addition, the long-term process performance was investigated and the best operating conditions in terms of H_2 production yield and rate were found at HRTs ≤ 8 h and OLRs of 65–97.5 g TOC/(L·d). A survey of the most relevant metabolic routes involved in the fermentative process showed that acetate and butyrate production were the most important driving pattern towards H_2 generation. The study also outlined that homoacetogenesis was the dominant H_2 consuming pathway under all the conditions tested. Accordingly, on the basis of the findings of the present experimentation also corroborated by some recent studies in the sector, to date, the inhibition of homoacetogenic bacteria during fermentative H_2 production is deemed to be one of the most challenging issues to be tackled.

An additional outstanding point of dark fermentation is that H_2 yields generally observed among research studies can be three times (or even more) lower than those expected from a theoretical point of view, primarily due to the thermodynamic/biochemical limitations occurring within the fermentative process. In the present thesis, an attempt to address this issue was accomplished by designing a system (IBES) that combines dark fermentation with electrochemistry in order to enhance H_2 yield through a novel approach. The bio-electrochemical tests performed in the IBES, using cheese whey as substrate, achieved very promising results displaying a 3-times higher H_2 yield compared to the conventional dark fermentation; therefore, proving that any further research in this field might be worthwhile. Future perspectives include strategies to prevent the passivation of the anode, that was recognized as a possible limiting factor during the process, afterwards the potential implementation in continuous mode, in order to enable a proper energy balance of the system. Furthermore, improvements to the anodic chamber (e.g. by testing alternative materials) could be explored to further enhance the sustainability of the whole process.

Lastly, dark fermentation perspectives of real-scale application definitely involve the integration in a multi-stage scheme, where the first step is the H_2 collection and then, the organic matter retained in the

metabolic products can be further consumed in post treatment stages. To this aim, the latest topic investigated within the thesis was the feasibility of two different bio-electrochemical systems as post-processes. They were applied to the effluent deriving from the IBES of the previously experimentation since, as well as for conventional dark fermentation, part of the carbon content of the starting substrate was retained in form of organic metabolites. The systems were able to provide further valorization of the organic waste through two different approaches: in the first case, electricity was generated thanks to the consumption of the organic acids and ethanol provided by the electro-active biomass of a microbial fuel cell featuring an innovative design; in the second case, the conversion of CO_2 into bio-methane was performed using a microbial electrolysis cell that operates via the consumption of organic acids and ethanol. The results showed that both types of reactors can be valid post-treatments allowing for energy recovery from the complex substrate such as IBES or stand-alone dark fermentation effluent, thus further investigations aimed at deepening the understanding of the reactions involved and improving the system configuration might be considered to achieve greater efficiency.

The intention of this research thesis was to expand the knowledge in the field of organic waste valorization via biological and bio-electrochemical processes, in the belief that the current gap between lab-scale experimentation and full-scale implementation could be narrowed. More generally, other possible future developments in this context may include the study of different multi-stage layouts involving alternative post-treatments for the IBES effluent, for example aimed at recovering organic acids in the form of high-value substances rather than energy. Moreover, it might be of interest to explore the outcome of the same processes investigated here using cheese whey when dealing with other organic substrates such as food waste. Finally, multi-stage treatment layouts would need to be carefully assessed in terms of energy and material flows and yields as well as direct and indirect impacts and advantages in order to establish the most sustainable solution.

References

Aelterman P, Rabaey K, The Pham H, et al (2006) Continuous electricity generation at high voltages and currents using stacked microbial fuel cells. Commun Agric Appl Biol Sci 71:63–66

Aghajani Delavar M, Wang J (2021) Numerical investigation of pH control on dark fermentation and hydrogen production in a microbioreactor. Fuel 292:120355. https://doi.org/10.1016/J.FUEL.2021.120355

Akhlaghi M, Boni MR, De Gioannis G, et al (2017a) A parametric response surface study of fermentative hydrogen production from cheese whey. Bioresour Technol 244:473–483. https://doi.org/10.1016/j.biortech.2017.07.158

Akhlaghi M, Boni MR, De Gioannis G, et al (2017b) A parametric response surface study of fermentative hydrogen production from cheese whey. Bioresour Technol 244:473–483. https://doi.org/10.1016/J.BIORTECH.2017.07.158

Akhlaghi M, Boni MR, Polettini A, et al (2019) Fermentative H2 production from food waste: Parametric analysis of factor effects. Bioresour Technol 276:349–360. https://doi.org/10.1016/J.BIORTECH.2019.01.012

Alexandropoulou M, Antonopoulou G, Trably E, et al (2018) Continuous biohydrogen production from a food industry waste : Influence of operational parameters and microbial community analysis. J Clean Prod 174:1054–1063. https://doi.org/10.1016/j.jclepro.2017.11.078

Antonopoulou G, Gavala HN, Skiadas I V., Lyberatos G (2012) Modeling of fermentative hydrogen production from sweet sorghum extract based on modified ADM1. Int J Hydrogen Energy 37:191–208. https://doi.org/10.1016/J.IJHYDENE.2011.09.081

Antonopoulou G, Gavala HN, Skiadas I V, et al (2008a) Biofuels generation from sweet sorghum: fermentative hydrogen production and anaerobic digestion of the remaining biomass. Bioresour Technol 99:110–9. https://doi.org/10.1016/j.biortech.2006.11.048

Antonopoulou G, Stamatelatou K, Bebelis S, Lyberatos G (2010) Electricity generation from synthetic substrates and cheese whey using a two chamber microbial fuel cell. Biochem Eng J 50:10–15. https://doi.org/10.1016/J.BEJ.2010.02.008

Antonopoulou G, Stamatelatou K, Venetsaneas N, et al (2008b) Biohydrogen and methane production from cheese whey in a two-stage anaerobic process. Ind Eng Chem Res 47:5227–5233. https://doi.org/10.1021/ie071622x

APHA, AWWA, WEF (2017) Standard Methods for the Examination of Water and Wastewater, 23rd Edition

Arellano-García L, Velázquez-Fernández JB, Macías-Muro M, Marino-Marmolejo EN (2021) Continuous hydrogen production and microbial community profile in the dark fermentation of tequila vinasse: Response to increasing loading rates and immobilization of biomass. Biochem

Eng J 172:108049. https://doi.org/10.1016/J.BEJ.2021.108049

Arooj MF, Han SK, Kim SH, et al (2008a) Continuous biohydrogen production in a CSTR using starch as a substrate. Int J Hydrogen Energy 33:3289–3294. https://doi.org/10.1016/J.IJHYDENE.2008.04.022

Arooj MF, Han SK, Kim SH, et al (2008b) Effect of HRT on ASBR converting starch into biological hydrogen. Int J Hydrogen Energy 33:6509–6514. https://doi.org/10.1016/J.IJHYDENE.2008.06.077

Asunis F, De Gioannis G, Dessì P, et al (2020) The dairy biorefinery: Integrating treatment processes for cheese whey valorisation. J Environ Manage 276:111240. https://doi.org/10.1016/j.jenvman.2020.111240

Asunis F, De Gioannis G, Isipato M, et al (2019) Control of fermentation duration and pH to orient biochemicals and biofuels production from cheese whey. Bioresour Technol 289:121722. https://doi.org/10.1016/J.BIORTECH.2019.121722

Azbar N, Dokgöz FT, Keskin T, et al (2009a) Comparative Evaluation of Bio-Hydrogen Production From Cheese Whey Wastewater Under Thermophilic and Mesophilic Anaerobic Conditions. Int J Green Energy 6:192–200. https://doi.org/10.1080/15435070902785027

Azbar N, Dokgöz FT, Keskin T, et al (2009b) Comparative evaluation of bio-hydrogen production from cheese whey wastewater under thermophilic and mesophilic anaerobic conditions. Int J Green Energy 6:192–200. https://doi.org/10.1080/15435070902785027

Banu JR, Yukesh Kannah R, Dinesh Kumar M, et al (2018) Recent advances on biogranules formation in dark hydrogen fermentation system: Mechanism of formation and microbial characteristics. Bioresour Technol 268:787–796. https://doi.org/10.1016/J.BIORTECH.2018.07.034

Bastidas-Oyanedel JR, Bonk F, Thomsen MH, Schmidt JE (2015) Dark fermentation biorefinery in the present and future (bio)chemical industry. Rev Environ Sci Biotechnol 14:473–498. https://doi.org/10.1007/S11157-015-9369-3/TABLES/3

Benito Martin PC, Schlienz M, Greger M (2017) Production of bio-hydrogen and methane during semi-continuous digestion of maize silage in a two-stage system. Int J Hydrogen Energy 42:5768–5779. https://doi.org/10.1016/j.ijhydene.2017.01.020

Blanco VMC, Oliveira GHD, Zaiat M. Dark fermentative biohydrogen production from synthetic cheese whey in an anaerobic structured-bed reactor: Performance evaluation and kinetic modeling. Renew Energy 2019;139:1310–9. doi:10.1016/J.RENENE.2019.03.029.

Bosco F, Carletto RA, Marmo L (2018) An Integrated Cheese Whey Valorization Process. 64:

Cappai G, De Gioannis G, Friargiu M, et al (2014) An experimental study on fermentative H2 production from food waste as affected by pH. Waste Manag 34:. https://doi.org/10.1016/j.wasman.2014.04.014

Carrillo-Reyes J, Celis LB, Alatriste-Mondragón F, Razo-Flores E (2012) Different start-up strategies to enhance biohydrogen production from cheese whey in UASB reactors. Int J Hydrogen Energy

37:5591–5601. https://doi.org/10.1016/J.IJHYDENE.2012.01.004

Carrillo-Reyes J, Trably E, Bernet N, et al (2016) High robustness of a simplified microbial consortium producing hydrogen in long term operation of a biofilm fermentative reactor. Int J Hydrogen Energy 41:2367–2376. https://doi.org/10.1016/J.IJHYDENE.2015.11.131

Carvalho F, Prazeres AR, Rivas J (2013) Cheese whey wastewater: Characterization and treatment. Sci Total Environ 445–446:385–396. https://doi.org/10.1016/J.SCITOTENV.2012.12.038

Castelló E, Braga L, Fuentes L, Etchebehere C (2018) Possible causes for the instability in the H2 production from cheese whey in a CSTR. Int J Hydrogen Energy 43:2654–2665. https://doi.org/10.1016/J.IJHYDENE.2017.12.104

Castelló E, Nunes Ferraz-Junior AD, Andreani C, et al (2020) Stability problems in the hydrogen production by dark fermentation: Possible causes and solutions. Renew Sustain Energy Rev 119:. https://doi.org/10.1016/j.rser.2019.109602

Castillo Martinez FA, Balciunas EM, Salgado JM, et al (2013) Lactic acid properties, applications and production: A review. Trends Food Sci Technol 30:70–83. https://doi.org/10.1016/J.TIFS.2012.11.007

Cerrillo M, Vinas M, Bonmatí A (2017) Startup of Electromethanogenic Microbial Electrolysis Cells with Two Different Biomass Inocula for Biogas Upgrading. ACS Sustain Chem Eng 5:8852–8859. https://doi.org/10.1021/ACSSUSCHEMENG.7B01636/SUPPL_FILE/SC7B01636_SI_001.PDF

Chae K-J, Choi M-J, Lee J, et al (2008) Biohydrogen production via biocatalyzed electrolysis in acetate-fed bioelectrochemical cells and microbial community analysis. Int J Hydrogen Energy 33:5184–5192. https://doi.org/10.1016/J.IJHYDENE.2008.05.013

Cheng KY, Ho G, Cord-Ruwisch R (2011) Novel methanogenic rotatable bioelectrochemical system operated with polarity inversion. Environ Sci Technol 45:796–802. https://doi.org/10.1021/ES102482J/SUPPL_FILE/ES102482J_SI_001.PDF

Cheng S, Liu H, Logan BE (2006) Increased Power Generation in a Continuous Flow MFC with Advective Flow through the Porous Anode and Reduced Electrode Spacing. https://doi.org/10.1021/es051652w

Cheng S, Logan BE (2007) Sustainable and efficient biohydrogen production via electrohydrogenesis. PNAS 104:. https://doi.org/10.1111/j.1365

Cheng S, Xing D, Call DF, Logan BE (2009) Direct biological conversion of electrical current into methane by electromethanogenesis. Environ Sci Technol 43:3953–3958. https://doi.org/10.1021/es803531g

Choi JDR, Chang HN, Han JI (2011) Performance of microbial fuel cell with volatile fatty acids from food wastes. Biotechnol Lett 33:705–714. https://doi.org/10.1007/S10529-010-0507-2/TABLES/2

Chookaew T, Prasertsan P, Ren ZJ (2014) Two-stage conversion of crude glycerol to energy using dark fermentation linked with microbial fuel cell or microbial electrolysis cell. N Biotechnol 31:179–184. https://doi.org/10.1016/J.NBT.2013.12.004

Da Silva Veras T, Mozer TS, da Costa Rubim Messeder dos Santos D, da Silva César A (2017) Hydrogen: Trends, production and characterization of the main process worldwide. Int. J. Hydrogen Energy

Davila-Vazquez G, Cota-Navarro CB, Rosales-Colunga LM, et al (2009) Continuous biohydrogen production using cheese whey: Improving the hydrogen production rate. Int J Hydrogen Energy 34:4296–4304. https://doi.org/10.1016/j.ijhydene.2009.02.063

De Gioannis G, Friargiu M, Massi E, et al (2014) Biohydrogen production from dark fermentation of cheese whey: Influence of pH. Int J Hydrogen Energy 39:. https://doi.org/10.1016/j.ijhydene.2014.10.046

De Gioannis G, Muntoni A, Polettini A, Pomi R (2013) A review of dark fermentative hydrogen production from biodegradable municipal waste fractions. Waste Manag 33:1345–1361. https://doi.org/10.1016/J.WASMAN.2013.02.019

Dębowski M, Korzeniewska E, Filipkowska Z, et al (2014) Possibility of hydrogen production during cheese whey fermentation process by different strains of psychrophilic bacteria. Int J Hydrogen Energy 39:1972–1978. https://doi.org/10.1016/j.ijhydene.2013.11.082

Del Pilar Anzola-Rojas M, Da Fonseca SG, Da Silva CC, et al (2015) The use of the carbon/nitrogen ratio and specific organic loading rate as tools for improving biohydrogen production in fixed-bed reactors. Biotechnol Reports 5:46–54. https://doi.org/10.1016/J.BTRE.2014.10.010

Dessì P, Lakaniemi AM, Lens PNL (2017) Biohydrogen production from xylose by fresh and digested activated sludge at 37, 55 and 70 °C. Water Res 115:120–129. https://doi.org/10.1016/j.watres.2017.02.063

Dinamarca C, Bakke R (2009) Apparent hydrogen consumption in acid reactors: observations and implications. Water Sci Technol 59:1441–1447. https://doi.org/10.2166/WST.2009.135

Dinamarca C, Gañán M, Liu J, Bakke R (2011) H2 consumption by anaerobic non-methanogenic mixed cultures. Water Sci Technol 63:1582–1589. https://doi.org/10.2166/WST.2011.214

Dubois M, Gilles KA, Hamilton JK, et al (1956) Colorimetric Method for Determination of Sugars and Related Substances. Anal Chem 28:350–356. https://doi.org/10.1021/ac60111a017

DuBois M, Gilles KA, Hamilton JK, et al (2002) Colorimetric Method for Determination of Sugars and Related Substances. Microb Cell Fact 8:59. https://doi.org/10.1021/AC60111A017

Elbeshbishy E, Dhar BR, Nakhla G, Lee HS (2017) A critical review on inhibition of dark biohydrogen fermentation. Renew. Sustain. Energy Rev.

Etchebehere C, Castelló E, Wenzel J, et al (2016) Microbial communities from 20 different hydrogen-producing reactors studied by 454 pyrosequencing. Appl Microbiol Biotechnol 100:3371–3384. https://doi.org/10.1007/S00253-016-7325-Y/FIGURES/5

European Commission (2019) The European Green Deal. https://eur-lex.europa.eu/legal-content/EN/TXT/?qid=1576150542719&uri=COM%3A2019%3A640%3AFIN

Ferchichi M, Crabbe E, Gil G-H, et al (2005) Influence of initial pH on hydrogen production from cheese whey. J Biotechnol 120:402–409. https://doi.org/10.1016/j.jbiotec.2005.05.017

Ferraz Júnior ADN, Etchebehere C, Zaiat M (2015) High organic loading rate on thermophilic hydrogen production and metagenomic study at an anaerobic packed-bed reactor treating a residual liquid stream of a Brazilian biorefinery. Bioresour Technol 186:81–88. https://doi.org/10.1016/J.BIORTECH.2015.03.035

Ferreira Rosa PR, Santos SC, Silva EL (2014a) Different ratios of carbon sources in the fermentation of cheese whey and glucose as substrates for hydrogen and ethanol production in continuous reactors. Int J Hydrogen Energy 39:1288–1296. https://doi.org/10.1016/j.ijhydene.2013.11.011

Ferreira Rosa PR, Santos SC, Silva EL (2014b) Different ratios of carbon sources in the fermentation of cheese whey and glucose as substrates for hydrogen and ethanol production in continuous reactors. Int J Hydrogen Energy 39:1288–1296

Freguia S, Rabaey K, Yuan Z, Keller J (2007) Electron and carbon balances in microbial fuel cells reveal temporary bacterial storage behavior during electricity generation. Environ Sci Technol 41:2915–2921. https://doi.org/10.1021/ES062611I/SUPPL_FILE/ES062611ISI20070208_110248.PDF

Fuess LT, Ferraz ADN, Machado CB, Zaiat M (2018) Temporal dynamics and metabolic correlation between lactate-producing and hydrogen-producing bacteria in sugarcane vinasse dark fermentation: The key role of lactate. Bioresour Technol 247:426–433. https://doi.org/10.1016/j.biortech.2017.09.121

García-Depraect O, Muñoz R, Rodríguez E, et al (2021) Microbial ecology of a lactate-driven dark fermentation process producing hydrogen under carbohydrate-limiting conditions. Int J Hydrogen Energy 46:11284–11296. https://doi.org/10.1016/J.IJHYDENE.2020.08.209

Gavala HN, Skiadas I V., Ahring BK (2006) Biological hydrogen production in suspended and attached growth anaerobic reactor systems. Int J Hydrogen Energy 31:1164–1175. https://doi.org/10.1016/J.IJHYDENE.2005.09.009

Ghimire A, Frunzo L, Pirozzi F, et al (2015) A review on dark fermentative biohydrogen production from organic biomass: Process parameters and use of by-products. Appl Energy 144:73–95. https://doi.org/10.1016/J.APENERGY.2015.01.045

Ghimire A, Luongo V, Frunzo L, et al (2017) Continuous biohydrogen production by thermophilic dark fermentation of cheese whey: Use of buffalo manure as buffering agent. Int J Hydrogen Energy 42:4861–4869. https://doi.org/10.1016/j.ijhydene.2016.11.185

Gokfiliz-Yildiz P, Karapinar I (2018) Optimization of particle number, substrate concentration and temperature of batch immobilized reactor system for biohydrogen production by dark fermentation. Int J Hydrogen Energy 43:10655–10665. https://doi.org/10.1016/J.IJHYDENE.2018.01.036

Gomes BC, Rosa PRF, Etchebehere C, et al (2015) Role of homo-and heterofermentative lactic acid bacteria on hydrogen-producing reactors operated with cheese whey wastewater. Int J Hydrogen Energy 40:8650–8660. https://doi.org/10.1016/j.ijhydene.2015.05.035

Guellout Z, Clion V, Benguerba Y, Dumas C, Ernst B. Study of the dark fermentative hydrogen production using modified ADM1 models. Biochem Eng J 2018;132:9–19. doi:10.1016/J.BEJ.2017.12.015.

Guo R, Wang B, Jia Y, Wang M (2017) Development of acid block anion exchange membrane by structure design and its possible application in waste acid recovery. Sep Purif Technol 186:188–196. https://doi.org/10.1016/J.SEPPUR.2017.06.006

Guo XM, Trably E, Latrille E, et al (2010) Hydrogen production from agricultural waste by dark fermentation: A review. Int J Hydrogen Energy. https://doi.org/doi:10.1016/j.ijhydene.2010.03.008

Hafez H, Nakhla G, El. Naggar MH, et al (2010) Effect of organic loading on a novel hydrogen bioreactor. Int J Hydrogen Energy 35:81–92. https://doi.org/10.1016/J.IJHYDENE.2009.10.051

Hallenbeck PC (2009) Fermentative hydrogen production: Principles, progress, and prognosis. Int J Hydrogen Energy 34:7379–7389. https://doi.org/10.1016/j.ijhydene.2008.12.080

Hallenbeck PC, Abo-Hashesh M, Ghosh D (2012) Strategies for improving biological hydrogen production. Bioresour. Technol.

Hernández-Mendoza C, Buitrón G (2014) Suppression of methanogenic activity in anaerobic granular biomass for hydrogen production. J Chem Technol Biotechnol 89:143–149. https://doi.org/10.1002/JCTB.4143

Hitit ZY, Hallenbeck PC (2021) Analytical procedures, data reporting and selected reference values for biological hydrogen production. Biomass and Bioenergy 147:106014. https://doi.org/10.1016/j.biombioe.2021.106014

IEA (2021) World Energy Outlook 2021 – Analysis - IEA. https://www.iea.org/reports/world-energy-outlook-2021. Accessed 24 Nov 2021

IEA (2019) World Energy Outlook 2019 – Analysis - IEA. https://www.iea.org/reports/world-energy-outlook-2019. Accessed 23 Mar 2020

Jafary T, Wan Daud WR, Ghasemi M, et al (2018) Clean hydrogen production in a full biological microbial electrolysis cell. Int J Hydrogen Energy. https://doi.org/10.1016/J.IJHYDENE.2018.01.010

Jeremiasse AW, Hamelers HVM, Buisman CJN (2010) Microbial electrolysis cell with a microbial biocathode. Bioelectrochemistry 78:39–43. https://doi.org/10.1016/J.BIOELECHEM.2009.05.005

Jia X, Wang Y, Ren L, et al (2019) Early warning indicators and microbial community dynamics during unstable stages of continuous hydrogen production from food wastes by thermophilic dark fermentation. Int J Hydrogen Energy 44:30000–30013.

https://doi.org/10.1016/j.ijhydene.2019.08.082

Jones DT, Woods DR (1986) Acetone-butanol fermentation revisited. Microbiol Rev 50:484–524. https://doi.org/10.1128/mmbr.50.4.484-524.1986

Jones RJ, Massanet-Nicolau J, Mulder MJJ, et al (2017) Increased biohydrogen yields, volatile fatty acid production and substrate utilisation rates via the electrodialysis of a continually fed sucrose fermenter. Bioresour Technol 229:46–52. https://doi.org/10.1016/j.biortech.2017.01.015

Khanal SK, Chen WH, Li L, Sung S (2004) Biological hydrogen production: Effects of pH and intermediate products. Int J Hydrogen Energy 29:1123–1131. https://doi.org/10.1016/j.ijhydene.2003.11.002

Kim IS, Hwang MH, Jang NJ, et al (2004) Effect of low pH on the activity of hydrogen utilizing methanogen in bio-hydrogen process. Int J Hydrogen Energy 29:1133–1140. https://doi.org/10.1016/J.IJHYDENE.2003.08.017

Kim JR, Cheng S, Oh S-E, Logan BE (2007a) Power Generation Using Different Cation, Anion, and Ultrafiltration Membranes in Microbial Fuel Cells. Environ Sci Technol. https://doi.org/10.1021/es062202m

Kim JR, Jung SH, Regan JM, Logan BE (2007b) Electricity generation and microbial community analysis of alcohol powered microbial fuel cells. Bioresour Technol 98:2568–2577. https://doi.org/10.1016/j.biortech.2006.09.036

Kraemer JT, Bagley DM (2007) Improving the yield from fermentative hydrogen production. Biotechnol Lett 29:685–695. https://doi.org/10.1007/s10529-006-9299-9

Kroeker EJ, Schulte DD, Sparling AB, Lapp HM (1979) Anaerobic Treatment Process Stability. In: J. (Water Pollut. Control Fed. https://www.jstor.org/stable/25039893. Accessed 1 Dec 2021

Kumar G, Bakonyi P, Sivagurunathan P, et al (2015) Improved microbial conversion of de-oiled Jatropha waste into biohydrogen via inoculum pretreatment: Process optimization by experimental design approach. Biofuel Res J 2:209–214. https://doi.org/10.18331/BRJ2015.2.1.7

Kumar G, Sivagurunathan P, Park JH, et al (2016) HRT dependent performance and bacterial community population of granular hydrogen-producing mixed cultures fed with galactose. Bioresour Technol 206:188–194. https://doi.org/10.1016/J.BIORTECH.2016.01.104

Kyazze G, Martinez-Perez N, Dinsdale R, et al (2006) Influence of substrate concentration on the stability and yield of continuous biohydrogen production. Biotechnol Bioeng 93:971–979. https://doi.org/10.1002/BIT.20802

Lawrence AW, McCarty LP. Kinetics of methane fermentation in anaerobic treatment. J Water Pollut Control Fed 1969;41:R1–17.

Lee HS, Rittmann BE (2009) Evaluation of metabolism using stoichiometry in fermentative biohydrogen. Biotechnol Bioeng 102:749–758. https://doi.org/10.1002/bit.22107

Lin PJ, Chang JS, Yang LH, et al (2011) Enhancing the performance of pilot-scale fermentative hydrogen production by proper combinations of HRT and substrate concentration. Int J Hydrogen Energy 36:14289–14294. https://doi.org/10.1016/j.ijhydene.2011.04.147

Liu C-G, Xue C, Lin Y-H, Bai F-W (2013) Redox potential control and applications in microaerobic and anaerobic fermentations. Biotechnol Adv 31:257–265. https://doi.org/10.1016/J.BIOTECHADV.2012.11.005

Liu H, Cheng S, Logan BE (2005a) Production of electricity from acetate or butyrate using a single-chamber microbial fuel cell. Environ Sci Technol 39:658–662. https://doi.org/10.1021/es048927c

Liu H, Grot S, Logan BE (2005b) Electrochemically Assisted Microbial Production of Hydrogen from Acetate. https://doi.org/10.1021/es050244p

Liu H, Logan B (2004) Electricity generation using an air-cathode single chamber microbial fuel cell (MFC) in the absence of a proton exchange membrane. ACS Natl Meet B Abstr 228:4040–4046

Liu Q, Zhang X, Yu L, et al (2011) Fermentative hydrogen production from fresh leachate in batch and continuous bioreactors. Bioresour Technol 102:5411–5417. https://doi.org/10.1016/j.biortech.2010.10.061

Liu YQ, Liu Y, Tay JH (2004) The effects of extracellular polymeric substances on the formation and stability of biogranules. Appl Microbiol Biotechnol 65:143–148. https://doi.org/10.1007/S00253-004-1657-8

Ljungdahl LG, Hugenholtz J, Wiegel J (1989) Acetogenic and Acid-Producing Clostridia. In: Clostridia. Springer US, Boston, MA, pp 145–191

Logan B, Hamelers B, Rozendal R, et al (2006) Microbial Fuel Cells: Methodology and Technology. 40:5181–5192. https://doi.org/10.1021/es0605016

Lopez-Hidalgo AM, Alvarado-Cuevas ZD, De Leon-Rodriguez A (2018) Biohydrogen production from mixtures of agro-industrial wastes: Chemometric analysis, optimization and scaling up. Energy 159:32–41. https://doi.org/10.1016/j.energy.2018.06.124

Łukajtis R, Hołowacz I, Kucharska K, et al (2018) Hydrogen production from biomass using dark fermentation. Renew Sustain Energy Rev 91:665–694. https://doi.org/10.1016/j.rser.2018.04.043

Micolucci F, Gottardo M, Pavan P, et al (2018) Pilot scale comparison of single and double-stage thermophilic anaerobic digestion of food waste. J Clean Prod 171:1376–1385. https://doi.org/10.1016/J.JCLEPRO.2017.10.080

Mikheeva ER, Katraeva I V., Kovalev AA, et al (2021) The start-up of continuous biohydrogen production from cheese whey: Comparison of inoculum pretreatment methods and reactors with moving and fixed polyurethane carriers. Appl Sci 11:1–16. https://doi.org/10.3390/app11020510

Montecchio D, Yuan Y, Malpei F (2018) Hydrogen production dynamic during cheese whey Dark Fermentation: New insights from modelization. Int J Hydrogen Energy 43:17588–17601.

https://doi.org/10.1016/J.IJHYDENE.2018.07.146

Montgomery DC (2019) Introduction to Statistical Quality Control, 8th edn. John Wiley & Sons, Inc

Montiel-Corona V, Palomo-Briones R, Razo-Flores E (2020) Continuous thermophilic hydrogen production from an enzymatic hydrolysate of agave bagasse: Inoculum origin, homoacetogenesis and microbial community analysis. Bioresour Technol 306:123087. https://doi.org/10.1016/j.biortech.2020.123087

Moscoviz R, Toledo-Alarcón J, Trably E, Bernet N (2016) Electro-Fermentation: How To Drive Fermentation Using Electrochemical Systems. Trends Biotechnol. 34:856–865

Moscoviz R, Trably E, Bernet N, Carrère H (2018) The environmental biorefinery: state-of-the-art on the production of hydrogen and value-added biomolecules in mixed-culture fermentation. Green Chem

Muñoz-Páez KM, Alvarado-Michi EL, Moreno-Andrade I, et al (2020) Comparison of suspended and granular cell anaerobic bioreactors for hydrogen production from acid agave bagasse hydrolyzates. Int J Hydrogen Energy 45:275–285. https://doi.org/10.1016/j.ijhydene.2019.10.232

Nelabhotla ABT, Dinamarca C (2019) Bioelectrochemical CO 2 reduction to methane: MES integration in biogas production processes. Appl Sci 9:16–18. https://doi.org/10.3390/app9061056

Nigam PS, Singh A (2011) Production of liquid biofuels from renewable resources. Prog. Energy Combust. Sci.

Noike T, Takabatake H, Mizuno O, Ohba M (2002) Inhibition of hydrogen fermentation of organic wastes by lactic acid bacteria. Int J Hydrogen Energy 27:1367–1371. https://doi.org/10.1016/S0360-3199(02)00120-9

OECD-FAO (2019) Prospettive Agricole OCSE-FAO 2018-2027. https://www.fao.org/publications/card/en/c/I9166IT/. Accessed 24 Nov 2021

Oh S, Min B, Logan BE (2004) Cathode performance as a factor in electricity generation in microbial fuel cells. Environ Sci Technol 38:4900–4904. https://doi.org/10.1021/es049422p

Ottaviano LM, Ramos LR, Botta LS, et al (2017) Continuous thermophilic hydrogen production from cheese whey powder solution in an anaerobic fluidized bed reactor: Effect of hydraulic retention time and initial substrate concentration. Int J Hydrogen Energy 42:4848–4860. https://doi.org/10.1016/j.ijhydene.2016.11.168

Paiano P, Menini M, Zeppilli M, et al (2019) Electro-fermentation and redox mediators enhance glucose conversion into butyric acid with mixed microbial cultures. Bioelectrochemistry 130:. https://doi.org/10.1016/j.bioelechem.2019.107333

Pakarinen O, Lehtomäki A, Rintala J (2008) Batch dark fermentative hydrogen production from grass silage: The effect of inoculum, pH, temperature and VS ratio. Int J Hydrogen Energy 33:594–601. https://doi.org/10.1016/j.ijhydene.2007.10.008

Palomo-Briones R, Razo-Flores E, Bernet N, Trably E (2017) Dark-fermentative biohydrogen pathways and microbial networks in continuous stirred tank reactors: Novel insights on their control. Appl Energy 198:77–87. https://doi.org/10.1016/j.apenergy.2017.04.051

Palomo-Briones R, Trably E, López-Lozano NE, et al (2018) Hydrogen metabolic patterns driven by Clostridium-Streptococcus community shifts in a continuous stirred tank reactor. Appl Microbiol Biotechnol 102:2465–2475. https://doi.org/10.1007/s00253-018-8737-7

Parameswaran P, Torres CI, Lee HS, et al (2009) Syntrophic interactions among anode respiring bacteria (ARB) and non-ARB in a biofilm anode: Electron balances. Biotechnol Bioeng 103:513–523. https://doi.org/10.1002/bit.22267

Park DH, Zeikus JG (2003) Improved fuel cell and electrode designs for producing electricity from microbial degradation. Biotechnol Bioeng 81:348–355. https://doi.org/10.1002/bit.10501

Park JH, Chandrasekhar K, Jeon BH, et al (2021) State-of-the-art technologies for continuous high-rate biohydrogen production. Bioresour Technol 320:124304. https://doi.org/10.1016/j.biortech.2020.124304

Pawar SS, Van Niel EWJ (2013) Thermophilic biohydrogen production: How far are we? Appl Microbiol Biotechnol 97:7999–8009. https://doi.org/10.1007/S00253-013-5141-1/TABLES/1

Perera KRJ, Ketheesan B, Gadhamshetty V, Nirmalakhandan N (2010) Fermentative biohydrogen production: Evaluation of net energy gain. Int J Hydrogen Energy 35:12224–12233. https://doi.org/10.1016/J.IJHYDENE.2010.08.037

Polettini A, Pomi R, Rossi A, Zonfa T, De Gioannis G, Muntoni A. (2022) Continuous biohydrogen production from cheese whey - Factor-based assessment (submitted paper)

Potter MC (1911) Electrical effects accompanying the decomposition of organic compounds. Proc R Soc London Ser B, Contain Pap a Biol Character 84:260–276. https://doi.org/10.1098/rspb.1911.0073

Ramos LR, de Menezes CA, Soares LA, et al (2020) Controlling methane and hydrogen production from cheese whey in an EGSB reactor by changing the HRT. Bioprocess Biosyst Eng 43:673–684. https://doi.org/10.1007/s00449-019-02265-9

Ramos LR, Silva EL (2018) Continuous hydrogen production from cofermentation of sugarcane vinasse and cheese whey in a thermophilic anaerobic fluidized bed reactor. Int J Hydrogen Energy 43:13081–13089. https://doi.org/10.1016/j.ijhydene.2018.05.070

Rao R, Basak N (2021) Optimization and modelling of dark fermentative hydrogen production from cheese whey by Enterobacter aerogenes 2822. Int J Hydrogen Energy 46:1777–1800. https://doi.org/10.1016/j.ijhydene.2020.10.142

Rivera I, Buitrón G, Bakonyi P, et al (2015) Hydrogen production in a microbial electrolysis cell fed with a dark fermentation effluent. J Appl Electrochem 45:1223–1229. https://doi.org/10.1007/s10800-015-0864-6

Rossi R, Evans PJ, Logan BE (2019) Impact of flow recirculation and anode dimensions on

performance of a large scale microbial fuel cell. J Power Sources 412:294–300. https://doi.org/10.1016/j.jpowsour.2018.11.054

Rozenfeld S, Schechter M, Teller H, et al (2017) Novel RuCoSe as non-platinum catalysts for oxygen reduction reaction in microbial fuel cells. J Power Sources 362:140–146. https://doi.org/10.1016/j.jpowsour.2017.07.022

Rozenfeld S, Teller H, Schechter M, et al (2018) Exfoliated molybdenum di-sulfide (MoS2) electrode for hydrogen production in microbial electrolysis cell. Bioelectrochemistry 123:201–210. https://doi.org/10.1016/j.bioelechem.2018.05.007

Saady NMC (2013) Homoacetogenesis during hydrogen production by mixed cultures dark fermentation: Unresolved challenge. Int J Hydrogen Energy 38:13172–13191. https://doi.org/10.1016/J.IJHYDENE.2013.07.122

Sánchez C, Dessì P, Duffy M, Lens PNL (2020) Microbial electrochemical technologies: Electronic circuitry and characterization tools. Biosens. Bioelectron. 150:111884

Santoro C, Arbizzani C, Erable B, Ieropoulos I (2017) Microbial fuel cells: From fundamentals to applications. A review. J Power Sources. https://doi.org/10.1016/j.jpowsour.2017.03.109

Schievano A, Pepé Sciarria T, Vanbroekhoven K, et al (2016) Electro-Fermentation – Merging Electrochemistry with Fermentation in Industrial Applications. Trends Biotechnol. 34:866–878

Schut GJ, Adams MWW (2009) The iron-hydrogenase of Thermotoga maritima utilizes ferredoxin and NADH synergistically: A new perspective on anaerobic hydrogen production. J Bacteriol 191:4451–4457. https://doi.org/10.1128/JB.01582-08

Seelajaroen H, Spiess S, Haberbauer M, et al (2020) Enhanced methane producing microbial electrolysis cells for wastewater treatment using poly(neutral red) and chitosan modified electrodes. Sustain Energy Fuels 4:4238–4248. https://doi.org/10.1039/d0se00770f

Selembo PA, Merrill MD, Logan BE (2010) Hydrogen production with nickel powder cathode catalysts in microbial electrolysis cells. Int J Hydrogen Energy 35:428–437. https://doi.org/10.1016/j.ijhydene.2009.11.014

Serra PMD, Espírito-Santo A, Magrinho M (2020) A steady-state electrical model of a microbial fuel cell through multiple-cycle polarization curves. Renew Sustain Energy Rev 117:109439. https://doi.org/10.1016/j.rser.2019.109439

Shao W, Wang Q, Rupani PF, et al (2020) Biohydrogen production via thermophilic fermentation: A prospective application of Thermotoga species. Energy 197:117199. https://doi.org/10.1016/j.energy.2020.117199

Si B, Li J, Li B, et al (2015) The role of hydraulic retention time on controlling methanogenesis and homoacetogenesis in biohydrogen production using upflow anaerobic sludge blanket (UASB) reactor and packed bed reactor (PBR). Int J Hydrogen Energy 40:11414–11421. https://doi.org/10.1016/j.ijhydene.2015.04.035

Siegrist H, Vogt D, Garcia-Heras JL, Gujer W. Mathematical model for meso- and thermophilic

anaerobic sewage sludge digestion. Environ Sci Technol 2002;36:1113–23. doi:10.1021/es010139p.

Sikora A, Błaszczyk M, Jurkowski M, Zielenkiewicz U (2013) Lactic Acid Bacteria in Hydrogen-Producing Consortia: On Purpose or by Coincidence? In: Kongo JM (ed) Lactic Acid Bacteria - R & D for Food, Health and Livestock Purposes. InTech

Silva AN da, Macêdo WV, Sakamoto IK, et al (2019) Biohydrogen production from dairy industry wastewater in an anaerobic fluidized-bed reactor. Biomass and Bioenergy 120:257–264. https://doi.org/10.1016/j.biombioe.2018.11.025

Sivagurunathan P, Anburajan P, Kumar G, Kim SH (2016) Effect of hydraulic retention time (HRT) on biohydrogen production from galactose in an up-flow anaerobic sludge blanket reactor. Int J Hydrogen Energy 41:21670–21677. https://doi.org/10.1016/j.ijhydene.2016.06.047

Slobodkin A, Reysenbach AL, Mayer F, Wiegel J (1997) Isolation and characterization of the homoacetogenic thermophilic bacterium Moorella glycerini sp. nov. Int J Syst Bacteriol 47:969–974. https://doi.org/10.1099/00207713-47-4-969/CITE/REFWORKS

Soares JF, Confortin TC, Todero I, et al (2020) Dark fermentative biohydrogen production from lignocellulosic biomass: Technological challenges and future prospects. Renew Sustain Energy Rev 117:. https://doi.org/10.1016/j.rser.2019.109484

Soetaert K, van den Meersche K, van Oevelen D (2009) limSolve: Solving Linear Inverse Models. R package version 1.5

Son S, Koo B, Chai H, et al (2021) Comparison of hydrogen production and system performance in a microbial electrolysis cell containing cathodes made of non-platinum catalysts and binders. J Water Process Eng 40:101844. https://doi.org/10.1016/j.jwpe.2020.101844

Spirito CM, Richter H, Rabaey K, et al (2014) Chain elongation in anaerobic reactor microbiomes to recover resources from waste. Curr Opin Biotechnol 27:115–122. https://doi.org/10.1016/j.copbio.2014.01.003

Tapia-Venegas E, Ramirez-Morales JE, Silva-Illanes F, et al (2015) Biohydrogen production by dark fermentation: scaling-up and technologies integration for a sustainable system. Rev Environ Sci Biotechnol 14:761–785. https://doi.org/10.1007/s11157-015-9383-5

Tenca A, Schievano A, Perazzolo F, et al (2011) Biohydrogen from thermophilic co-fermentation of swine manure with fruit and vegetable waste: Maximizing stable production without pH control. Bioresour Technol 102:8582–8588. https://doi.org/10.1016/j.biortech.2011.03.102

Thauer RK, Jungermann K, Decker K (1977a) Energy conservation in chemotrophic anaerobic bacteria. Bacteriol Rev 41:100–80

Thauer RK, Jungermann K, Decker K (1977b) Energy Conservation in Chemotrophic Anaerobic Bacteria. Bacteriol Rev 41:100–180. https://doi.org/10.1108/eb027807

Toledo-Alarcón J, Moscoviz R, Trably E, Bernet N (2019) Glucose electro-fermentation as main driver for efficient H2-producing bacteria selection in mixed cultures. Int J Hydrogen Energy 4:2230–

2238. https://doi.org/10.1016/j.ijhydene.2018.07.091

Tremouli A, Antonopoulou G, Bebelis S, Lyberatos G (2013) Operation and characterization of a microbial fuel cell fed with pretreated cheese whey at different organic loads. Bioresour Technol 131:380–389. https://doi.org/10.1016/j.biortech.2012.12.173

Tremouli A, Karydogiannis I, Pandis PK, et al (2019a) Bioelectricity production from fermentable household waste extract using a single chamber microbial fuel cell. Energy Procedia 161:2–9. https://doi.org/10.1016/j.egypro.2019.02.051

Tremouli A, Kamperidis T, Pandis PK, et al (2021) Exploitation of Digestate from Thermophilic and Mesophilic Anaerobic Digesters Fed with Fermentable Food Waste Using the MFC Technology. Waste and Biomass Valorization 12:5361–5370. https://doi.org/10.1007/s12649-021-01414-0

Tremouli A, Pandis PK, Karydogiannis I, et al (2019b) Operation and Electro(chemical) characterization of a microbial fuel cell stack fed with fermentable household waste extract. Glob NEST J 21:253–257. https://doi.org/10.30955/gnj.002996

UN (2019) World Population Prospects 2019

UNEP (2021) UNEP Food Waste Index Report 2021 | UNEP - UN Environment Programme. https://www.unep.org/resources/report/unep-food-waste-index-report-2021. Accessed 25 Nov 2021

UNFCCC (2021) Glasgow Climate Change Conference – October-November 2021 | UNFCCC. https://unfccc.int/conference/glasgow-climate-change-conference-october-november-2021. Accessed 24 Nov 2021

Valentín-Reyes J, García-Reyes RB, García-González A, Álvarez-Valencia LH, Rivas-García P, Cerino-Córdova F de J. Mathematical modelling for biohydrogen production by Clostridium beijerinckii. Int J Hydrogen Energy 2018;43:17602–10. doi:10.1016/J.IJHYDENE.2018.07.200

Van Eerten-Jansen MCAA, Jansen NC, Plugge CM, et al (2015) Analysis of the mechanisms of bioelectrochemical methane production by mixed cultures. J Chem Technol Biotechnol 90:963–970. https://doi.org/10.1002/jctb.4413

Van Ginkel S, Logan BE (2005) Inhibition of biohydrogen production by undissociated acetic and butyric acids. Environ Sci Technol 39:9351–9356. https://doi.org/10.1021/es0510515

Venetsaneas N, Antonopoulou G, Stamatelatou K, et al (2009) Using cheese whey for hydrogen and methane generation in a two-stage continuous process with alternative pH controlling approaches. Bioresour Technol 100:3713–7. https://doi.org/10.1016/j.biortech.2009.01.025

Villano M, Aulenta F, Ciucci C, et al (2010) Bioelectrochemical reduction of CO2 to CH4 via direct and indirect extracellular electron transfer by a hydrogenophilic methanogenic culture. Bioresour Technol 101:3085–3090. https://doi.org/10.1016/j.biortech.2009.12.077

Villano M, Scardala S, Aulenta F, Majone M (2013) Carbon and nitrogen removal and enhanced methane production in a microbial electrolysis cell. Bioresour Technol 130:366–371. https://doi.org/10.1016/J.BIORTECH.2012.11.080

Wang A, Sun D, Cao G, et al (2011) Integrated hydrogen production process from cellulose by combining dark fermentation, microbial fuel cells, and a microbial electrolysis cell. Bioresour Technol 102:4137–4143. https://doi.org/10.1016/j.biortech.2010.10.137

Wang B, Wan W, Wang J (2008) Inhibitory effect of ethanol, acetic acid, propionic acid and butyric acid on fermentative hydrogen production. Int J Hydrogen Energy 33:7013–7019. https://doi.org/10.1016/J.IJHYDENE.2008.09.027

Wu X, Zhu J, Dong C, et al (2009) Continuous biohydrogen production from liquid swine manure supplemented with glucose using an anaerobic sequencing batch reactor. Int J Hydrogen Energy 34:6636–6645. https://doi.org/10.1016/J.IJHYDENE.2009.06.058

Xu T (2005) Ion exchange membranes: State of their development and perspective. J Memb Sci 263:1–29. https://doi.org/10.1016/j.memsci.2005.05.002

Xue G, Lai S, Li X, et al (2018) Efficient bioconversion of organic wastes to high optical activity of L-lactic acid stimulated by cathode in mixed microbial consortium. Water Res 131:1–10. https://doi.org/10.1016/j.watres.2017.12.024

Yasri N, Roberts EPL, Gunasekaran S (2019) The electrochemical perspective of bioelectrocatalytic activities in microbial electrolysis and microbial fuel cells. Energy Reports 5:1116–1136. https://doi.org/10.1016/j.egyr.2019.08.007

Yu Z, Leng X, Zhao S, et al (2018) A review on the applications of microbial electrolysis cells in anaerobic digestion. Bioresour Technol 255:340–348. https://doi.org/10.1016/j.biortech.2018.02.003

Yun JH, Cho KS (2016) Effect of hydraulic retention time on suppression of methanogens during a continuous biohydrogen production process using molasses wastewater. https://doi.org/101080/1093452920161221221 52:37–44. https://doi.org/10.1080/10934529.2016.1221221

Zhang Z, Song Y, Zheng S, et al (2019) Electro-conversion of carbon dioxide (CO2) to low-carbon methane by bioelectromethanogenesis process in microbial electrolysis cells: The current status and future perspective. Bioresour Technol 279:339–349. https://doi.org/10.1016/j.biortech.2019.01.145

Zhen G, Kobayashi T, Lu X, Xu K (2015) Understanding methane bioelectrosynthesis from carbon dioxide in a two-chamber microbial electrolysis cells (MECs) containing a carbon biocathode. Bioresour Technol 186:141–148. https://doi.org/10.1016/J.BIORTECH.2015.03.064

Zhu J, Wu X, Miller C, et al (2007) Biohydrogen production through fermentation using liquid swine manure as substrate. http://dx.doi.org/101080/03601230701312779 42:393–401. https://doi.org/10.1080/03601230701312779

Appendix – Conference publications

BIO-ELECTROCHEMICAL PRODUCTION OF HYDROGEN AND ELECTRICITY FROM ORGANIC WASTE

A. Dell'Era[1], M. Pasquali[1], A. Polettini[2], R. Pomi[2], A. Rossi[2], T. Zonfa[2]

[1] *Department of Basic and Applied Sciences for Engineering, University of Rome "La Sapienza", Via del Castro Laurenziano 7, 00161 Rome, Italy*
[2] *Department of Civil and Environmental Engineering, University of Rome "La Sapienza", Via Eudossiana 18, 00184 Rome, Italy*

ABSTRACT: This study presents an integrated bio-electrochemical process meant to enhance the hydrogen production yield of dark fermentation. An experimental set-up consisting of a galvanic cell combined with a fermentation reactor was used to achieve higher hydrogen yields through the electrochemical conversion of the protons released by the organic acids generated during fermentation of a model substrate. The electrochemical conversion of protons into hydrogen in the galvanic cell simultaneously produces electricity and also has the positive outcome of contrasting acidification. The results of preliminary tests of the integrated bio-electrochemical process are presented to allow for a preliminary investigation of the associated potential benefits.

Keywords: organic waste; dark fermentation; hydrogen; bio-electrochemical process; electricity production

1. Introduction

The present study addresses the opportunities for the production of sustainable energy carriers, such as bio-hydrogen (bio-H_2), from organic residues. H_2 can be used in both power generation systems and combustion processes, providing the great advantage of clean combustion. Moreover, H_2 is considered a very competitive energy carrier compared to other fuels, thanks to its high net heating value. Nowadays, its use as a clean energy source is yet uncommon; currently, the main use is in ammonia production and hydrogenation of coal and petroleum during hydrocracking of traditional fuels. In addition, H_2 is still primarily derived from non-renewable sources, with a high associated energy consumption, high temperatures needed (above 700°C) and relevant CO_2 emissions. Water electrolysis is one of the most well-known methods to produce H_2 from renewable sources, but its full application has some drawbacks including the relatively low efficiency and the high production cost compared with hydrocarbon reforming. Moreover, electrolysis requires large energy inputs, implying that it could be sustainable only if supplied by clean power.
The considerations above show that there is an urgent need for a regulatory framework and infrastructure improvement to enhance worldwide H_2 exploitation in the energy sector, along with extensive research on novel production methods.
Several bioprocesses have been investigated over the last decades to produce H_2 through sustainable methods. Among them, dark fermentation (DF) is considered one of the most promising options. The

main reason is that DF may remove the major drawbacks associated with other biological processes (including direct or indirect photolysis and photo-fermentation), associated to the intermittent production of H_2 and the need of a light source to support the process. Compared to the other biological processes, dark fermentative H_2 production has the additional advantages of higher production rate, flexibility of operation under different temperature and pressure conditions, lower net energy input and, noteworthy, applicability to a range of residual substrates including organic waste and carbohydrate-based wastewaters (Da Silva Veras et al. 2017). Various heterotrophic microorganisms can take part to DF. They are capable of breaking down carbohydrate-rich substrates under anaerobic conditions through different biochemical pathways, leading to several metabolic products that include H_2 and CO_2 as the gaseous outputs, and liquid end-products including volatile organic acids and/or alcohols.
The key feature that makes DF attractive for organic waste treatment is associated to the potential of producing H_2 using a renewable source, at the same time stabilizing organic matter. However, there are still issues that need further investigation. These include the understanding of the influence of operational parameters of the process, its stability under continuous operation, and the feasibility of integration with additional treatment stages (either concomitantly or sequentially), with the aim of maximizing the exploitation of the organic substrate. In fact, despite the above-mentioned advantages, DF also has some limitations related to the biochemical nature of the process itself, which make the actual H_2 yield attained lower than that expected on a theoretical basis.
This work aims to address the biochemical limitations of fermentative H_2 production through an innovative approach, which involves the integration of DF with electrochemical methods to better exploit the energy content of organic residues. Currently, there are studies on bio-electrochemical systems (BESs), such as Microbial Electrolysis Cells (MECs) and Microbial Fuel Cells (MFCs), that can be valid post-treatments for DF effluents. Indeed, they can further degrade the organic matter and produce additional H_2 or electricity. However, these processes can only be applied downstream of DF and do not bring any improvement to the DF itself. The innovative approach proposed in this work lies in the development of a BES that integrates the DF process with electrochemical conversion in the same reactor, without excluding the possibility of treating the effluent with MECs and/or MFCs for further degradation of the digestate produced.

2. Integration of electrochemical methods and biochemical processes for H_2 production

2.1 Main features of dark fermentation

H_2 production during DF is the result of various biochemical reactions, associated to the metabolic activity of chemoheterotrophic microorganisms, which lead to cell synthesis and energy production for their own survival under anaerobic and light-independent conditions, consuming the organic substrate and providing various metabolic end-products. The analysis of end-products in fermentative processes is a key issue because the distribution pattern reflects the metabolic routes followed by hydrogen-producing microorganisms and it is correlated with the H_2 yield. The main end-products in the liquid phase that are generally detected during DF are volatile fatty acids (VFAs) and alcohols (Ghimire et al. 2015), including mainly acetic acid, butyric acid, propionic acid and ethanol. The complete reaction of the acetic pathway shows that is stoichiometrically possible to achieve 4 moles of H_2 per mole of glucose consumed (1):

$$C_6H_{12}O_6+2H_2O\rightarrow 2CH_3COOH+2CO_2+4H_2 \quad (1)$$

This amount is considered as an upper threshold, which is referred to as the Tauher limit (Thauer et al.1977). It refers to the fact that, from a potential of 12 moles of H_2 available in one mole of glucose (2) a maximum of 4 moles can be obtained, since glucose utilization is always necessarily accompanied by the formation of other metabolites, among which acetic acid is the one that allows the greatest amount of H_2.

$$C_6H_{12}O_6+6H_2O\rightarrow 12H_2+6CO_2 \quad (2)$$

However, a thermodynamic limitation occurs when metabolic products are accumulated in the system as the process progresses, so the more by-products are accumulated in the medium the harder the theoretical yield is approached, as observed in many research studies. Moreover, conditions suitable for the growth of homoacetogenic bacteria give rise to homoacetogenesis, one of the processes that can reduce the H_2 yield, as shown by the equation (3) (Jones et al. 2017):

$$2H_2+2CO_2\rightarrow CH_3COOH+2H_2O \quad (3)$$

This is a reason why the presence of acetic acid among the end-products is not necessarily correlated with higher H_2 yields.

Another possible route is the butyric fermentation (4), that leads to 2 moles of H_2 and 1 mole of butyric acid per mole of glucose consumed:

$$C_6H_{12}O_6\rightarrow CH_3CH_2CH_2COOH+2CO_2+2H_2 \quad (4)$$

This is the preferable way along with the acetic route in order to produce H_2, so that acetate and butyrate are usually the most abundant species among the DF end-products.

However, several other reactions can take place concomitantly with these pathways, depending on various factors including the environmental and operating conditions. For this reason, it is essential to control them in order to drive the process towards efficient H_2 production. For instance, propionic acid formation involves a H_2-consuming reaction (5), which negatively affects the net H_2 yield:

$$C_6H_{12}O_6+2H_2\rightarrow 2CH_3CH_2COOH+2H_2O \quad (5)$$

Many other VFAs and solvents can be detected in smaller quantities in DF, depending on the environmental conditions and the microbial communities.

2.2 Theoretical principles of the proposed integrated bio-electrochemical systems

The integrated bio-electrochemical system (IBES) proposed here is aimed at enhancing the H_2 yield of DF through a beneficial combination of the biochemical and electrochemical processes. In order to overcome the biochemical threshold mentioned above, the proposed IBES is based on the electrochemical reduction of the protons (H^+) released from the dissociation of the VFAs produced during the biological process. Assuming acetic acid as representative of the VFAs generated, the dissociation reaction (equation 6) is written as:

$$CH_3COOH\leftrightarrow CH_3COO^-+H^+ \quad (6)$$

The protons can be reduced to H_2 according to reaction (7) if the required amount of electrons is supplied to the biochemical reactor by the electrochemical compartment.

$2H^{+}+2e^{-}\leftrightarrow H_2$ (7)

The main aspect that makes the IBES different from other bio-electrochemical systems, such as MFCs and MECs, is that the biological and electrochemical reactions occur simultaneously in two different compartments of the same reactor (Figure 1). The digestate from the biological compartment can then be further treated in subsequent stages through other BESs for further degradation of the residual organic matter, using the available content of the residual VFAs (Rivera et al. 2015).

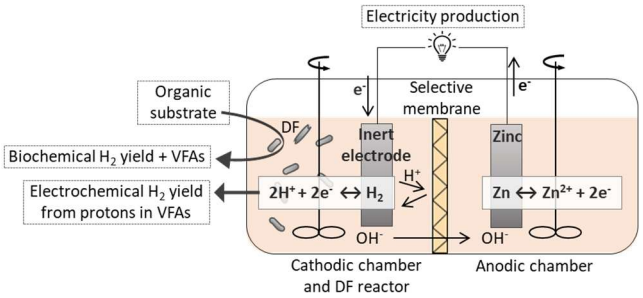

Figure 1. Schematic representation of the integrated bio-electrochemical system (IBES).

In order to supply the electrons needed for proton reduction in the biological compartment, the IBES mimics the functions of a galvanic cell. An inert electrode (cathode) is placed in the fermentation medium, which is connected through an external electric circuit to a second reducing electrode (anode), placed in an electrolytic solution in a separate chamber. The electric current flow occurs from the reducing electrode to the inert one, which does not participate directly in the reaction, but has rather the role of carrying the electrons into the fermentation reactor allowing them to react with protons. The reactions that occur in the cathodic (8) and anodic (9) chambers are shown below, with corresponding reduction potentials under standard conditions (E^0), assuming zinc as the reducing species.

$2H^{+}+2e^{-}\leftrightarrow H_2$ $E^0(2H^{+}/H_2)=0.000V$ (8)

$Zn\leftrightarrow Zn^{2+}+2e^{-}$ $E^0(Zn_2{}^{+}/Zn) = - 0.762V$ (9)

The overall cell electromotive force under standard conditions (ΔE^0), that is defined as the potential difference between cathode and anode, in this system is as follows:

$\Delta E^0=E^0(2H^{+}/H_2)-E^0(Zn^{2+}/Zn)=0.762V$ (10)

According to the thermodynamics of the process, it can be observed that the Gibbs free energy is negative (11), therefore the redox reaction takes place spontaneously as the reduction potential of the anode is adequately low.

$\Delta G^0=-nF\Delta E^0=-147kJ$ (11)

Where *n* is the number of electrons exchanged in the reaction and *F* is Faraday's constant (9.64853 x 10^4 C mol^{-1}).

The potential advantages of the IBES include the increased H_2 production compared to the biochemical yield as well as electricity generation. Hence, there is a better exploitation of the energy potential contained in the substrate through the reuse of metabolites formed in the fermentation reactor.

Moreover, the transformation of protons can also have a positive effect on acidification phenomena, as it contributes to pH buffering and consequently reduces the amount of chemicals required to control pH within the optimal range for the fermentation process.

3. Materials and methods

Three different experimental set-ups (Figure 2 A, B, C) were designed in order to identify the most suitable materials and configuration for the IBES. System A is composed of two physically separated compartments (200 mL volume), where the electrolytic solutions interact through a sodium chloride-based salt bridge. System B is composed of two chambers of similar size to the system A but connected through an Anionic Exchange Membrane (*AEM*, type FAB-PK-130 by Fumasep), having a surface area to volume ratio of 0.12 cm^2/mL. In system B, the AEM guarantees the separation of the electrolytic solutions, but at the same time allows the flow of anions from the cathodic to the anodic compartments, required to maintain electroneutrality. These two configurations were only used for preliminary tests, since the compartments are open and it is not possible to measure the amount of H_2 produced. In this case, the process was monitored through the following parameters: cell voltage ΔV, electrical current intensity I and pH change of the cathodic solution. The continuous electric measurements were performed through a NI FieldPoint in configurations A and B, with an external fixed load of 90 Ohm, in combination with LabVIEW as the data acquisition software. In a number of dedicated tests, a potentiometer was also used to derive the electric potential curves by adjusting the external load.

The total amount of charge Q exchanged during the electrochemical process was calculated according to the following equation (12).

$$Q=\int_0^t I(t)dt \tag{12}$$

According to reaction (7), the theoretical amount of H_2 generated can be calculated from the amount of displaced electrons under the hypothesis that these are only used for proton reduction, as follows:

$$H_{2teo}=Q/_{2F} \tag{13}$$

The third configuration (C) was designed to gain better insight into electrochemical H_2 production. This configuration consisted of two gas-tight bottles connected through a flange. Like configuration B, the separation of the liquid solutions in the two chambers was accomplished using an AEM. Due to geometrical constraints of the chambers, in this case the AEM surface area to volume ratio was 0.025 cm^2/mL. A eudiometer was connected to the cathodic compartment to allow for volumetric gas measurement and gas sampling for subsent gas-chromatographic analysis (VARIAN Model 3600 CX). The preliminary tests were carried out using acetic acid in the cathodic chamber as representative of the VFAs generated during DF. Different initial acetate concentrations were used to obtain a range of initial pH values. Different electrodes were tested for the cathode material: graphite sheet, platinum sheet, titanium grid, nickel grid and porous carbon. These were selected due to their electrical conductivity characteristics, recognized inert behaviour with respect to redox reactions and absence of potential toxic effects on microorganisms. The anodic chamber was filled with zinc sulphate at 0.5M concentrations, while a metallic zinc plate was used as the anode.

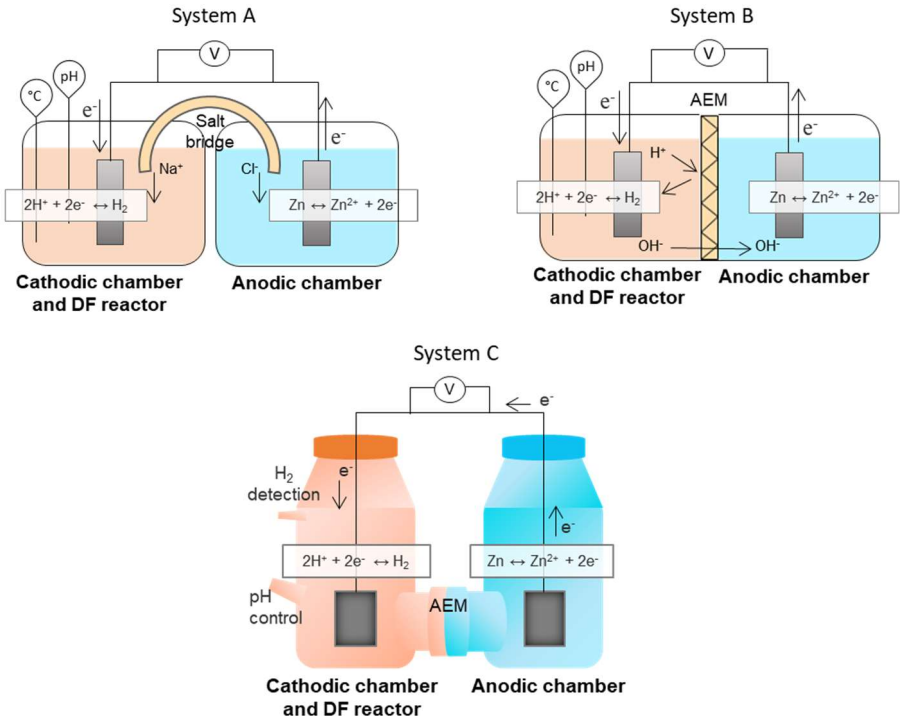

Figure 2. Reactor configurations used for testing the integrated bio-electrochemical system (IBES). A: two physically separated compartments, where the necessary ions are provided by the salt bridge in order to maintain the electroneutrality of the cell; B: two chambers separated by an anionic exchange membrane that guarantees the separation of the electrolytic solutions, but at the same time allows the flow of anions from the cathodic to the anodic compartments; C: two gastight bottles connected through a flange containing the separation AEM, which in this case has a lower area to volume ratio than in system B.

4. Results and discussion

An initial set of experimental tests was conducted to select the best electrodes using system A. In the anodic chamber, the use of a 15-cm^2 zinc plate or a 1-cm^2 surface rod made of pressed zinc powder produced no significant differences. On the other hand, in terms of electricity production, the main differences were observed when changing the nature of the cathode electrode; the influence of both the cathode shape and position, as well as the material type, was evident. The highest electric current intensities were obtained with the titanium grid electrode. Using platinum as the cathode material, despite this being known as an excellent conductor, producing half the electric current intensity of that obtained with titanium, probably due to the smaller size of the platinum sheet used (surface area = 2 cm^2). The lowest electric current intensities were detected using the graphite sheet at the cathode.
The tests conducted using the A configuration also showed the presence of a high overpotential. As indicated by various studies on other types of BESs, cell systems equipped with salt bridges connecting the two electrode compartments generate high internal resistances (Logan et al. 2006). In order to optimize the IBES efficiency by reducing the internal resistance, the B configuration was developed.

Using the titanium cathode produced a cell voltage of 0.20 V in configuration A and 0.43 V in configuration B, and resulted in current intensities of 2.2 and 4.7 mA (average of the values measured during the first hour of the tests at 90 Ohm as the external load). Moreover, it was found that the interelectrode distance largely influences cell efficiency, as observed in other experimental studies on BESs (Cheng et al. 2006). Thus, placing the electrodes right next to the membrane would produce the largest benefits in terms of current circulation.

The power curve (Figure 3) was derived to identify the electrical characteristics of the cell in configuration B using titanium grid as the cathode and metallic zinc plate as the anode. The potentiometer located in the circuit allowed to gradually vary the resistive load applied between 500 Ohm and 1.3 Ohm. The cell voltage was measured continuously for a few minutes following each resistance variation, thus avoiding excessive changes in the electrolyte solutions but ensuring the setting of equilibrium conditions. The corresponding electric current (I) was obtained in accordance with the Ohm's law. A maximum power value (*P*) of 2.5 mW was obtained at 8.5 mA, with a resistive load of 33.5 Ohm. Figure 3 also shows that the highest voltage was obtained for the high resistive load applied, while maximizing the electric current flow would require to keep the resistive load to a minimum.

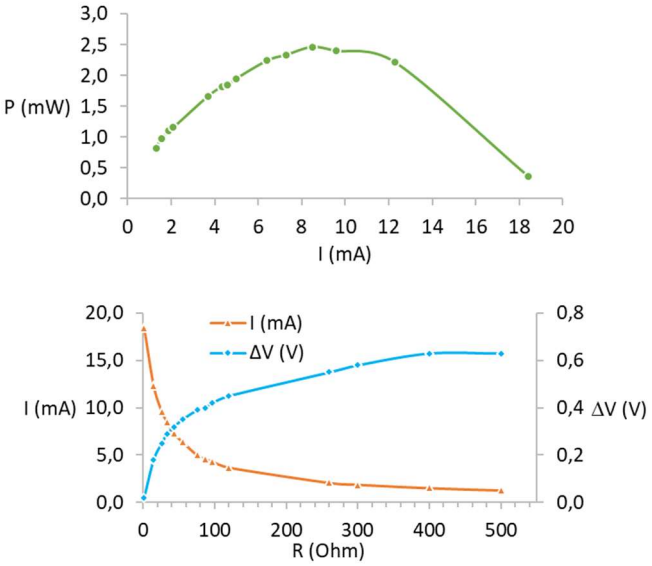

Figure 3. Power curve and external resistive load variation for the IBES in B-Titanium configuration.

The time evolution of the process was analysed for the B-type cell by fixing the resistive load to the minimum value in order to maximize the electrons flow. Two other cathodes were tested in addition to the titanium grid previously identified in the tests in configuration A, namely a nickel mesh (B-nickel configuration) and a porous carbon (B-carbon configuration); nickel sulphate was applied by electrodeposition on the latter in order to decrease the activation overpotential on the electrode surface for hydrogen production. Table 1 provides a summary of the characteristics and the main results of the preliminary tests that were carried out in the B and C systems.

Table 1. Main characteristics of systems B and C.

Configuration	B-Nickel	B-Carbon	B-Titanium	C-Titanium
Volume of cathodic solution (mL)	195	210	210	500
AEM surface (cm^2)	24.0	24.0	24.0	12.5
Test duration (h)	96	72	96	312
Initial pH of the cathodic solution	2.7	3.0	2.9	3.9
Acetic acid in the cathodic solution (mol)	0.039	0.012	0.019	0.0004
Final pH of the cathodic solution	7.3	7.8	6.9	7.4
Initial current intensity (mA)	22.9	22.0	19.2	3.2
Electrons releasedby anode consumption (mol)	0.057	0.031	0.057	-
Electrons transferred according to the total charge (mol)	0.045	0.032	0.052	0.018
Potential H_2 produced according to the total charge (mol)	0.023	0.016	0.026	0.009

The progressive pH increase observed till the end of each test confirms the trend expected on the basis of the theoretical principles presented in section 2.2. As indicated by the sample test in Figure 4, the electric current generally displayed the highest values within the first minutes from the onset of the test; subsequently, the current profile decreased rapidly and then continued with a gradual smoother decrease caused by the ionic concentration variation taking place in the electrolyte solutions. When the pH of the cathodic solution reached ~4.0 units, it was observed to undergo a sudden sharp increase, causing an associated rapid decrease in the current intensity. Under these conditions the electron transfer was stopped, and so was the observed pH growth. The final pH was found to stabilize at values between 7.0 and 8.0 units depending on the specific test.

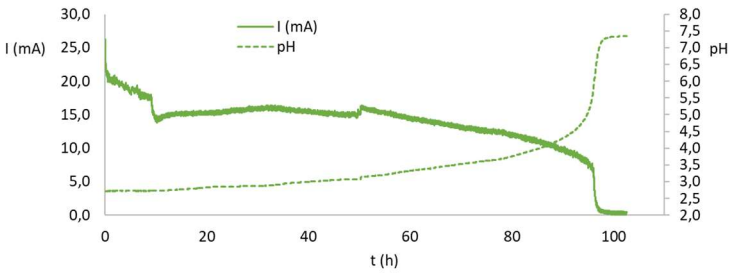

Figure 4. Electric current and pH trend in IBES B-Nickel configuration.

The tests performed with configuration B show that the observed pH changes were directly correlated with the amount of electrons mobilized. Moreover, the observed shape of the pH profile over time appeared to mirror the expected effect of continued dissociation of acetate as protons are subtracted from the solution and converted to H_2. Based on theoretical considerations, the acetate fraction in the dissociated form at pH = 2.7 is less than 1%, and increases to 15% at pH 4 and further to 99% at pH 7. It is thus clear that, when pH approaches the alkaline range, acetate deprotonation is virtually complete and no further protons can be made available to support the reduction to H_2. This consideration is further supported by the results depicted in Figure 5, which shows the effect of a second acetate addition

to the solution. When the electric current flow was stopped and pH reached a plateau of ~7, acetate was added to restore the pH of the cathodic solution to 4.0, the electric current suddenly reached an intensity of 10 mA and the cell operation was similar to the previous period, with pH rising with a similar profile to a final value of 7.1 after ~12 hours. This result suggests that, when the electrochemical system is coupled with a fermentation reactor, in principle the continuous production of VFAs would be able to provide the continuous supply of protons required to allow a stable flow of electrons.
Lastly, it is worth mentioning that, as known from literature, pHs between 5.0 and 6.5 are recommended for hydrogenesis (Elbeshbishy et al. 2017). To this regard, the results obtained with the acetate solution appear to be promising because they show a rapid increase in pH values above 5.

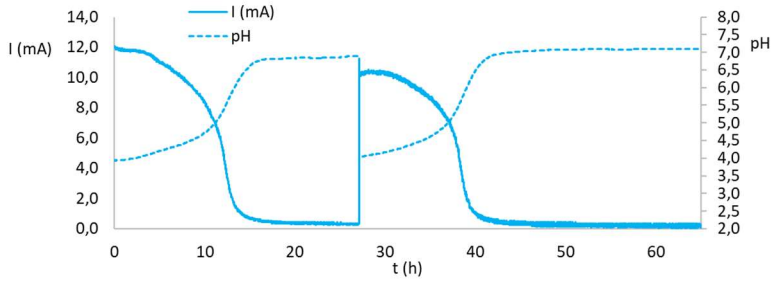

Figure 5. Electric current and pH trend in IBES B-Titanium system.

Table 1 also shows that the amount of electrons that would theoretically account for the amount of metallic Zn oxidized at the anode displays a perfect match with the amount of electric current generated in the system. The theoretical amount of H_2 produced on the basis of the total charge generated, estimated through equations (12) and (13), in turn depends on the number of protons made available by acetate dissolution. The electron moles released at the anode and transferred to the cathode were higher than the proton moles available, even if acetic acid was assumed to be entirely deprotonated. The electron balance thus suggests that the electric current generated was not fully used for proton reduction to H_2, and likely further concomitant electrochemical processes contributed to the generation of the electric current. While these phenomena are unclear and need to be investigated in detail, it may be hypothesized that possible causes of deviation from the expected reactions may include interactions of the cathode metal species. For configuration C, the less favourable ratio between the AEM surface and the cell volume, dictated by technical constraints, was also observed to exert a negative effect on the IBES yield. This resulted in a lower amount of electrons mobilized and an associated increase in the process duration in terms of evolution of pH buffering. The process was also found to evolve at a lower rate compared to configuration B, indicating that an improved size ratio of the AEM and a reduction of the internal resistances of the system would be required to improve the process performance (Figure 6).

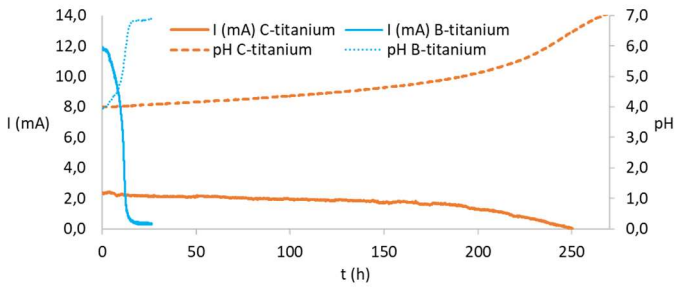

Figure 6. Lower AEM surface to volume ratio in system C produces lower initial electric current and slower evolution of the pH buffering process over time.

5. Conclusions

This work was aimed at addressing the intrinsic biochemical limitations of DF through the development of an integrated electrochemical/biochemical process able to produce H_2 from organic waste substrates. The proposed IBES is based on the concept that the protons deriving from the dissociation of the VFAs produced during DF can be electrochemically converted to H_2, thus enhancing the H_2 yield of DF and controlling system acidification.

The experimental IBES tested was designed as a galvanic cell that allows the process to be energetically self-sufficient and leads to the production of a surplus electric current that can be used for both internal and external purposes. Acetate was used as a model VFA to simulate the composition of DF digestate. The preliminary experimental results showed an effect of the process in terms of pH increase in the cathodic compartment associated to the production of electricity. The preliminary tests highlighted the importance of optimizing the system configuration in terms of minimization of ohmic resistances and maximization of the membrane surface area per unit reactor volume.

Further investigation of potential interfering reactions that may cause deviations from the expected H_2 yield, including electrochemical effects on the metabolic reactions of DF, are required to derive a thorough assessment of process viability. Future experiments will be conducted by simultaneously carrying out DF and the electrochemical process with organic substrate, in order to quantify the H_2 production and to make a comparison between the overall energy yields of the IBES and the stand-alone biochemical process.

References

Cheng, Shaoan, Hong Liu, and Bruce E. Logan. 2006. “Increased Power Generation in a Continuous Flow MFC with Advective Flow through the Porous Anode and Reduced Electrode Spacing.” https://doi.org/10.1021/es051652w.

Elbeshbishy, Elsayed, Bipro Ranjan Dhar, George Nakhla, and Hyung Sool Lee. 2017. “A Critical Review on Inhibition of Dark Biohydrogen Fermentation.” Renewable and Sustainable Energy Reviews. https://doi.org/10.1016/j.rser.2017.05.075.

Ghimire, Anish, Luigi Frunzo, Francesco Pirozzi, Eric Trably, Renaud Escudie, Piet N.L. Lens, and Giovanni Esposito. 2015. “A Review on Dark Fermentative Biohydrogen Production from Organic Biomass: Process Parameters and Use of by-Products.” Applied Energy 144 (April): 73–95. https://doi.org/10.1016/J.APENERGY.2015.01.045.

Jones, Rhys Jon, Jaime Massanet-Nicolau, Martijn J.J. Mulder, Giuliano Premier, Richard Dinsdale, and Alan Guwy. 2017. "Increased Biohydrogen Yields, Volatile Fatty Acid Production and Substrate Utilisation Rates via the Electrodialysis of a Continually Fed Sucrose Fermenter." Bioresource Technology 229: 46–52. https://doi.org/10.1016/j.biortech.2017.01.015.

Logan, Bruce, Bert Hamelers, RENE ROZENDAL, UWE SCHRODER, JURG KELLER, STEFANO FREGUIA, Peter AELTERMAN, Willy VERSTRAETE, and KORNEEL RABAEY. 2006. "Microbial Fuel Cells: Methodology and Technology" 40 (17): 5181–92. https://doi.org/10.1021/es0605016.

Rivera, Isaac, Germán Buitrón, Péter Bakonyi, Nándor Nemestóthy, and Katalin Bélafi-Bakó. 2015. "Hydrogen Production in a Microbial Electrolysis Cell Fed with a Dark Fermentation Effluent." Journal of Applied Electrochemistry 45 (11): 1223–29. https://doi.org/10.1007/s10800-015-0864-6.

Silva Veras, Tatiane da, Thiago Simonato Mozer, Danielle da Costa Rubim Messeder dos Santos, and Aldara da Silva César. 2017. "Hydrogen: Trends, Production and Characterization of the Main Process Worldwide." International Journal of Hydrogen Energy. https://doi.org/10.1016/j.ijhydene.2016.08.219.

Thauer, Rudolf K., Kurt Jungermann, and Karl Decker. 1977. "Energy Conservation in Chemotrophic Anaerobic Bacteria." Bacteriological Reviews 41: 100–180. https://doi.org/10.1108/eb027807.

BIO-H_2 PRODUCTION FROM CHEESE WHEY AND WASTEWATER SLUDGE IN SEMI-CONTINUOUS SYSTEMS

M.R. BONI*, G. DE GIOANNIS**, A. MUNTONI**, A. POLETTINI*, R. POMI*, A. ROSSI*, D. SPIGA**, T. ZONFA*

** Department of Civil and Environmental Engineering, University of Rome "La Sapienza", Via Eudossiana, 18, 00184 Rome (Italy)*

*** Department of Civil and Environmental Engineering and Architecture, University of Cagliari, Piazza D'Armi, 1, 09123, Italy*

Abstract

In the present work, a lab-scale experimental campaign on dark fermentation of milk powder (used as a surrogate of cheese whey) was conducted in order to assess the bio-hydrogen production potential of cheese whey. The experiments were performed in automated semi-continuous reactors and were aimed at estimating the effect of the Organic Loading Rate (OLR) and Hydraulic Retention Time (HRT) on the H_2 yield. Hydrogenogenic biomass was harvested from aerobic wastewater sludge by applying a thermal pre-treatment (105 °C, 30 min) and used as the initial inoculum. The experiments were conducted at a set-point pH of 6.5, which was automatically adjusted by the control system. In total, 20 fermentation tests were run, with HRT ranging from 4 to 20 h and OLR from 16 to 129 g TOC/(L·d). The biogas composition was evaluated by periodic gas sampling. The evolution of digestate composition was monitored through periodic measurements of volatile fatty acids, total organic carbon and soluble carbohydrates in order to derive information about the prevalent metabolic pathways and draw the carbon mass balance.

Keywords: fermentative H_2 production, cheese whey, semi-continuous tests

Introduction

The management of food processing residues such as cheese whey from dairy industry represents a critical issue due to the large unit volumes produced and the typical high content of biodegradable matter. The cheese-making process generates from 0.5 to 9 L of cheese whey per kg of cheese produced (Carvalho et al. 2013). Worldwide, only approximately a half of the cheese whey is valorised to produce food and feed products (Bosco et al. 2018), while the remaining part is disposed after physico-chemical or biological treatment. A portion of the produced cheese whey can also be directly applied to soil.

In view of designing a feasible management scenario for cheese whey, one of the practicable options includes the exploitation of its energy content through fermentation aimed at bio-hydrogen

production. In particular, dark fermentation of cheese whey has been widely investigated over the last decade (Ferchichi et al. 2005; Antonopoulou et al. 2008b; Azbar et al. 2009b; De Gioannis et al. 2014; Dębowski et al. 2014; Ferreira Rosa et al. 2014b; Akhlaghi et al. 2017a; Asunis et al. 2019, 2020), and the process has been found to variously depend on numerous and interconnected factors such as substrate composition, concentration and pre-treatment methods, presence/type of inoculum and inoculum pre-treatment, inoculum-to-substrate ratio, reactor type and operation regime, applied operating conditions (e.g. pH, hydraulic and cell residence time, temperature, organic loading rate, etc.). The influence of such factors has been studied extensively in batch conditions spanning a range of different approaches, including direct analytical characterization of cheese whey degradation and related formation of metabolic products, detailed microbial analysis of the existing biomass, biochemical modelling of the metabolic pathways and statistical processing of fermentation performance data. However, since H_2 is an intermediate product of the fermentation process and tends to be preferentially recycled within the metabolic pathways to optimize energy utilization by biomass, the stability of H_2 production under continuous process operation is a rather challenging target. Therefore, despite the advances made in the understanding of fermentative H_2 production, numerous open questions remain as to the feasibility of full-scale implementation of the process.

In the present work, we aimed at exploring the H_2 production potential of cheese whey under continuous operation and identifying the optimal conditions for the fermentation process by assessing the process stability.

Materials and Methods

In the present work, a lab-scale experimental campaign on dark fermentation of milk powder (MP, used as a surrogate of cheese whey) was conducted in order to assess the bio-hydrogen production potential of cheese whey. MP was dissolved in deionized water to a TS concentration of 11% by weight, and then diluted at different ratios (depending on the specific experimental condition adopted) in view of the fermentation tests.

Hydrogenogenic biomass was harvested from aerobic wastewater sludge (activated sludge, AS) by applying a thermal pre-treatment (105 °C, 30 min) and used as the initial inoculum.

The main characterization parameters for MP and AS are reported in Table 1.

Table 1. *Characterization parameters for MP and AS*

Parameter	Unit of measure	MP	AS
Total Solids	g/L	1109 ± 10.4	20.5 ± 1.8
Volatile Solids	g/L	1076 ± 6.8	16.0 ± 1.4
Total suspended solids	g/L	441 ±26.3	18.2 ± 0.1
Total Organic Carbon (TOC)	g C/L	487 ± 8.3	9.0 ± 0.7
Soluble carbohydrates	g hexose/L	637 ± 2.5	0.7 ± 0.08

The experiments were conducted in automated semi-continuous reactors and were aimed at estimating the effect of the Organic Loading Rate (OLR) and Hydraulic Retention Time (HRT) on the H_2 yield. The experiments were performed at a set-point pH of 6.5, which was automatically adjusted

through a customized pH control system. In total, 19 fermentation tests were run (see Table 2), with HRTs ranging from 4 to 20 h and OLRs from 16 to 130 g TOC/(L·d). The volumetric biogas production was automatically recorded during the fermentation tests, with measurements taken every minute and then mediated over a time span of 1 hour. The biogas composition in terms of volumetric concentration of the main components (H_2, CO_2, CH_4) was evaluated by periodic gas sampling. The evolution of digestate composition was monitored through periodic measurements of volatile fatty acids, total organic carbon and soluble carbohydrates in order to derive information about the prevalent metabolic pathways and draw the carbon mass balance.

Table 2. *Experimental conditions adopted in the semi-continuous tests*

Run no.	Run code	HRT (h)	OLR (g TOC/(L·d))
1	R-4-65	4	65
2	R-6-32.5	6	32.5
3	R-6-65	6	65
4	R-6-100	6	100
5	R-6-130	6	130
6	R-8-32.5	8	32.5
7	R-8-65	8	65
8	R-8-100	8	100
9	R-8-130	8	130
10	R-12-65	12	65
11	R-12-100	12	100
12	R-16-16	16	16
13	R-16-32.5	16	32.5
14	R-16-52	16	52
15	R-16-65	16	65
16	R-16-130	16	130
17	R-20-32.5	20	32.5
18	R-20-52	20	52
19	R-20-65	20	65

Results and discussion

The observed evolution of biogas production during the fermentation process was found to depend largely on the operating conditions adopted. Fluctuations in the biogas volume recorded were detected to different degrees, as a consequence of both acclimation of biomass during the start-up phase and the intrinsic stability of the process under specific operating conditions. The stability of H_2 production was evaluated through the so-called stability index (SI), which was applied to the time series of the measured hourly H_2 production yields (HPY). The SI was calculated for consecutive operation cycles (each having a duration of 1 HRT) from the moving standard deviation (S.D.) and average (AVG) values of the hydrogen production yield, as indicated by the following equation:

$$SI_{period,j} = 1 - \frac{S.D.(HPY)_i|_{i=j-1}^{j-1+m}}{AVG(HPY)_i|_{i=j-1}^{j-1+m}}$$

where $j = 1, \ldots, N$; N = total no. of periods in one test (= t_{tot} – HRT +1); t_{tot} = total length of the time series; Δt_{meas} = time lapse between two consecutive measures; m = number of data points in one period (=HRT/Δt_{meas}); $AVG(HPY)_i|_{i=j-1}^{j-1+m}$ = moving average of m HPY values for the different periods; $S.D.(HPY)_i|_{i=j-1}^{j-1+m}$ = moving standard deviation of m HPY values for the different periods.

Each fermentation run was considered to have attained the stability condition when $SI_{period,j}$ was ≥ 0.75 for at least three consecutive cycles up to the end of the experiment.

The results of the experimental runs indicated different performances of the hydrogenogenic process in terms of both HPY and hydrogen production rate (HPR). Not all the investigated HRT-OLR combinations were able to produce a stable H_2 production over prolonged operation periods, so that a gradual washout of the hydrogenogenic biomass was observed in a number of tests (results not shown here). Only 11 experiments out of the 19 tests conducted were found to have attained the stability condition according to the definition provided above. Figure 1 provides a number of examples of the observed HPY for some of the stable runs, while a summary of the results obtained for both the stable and unstable runs is provided in Figure2 in terms of box plots showing the main statistical indicators of HPY.

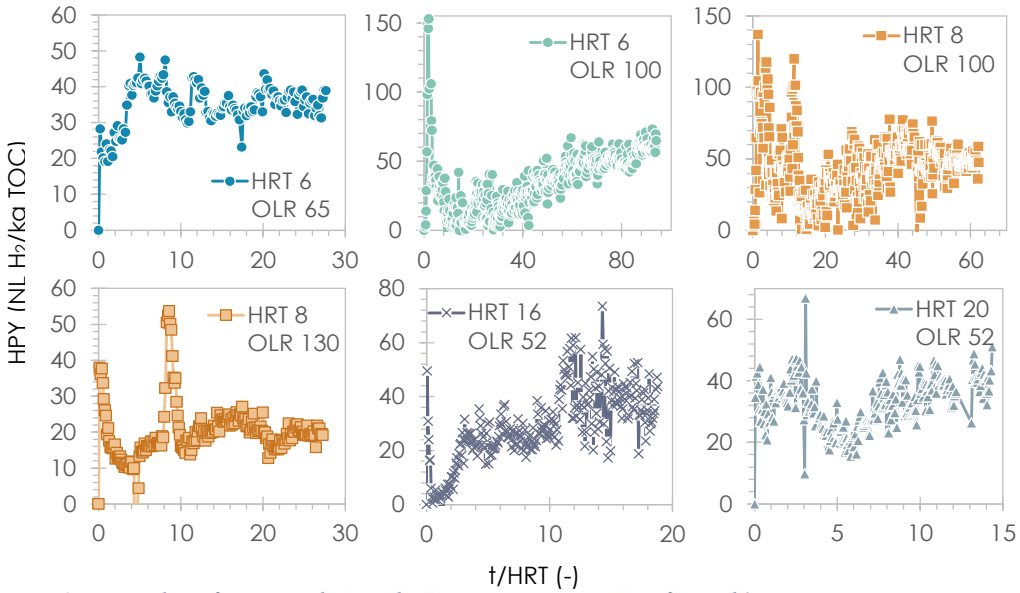

Figure 1. *Examples of HPY evolution during reactor operation for stable tests*

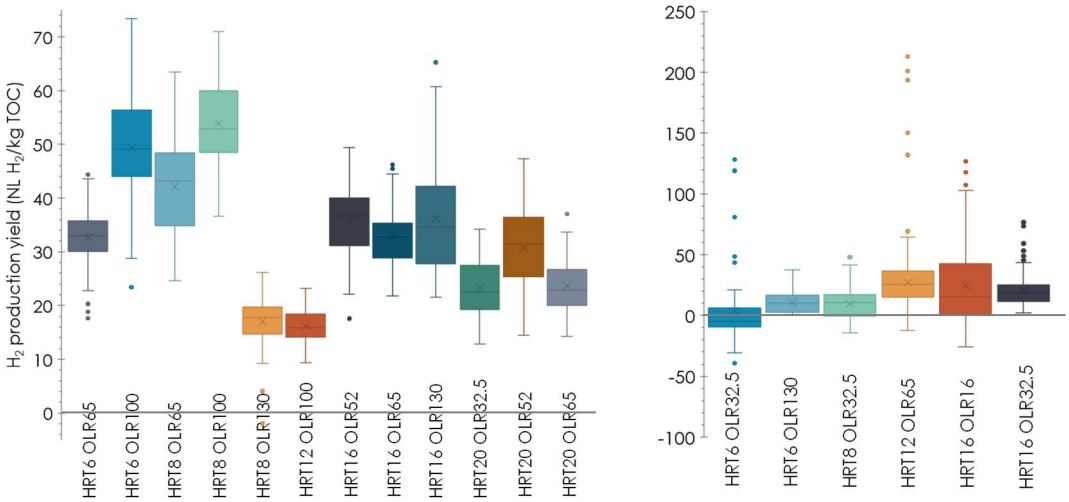

Figure 2. *Box plots of HPY for stable (left) and unstable (right) runs*

For the 11 stable runs, Table 3 also shows the results expressed in terms of average HPY and HPR (values calculated for the stability period only).

The experimental results indicate that the hydrogenogenic process required a suitable combination of HRT and OLR to ensure an adequate and stable H_2 production. The best process performance in terms of HPY (with values of 42-54 NL H_2/kg TOC) was attained at HRTs of 6 and 8 h and OLRs of 65 and 100 g TOC/(L·d). The best HPRs (4.8-5.3 NL H_2/d.L_{react}) were achieved at HRTs of 6 and 8 h and OLR of 100 g TOC/(L·d).

Table 3. Hydrogen production yield and rate attained during the stability period

Run code	HPY (NL H_2/kg TOC)	HPR (NL H_2/d.L_{react})
R-6-65	32.70	2.1
R-6-100	49.37	4.8
R-8-65	41.96	2.7
R-8-100	53.94	5.3
R-8-130	18.58	2.4
R-12-65	18.11	1.2
R-16-52	35.64	1.9
R-16-65	32.80	2.1
R-20-32.5	23.38	0.8
R-20-52	30.77	1.6
R-20-65	23.62	1.5

Conclusions

The results of the present study indicate the pivotal role of HRT and OLR in establishing suitable metabolic pathways for H_2 production and appropriate hydrogenogenic biomass growth. The analysis of the fermentation products indicated a prevalence of acetate and butyrate for the stable runs, but also the existence of numerous overlapping and often competing metabolic reactions, which resulted in notably lower H_2 production yields compared to the performance anticipated from previous batch tests. Further investigation is currently being conducted to identify suitable reactor operation strategies to maximize H_2 production.

References

Akhlaghi, M., Boni, M.R., De Gioannis, G., Muntoni, A., Polettini, A., Pomi, R., Rossi, A., Spiga, D., 2017. A parametric response surface study of fermentative hydrogen production from cheese whey. Bioresour. Technol. 244, 473–483. https://doi.org/10.1016/j.biortech.2017.07.158

Antonopoulou, G., Stamatelatou, K., Venetsaneas, N., Kornaros, M., Lyberatos, G., 2008. Biohydrogen and methane production from cheese whey in a two-stage anaerobic process. Ind. Eng. Chem. Res. 47, 5227–5233. https://doi.org/10.1021/ie071622x

Asunis, F., De Gioannis, G., Dessì, P., Isipato, M., Lens, P.N.L., Muntoni, A., Polettini, A., Pomi, R., Rossi, A., Spiga, D., 2020. The dairy biorefinery: Integrating treatment processes for cheese whey valorisation. J. Environ. Manage.

Asunis, F., De Gioannis, G., Isipato, M., Muntoni, A., Polettini, A., Pomi, R., Rossi, A., Spiga, D., 2019. Control of fermentation duration and pH to orient biochemicals and biofuels production from cheese whey. Bioresour. Technol. 289. https://doi.org/10.1016/j.biortech.2019.121722

Azbar, N., Dokgöz, F.T., Keskin, T., Eltem, R., Korkmaz, K.S., Gezgin, Y., Akbal, Z., Öncel, S., Dalay, M.C., Gönen, Ç., Tutuk, F., 2009. Comparative evaluation of bio-hydrogen production from cheese whey wastewater under thermophilic and mesophilic anaerobic conditions. Int. J. Green Energy 6, 192–200. https://doi.org/10.1080/15435070902785027

Bosco, F., Carletto, R.A., Marmo, L., 2018. An Integrated Cheese Whey Valorization Process 64.

Carvalho, F., Prazeres, A.R., Rivas, J., 2013. Cheese whey wastewater: characterization and treatment. Sci. Total Environ. 445–446, 385–96.

De Gioannis, G., Friargiu, M., Massi, E., Muntoni, A., Polettini, A., Pomi, R., Spiga, D., 2014. Biohydrogen production from dark fermentation of cheese whey: Influence of pH. Int. J. Hydrogen Energy 39. https://doi.org/10.1016/j.ijhydene.2014.10.046

Dębowski, M., Korzeniewska, E., Filipkowska, Z., Zieliński, M., Kwiatkowski, R., 2014. Possibility of hydrogen production during cheese whey fermentation process by different strains of psychrophilic bacteria. Int. J. Hydrogen Energy 39, 1972–1978. https://doi.org/10.1016/j.ijhydene.2013.11.082

Ferchichi, M., Crabbe, E., Gil, G.-H., Hintz, W., Almadidy, A., 2005. Influence of initial pH on hydrogen production from cheese whey. J. Biotechnol. 120, 402–409. https://doi.org/10.1016/j.jbiotec.2005.05.017

Ferreira Rosa, P.R., Santos, S.C., Silva, E.L., 2014. Different ratios of carbon sources in the fermentation of cheese whey and glucose as substrates for hydrogen and ethanol production in continuous reactors. Int. J. Hydrogen Energy 39, 1288–1296

SARDINIA2021 HYBRID EVENT / 11-15 OCTOBER 2021 / CAGLIARI / ITALY
18TH INTERNATIONAL SYMPOSIUM ON WASTE MANAGEMENT AND SUSTAINABLE LANDFILLING

Insight into the integration of dark fermentation with electrochemical methods for H_2 and electricity production

A. Dell'Era[1], M. Pasquali[1], A. Polettini[2], R. Pomi[2], A. Rossi[2], T. Zonfa[2]

[1] Department of Basic and Applied Sciences for Engineering, University of Rome "La Sapienza", Via del Castro Laurenziano 7, 00161 Rome, Italy
[2] Department of Civil and Environmental Engineering, University of Rome "La Sapienza", Via Eudossiana 18, 00184 Rome, Italy

ABSTRACT: This work aims at addressing the biochemical barriers through an innovative approach, which involves the integration of dark fermentation (DF) with an electrochemical compartment by designing and implementing an integrated bio-electrochemical system (IBES). The key role of the IBES is to induce the electrochemical conversion of the protons released by the organic acids generated during DF. To this aim, the IBES is designed as a galvanic cell combined with a DF reactor, producing electricity as a result of the electron exchange between the two compartments. The integrated process provides a twofold advantage: the protons that are electrochemically converted to H_2 increase the overall yield of the process and also contribute to pH buffering by reducing system acidification caused by the accumulation of organic acids associated to DF.

Keywords: dark fermentation; hydrogen; organic waste; bio-electrochemical process; electricity production.

1. Introduction

Dark fermentation (DF) is one of the most promising biochemical processes for sustainable management of organic waste through bio-H_2 production. DF offers several advantages compared to other bio-H2 production processes, including higher production rate, flexibility of operation under different temperature and pressure conditions, and lower net energy input. It may also be applied to a wide range of organic substrates such as waste and wastewater (da Silva Veras et al. 2017). Nevertheless, there are still issues that need further investigation in order to improve the efficiency of the process. These include the intrinsic limitations related to biochemical constraints, which lead to notably lower H_2 yields compared to those expected on a theoretical basis. It is known that H_2 production during DF is the result of various biochemical reactions, associated to the metabolic activity of microbial community, which lead to cell synthesis and energy production for their own survival by consuming the organic substrate and providing various metabolic end-products besides H_2.
The main end-products include volatile fatty acids (VFAs) and alcohols, in particular acetate, butyrate, propionate and ethanol (Ghimire et al. 2015). According to the Thauer limit (Thauer et al.1977), under the best operating conditions the expected H_2 yield is at most 4 moles per mole of hexose consumed, as shown by the reaction for the acetic pathway (1):

$C_6H_{12}O_6 + 2H_2O \rightarrow 2CH_3COOH + 2CO_2 + 4H_2$ (1)

However, several other reactions can take place concomitantly with this pathway, also leading to lower yields, depending on various factors including the environmental and operating conditions. This implies that H_2 production in the biochemical process is systematically complemented with by-products, therefore there is further potential for energy recovery from the end-products of DF.

This work aims to address the biochemical limitations of fermentative H_2 production through an innovative approach, which involves the integration of DF with electrochemical methods to better exploit the energy content of organic residues. The innovative approach proposed in this work lies in the development of a bioelectrochemical system that integrates the DF process with electrochemical conversion of protons in VFAs during the biochemical process.

2. Integrated bio-electrochemical system (IBES) for dark fermentation

The integrated bio-electrochemical process (Figure 1) is aimed at improving the H_2 yield by acting on the protons generated by dissociation of the VFAs produced during the biochemical process:

$R\text{-}COOH \leftrightarrow R\text{-}COO^- + H^+$ (2)

The protons are reduced to H_2 according to reaction (3) by delivering the required electrons through the oxidation of a metallic element in the anodic chamber.

$2H^+ + 2e^- \leftrightarrow H_2$ (3)

An inert electrode (cathode) is placed in the fermentation medium, which is connected through an external electric circuit to a second reducing electrode (anode), placed in an electrolytic solution in a separate chamber. The electric current flow occurs from the reducing electrode to the inert one, which does not participate directly in the reaction, but has rather the role of carrying the electrons into the fermentation reactor allowing them to reduce protons. The reactions that occur in the cathodic (4) and anodic (5) chambers are shown below, along with the corresponding reduction potentials under standard conditions (E^0), assuming zinc as an example of anode.

$2H^+ + 2e^- \leftrightarrow H_2$ $E^0(2H^+/H_2) = 0.000V$ (4)

$Zn \leftrightarrow Zn^{2+} + 2e^-$ $E^0(Zn_2^+/Zn) = -0.762V$ (5)

The overall cell electromotive force under standard conditions (ΔE^0), that is defined as the potential difference between the cathode and the anode, for this system is as follows:

$\Delta E^0 = E^0(2H^+/H_2) - E^0(Zn^{2+}/Zn) = 0.762V$ (6)

According to the process thermodynamics, it can be observed that the Gibbs free energy is negative (7), therefore the redox reaction takes place spontaneously as the reduction potential of the anode is adequately low.

$\Delta G^0 = -nF\Delta E^0 = -147$ kJ (7)

Where *n* is the number of electrons exchanged in the reaction and *F* is Faraday's constant (9.64853 x 10^4 C mol^{-1}).

Consequently, the integrated bio-electrochemical process provides an additional generation of H_2 compared to the biochemical reactions, due to the electrochemical transformation that exploit the metabolic products. Moreover, the system is designed as a galvanic cell that allows the process to be energetically self-sufficient. Finally, the protons conversion offers a secondary benefit, since it prevents the acidification of the fermentative medium, which would otherwise be achieved with chemical agents in order to maintain the pH range suitable for the microorganisms.

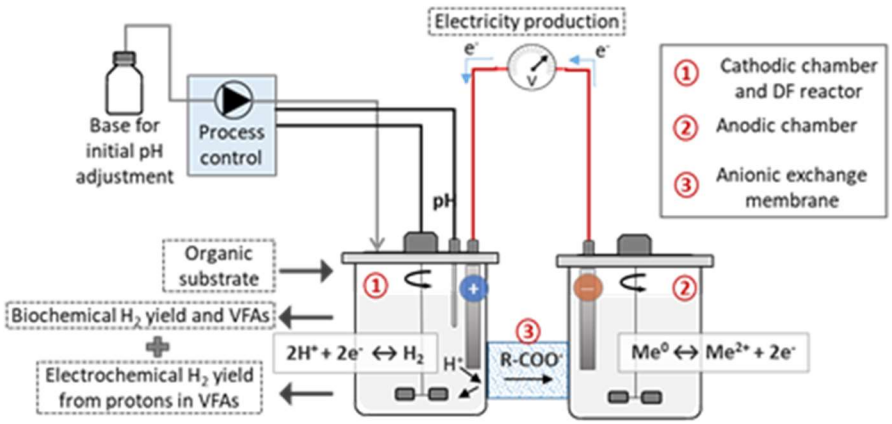

Figure 1. Layout of the IBES

3. Materials and Methods

Four different experimental set-ups (named A, B, C, D) were designed in order to identify the most suitable materials and configuration for the IBES. Acetic and butyric acid were used as model substrates to simulate the metabolic products of DF in all the configurations for a preliminary evaluation of the process. Subsequently, the bio-electrochemical process was investigated through dark fermentation of cheese whey in configuration D. In the latter case, a stand-alone dark fermentation reactor was employed with same substrate in batch mode for comparison with the IBES.

The four set-ups consist of two compartments: the cathodic chamber, in which DF occurs simultaneously with the electrochemical conversion of protons, and the anodic chamber, in which the oxidation of a metal takes place. In the A system, a sodium chloride salt bridge was tested to ensure the cell electroneutrality; in the other three systems, an anionic exchange membrane (AEM) was used for the same purpose, with a surface area to volume ratio of 120 cm^2/L for system B, 23 cm^2/L for C and 135 cm^2/L for D.

Different electrodes were tested for the cathode material, which has the role of conveying electrons into the fermentation medium, including graphite sheet, platinum sheet, titanium grid, nickel grid and porous carbon. These were selected due to their electrical conductivity characteristics, recognized inert behaviour with respect to redox reactions and absence of potential toxic effects on microorganisms. The anodic chamber was filled with zinc sulphate at 0.5M concentrations, while a metallic zinc plate was used as the anode. Systems A and B were only used for preliminary tests, since the compartments are open and it is not possible to measure the amount of H_2 produced; in this case, the process was

monitored through continuous measurement of the cell voltage ΔV, electric current intensity I and pH change of the cathodic solution. Systems C and D were equipped with a eudiometer for volumetric gas measurement and sampling for subsequent gas-chromatographic analysis (Model 3600 CX, VARIAN). In systems A and B, the continuous voltage measurements were performed through a NI FieldPoint, with an external fixed load of 90 Ω. In system C and D, a NI cDAQ-9174 was used for the same purpose, with an external fixed load of 1 GΩ. Both measurement systems were combined with LabVIEW as the data acquisition software. In a number of dedicated tests, a potentiometer was also used to derive the electric potential curves by adjusting the external load.

The total amount of electric charge Q exchanged during the electrochemical process was calculated according to the following equation (8).

$$Q = \int_0^t I(t)dt \qquad (8)$$

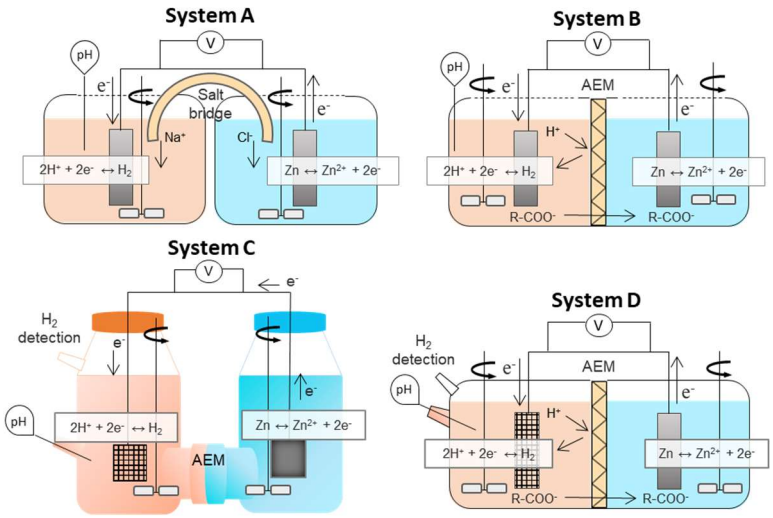

Figure 2. Experimental set-ups for the integrated bio-electrochemical process. System A is composed of two physically separated compartments, where the salt bridge provides maintenance of the cell electroneutrality. In system B, the two chambers are separated by an AEM with a A/V ratio of 120 cm^2L^{-1}. System C is made of two gastight bottles connected through a flange containing the separation AEM, with a A/V ratio of 23 cm^2L^{-1}. The system D is a PMMA cell with a A/V ratio of 135 cm^2L^{-1}.

4. Results and Discussion

The preliminary tests show an increase in pH values of the model solution (acetic acid) as an effect of the conversion of protons into H_2, which was also correlated with the electricity production. The result of the test performed with configuration B is shown as an example in Figure 3. The observed pH changes were directly correlated with the amount of electrons mobilized. Moreover, the observed shape of the pH profile over time appeared to mirror the expected effect of continued dissociation of acetate,

with the released protons being subtracted from the solution and converted into H_2. This was followed by a pH plateau when acid dissociation is complete, corresponding to the interruption of the electrons flow. Of course, when organic acids are continuously supplied by the biological process, a stable flow of electrons would be expected.

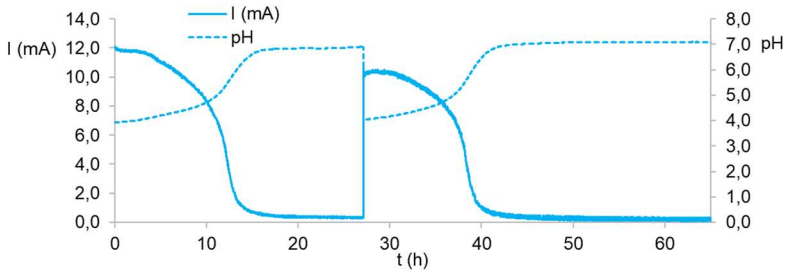

Figure 3. Electric current and pH trend in system B

Preliminary tests were also conducted to optimize the system configuration in terms of minimization of ohmic resistances and maximization of the membrane surface area per unit reactor volume. The three systems with the membrane and titanium grid were compared through their power curves (Figure 4) that were derived by changing the external resistive load applied by means of a potentiometer in the circuit. The results show that the A/V ratio strongly affect the cell efficiency in terms of power.

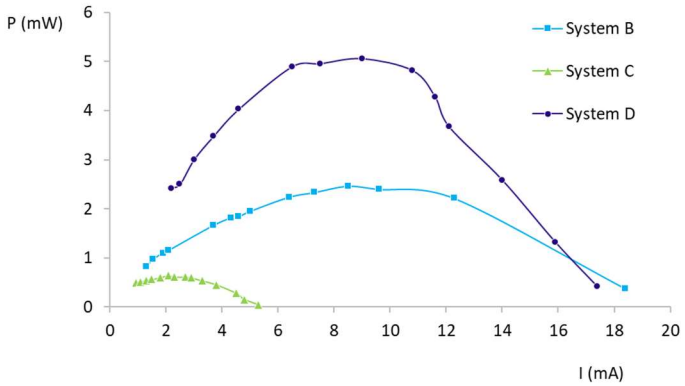

Figure 4. Power curves in system B, C and D with titanium grid as cathode.

In particular, the results with system C showed that the less favourable ratio between the AEM surface area and the cell volume, dictated by technical constraints, had a negative effect on the IBES yield. Moreover, the process evolution over time was investigated by fixing the external resistive load to the minimum in order to maximize the electrical current flow instead of the power. In system B, the evolution over time was performed with three different cathodes (Nickel, Carbon and Titanium). Subsequently, in systems C and D the evolution tests were performed with titanium grid (tests C, D-1 and D-2 with acetic acid, D-HBu with butyric acid). In this case, the process in system C was found to evolve at a lower rate compared to configuration B and D, indicating that an improved size ratio of the

AEM and a reduction of the internal resistances of the system would be required to improve the process performance. In systems C and D, H_2 production could be observed directly, mainly in the first stage of the process (169 hours for system C, 51 h for D-1, 62 h for D-2 and 57 h for D-HBu).

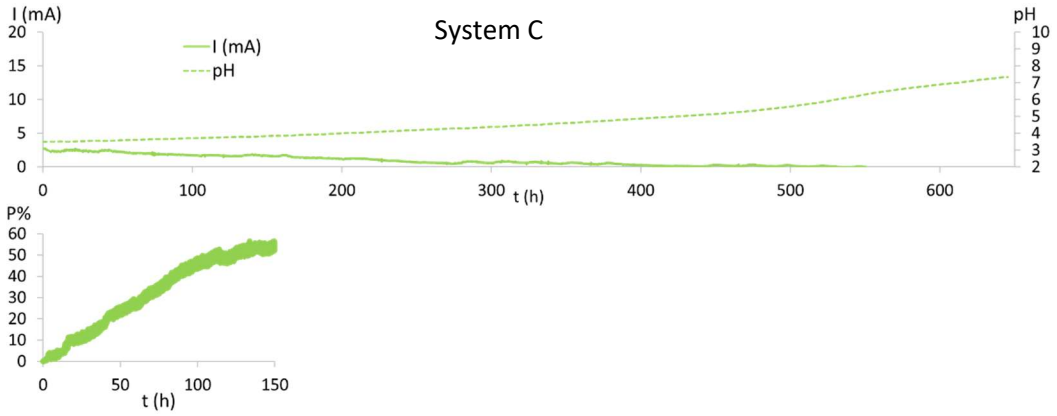

Figure 5. System C: Evolution over time of pH, electricity and H_2 production as percentage of H^+ reduced to H_2 compared to totally dissociated protons of the starting acetic acid (P%).

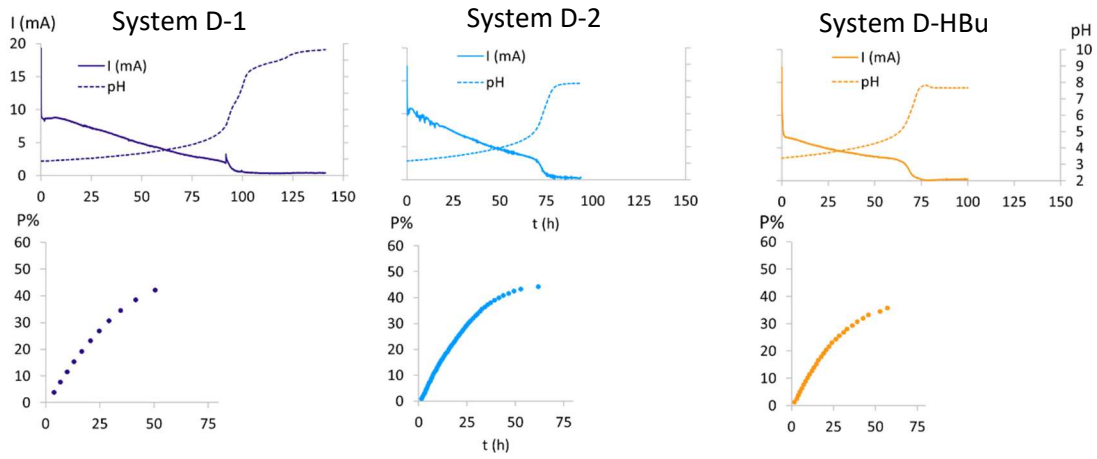

Figure 6. System D: Evolution over time of pH, electricity and H_2 production as percentage of H^+ reduced to H_2 compared to totally dissociated protons of the starting acid (P%).

It was observed that the faster dissociation of acetic acid in system D was also associated with a higher rate of H_2 production, although the longer process C duration resulted in a higher yield. However, in both systems the amount of protons reduced to H_2 appeared to be lower than the potential moles contained in the starting acetic acid, although the pH evolution seems to suggest that dissociation was complete. Moreover, the electron balance suggests that the electric current generated was not exclusively used for proton reduction to H_2, and likely further concomitant electrochemical processes

contributed to the generation of the electric current. It may be hypothesized that possible causes of deviation from the expected reactions may include interactions of the cathode metal species. In order to better understand the possible causes and any interfering processes, additional tests are currently being carried out.

Table1. Summary of mainly results in system C and D.

Configuration	C	D-1	D-2	D-HBu
Time to reach pH 7 (h)	612	99	76	76
Electrons released by Zn anode consumption (mol)	0.0135	0.0173	0.0153	0.0117
Electrons transferred according to the electricity produced (mol)	0.0196	0.0199	0.0174	0.0124
H_2 electrochemically produced from starting acetic acid (NL)	0.127	0.92	0.97	0.053
Time for total H_2 production (h)	169	51	62	57
Percentage of H^+ reduced to H_2 compared to totally dissociated protons of the starting acetic acid (P%)	57.6%	42.1%	44.3%	35.7%

Lastly, the bioelectrochemical process was carried out through D configuration by dark fermentation of cheese whey in order to implement the IBES under actual DF conditions. Both the IBES and the stand-alone DF reactor were filled with cheese whey previously corrected with sodium hydroxide (2M) to raise the initial pH to 7.5. Subsequently, the pH was uncontrolled in order to evaluate the action of the bioelectrochemical process without external agents. Both reactors were maintained under mesophilic conditions (38±1 °C).

The IBES showed 59,8% of improvement in H_2 yields, achieving the maximum of 2.6 $NmLH_2/g_{CW}$ compared to 1.0 $NmLH_2/g_{CW}$ in the control reactor. In this case, electrons released by zinc anode consumption were 0.0330 mol e^- with 0.0444 mol e^- of electrons transferred according to the electricity produced. The charge transferred is higher in this case due to the greater availability of protons provided by the fermentation medium compared to synthetic substrates of preliminary tests. According to the electrical current measured, the maximum H_2 volume potentially produced by the electrochemical process amounts to 497 $NmLH_2$, which would represent an improvement in H_2 yields of 31.1% compared to control reactor. This seems to support the idea that the electrochemical system acts on improving yields through a twofold influence, thus, in addition to H_2 yields from protons conversion, there is a general improvement in the biochemical process probably due to a small buffering effect on pH. Nevertheless, the buffer effect on pH is not enough to rapidly prevent from

acidification, so below pH 5 the values rapidly decrease and the biochemical process ends. This result shows that pH control with chemical agents may still be required during the bio-electrochemical process, although to a lesser extent than in stand-alone dark fermentation. Therefore, further experimental tests will be carried out to confirm this result and to further investigate the effect of the integration of the electrochemical conversion of protons with the biochemical process.

5. Conclusions

The aim of this experimental work was to create an integrated bio-electrochemical system (IBES) in order to improve H_2 yields during DF through protons of VFAs reduction into H_2.
The preliminary tests highlighted the importance of optimizing the system configuration in order to reduce internal resistances and to provide an appropriate H_2 generation rate as well as electricity production. Initial tests with real organic substrate confirm the improved H_2 yields provided by the IBES. Therefore, the advantages of the IBES include a higher H_2 production that helps to overcome the biochemical limits, as well as a small positive effect on the intrinsic acidification of the system. Moreover, the integrated system is designed as a galvanic cell, so there is an electricity production that could allow the process to be partially ergetically self-sufficient.
Further investigations are required on any overlapping secondary reactions caused by the circulation of the electrical charge, as shown as possible by preliminary tests. In addition, further experimental tests will be carried out with the real organic substrate in order to provide an overall assessment of the bio-electrochemical process.

References

Ghimire, Anish et al. 2015. “A Review on Dark Fermentative Biohydrogen Production from Organic Biomass: Process Parameters and Use of by-Products.” *Applied Energy* 144: 73–95. https://www.sciencedirect.com/science/article/pii/S0306261915000616 (December 19, 2018).

Da Silva Veras, Tatiane, Thiago Simonato Mozer, Danielle da Costa Rubim Messeder dos Santos, and Aldara da Silva César. 2017. “Hydrogen: Trends, Production and Characterization of the Main Process Worldwide.” *International Journal of Hydrogen Energy*.

Thauer, Rudolf K., Kurt Jungermann, and Karl Decker. 1977. “Energy Conservation in Chemotrophic Anaerobic Bacteria.” *bacteriological reviews* 41: 100–180.